

# Evaluation of the albedo parameterization of the Canadian Lake Ice Model and MODIS albedo products during the ice cover season

by

Nicolas Andreas Svacina

A thesis  
presented to the University of Waterloo  
in fulfillment of the  
thesis requirement for the degree of  
Master of Science  
in  
Geography

Waterloo, Ontario, Canada, 2013

©Nicolas Andreas Svacina 2013

## **Author's declaration**

I hereby declare that I am the sole author of this thesis. This is a true copy of the thesis, including any required final revisions, as accepted by my examiners.

I understand that my thesis may be made electronically available to the public.

## Abstract

Snow and lake ice have very high albedos compared to other surfaces found in nature. Surface albedo is an important component of the surface energy budget especially when albedos are high since albedo governs how much shortwave radiation is absorbed or reflected at a surface. In particular, snow and lake ice albedos have been shown to affect the timing of lake ice break-up. Lakes are found throughout the Northern Hemisphere and lake ice has been shown to be sensitive to climatic variability. Therefore, the modelling of lake ice phenology, using lake ice models such as the Canadian Lake Ice Model (CLIMo), is important to the study of climatic variability in the Arctic and sub-Arctic regions and accurate snow and lake ice albedo measurements are required to ensure the accuracy of the simulations. However, snow and lake ice albedo can vary from day-to-day depending on factors such as air temperature, presence of impurities, age, and composition. Some factors are more difficult than others to model (e.g. presence of impurities). It would be more straight forward to just gather field measurements, but such measurements would be costly and lakes can be in remote locations and difficult to access. Instead, CLIMo contains an albedo parameterization scheme that models the evolution of snow and lake ice albedo in its simulations. However, parts of the albedo parameterization are based on sea-ice observations (which inherently have higher albedos due to brine inclusions) and the albedo parameterization does not take ice type (e.g. clear ice or snow ice) into account. Satellite remote sensing via the Moderate Resolution Imaging Spectroradiometer (MODIS) provides methods for retrieving albedo that may help enhance CLIMo's albedo parameterization.

CLIMo's albedo parameterization as well the MODIS daily albedo products (MOD10A1 and MYD10A1) and 16-day product (MCD43A3) were evaluated against *in situ* albedo observations made over Malcolm Ramsay Lake near Churchill, Manitoba, during the winter of 2012. It was found that the snow albedo parameterization of CLIMo performs well when compared to average *in situ* observations, but the bare ice parameterization overestimated bare ice albedo observations. The MODIS albedo products compared well when evaluated against the *in situ* albedo observations and were able to capture changes in albedo throughout the study period. The MODIS albedo products were also compared against CLIMo's melting ice parameterization, because the equipment had to be removed from the lake to prevent it from falling into the water during the melt season. Cloud cover interfered with the MODIS observations, but the comparison suggests that MODIS albedo products retrieved higher albedo values than the melting ice parameterization of CLIMo.

The MODIS albedo products were then integrated directly into CLIMo in substitution of the albedo parameterization to see if they could enhance break-up date (ice off) simulations. MODIS albedo retrievals (MOD10A1, MYD10A1, and MCD43A3) were collected over Back Bay, Great Slave Lake (GSL) near Yellowknife, Northwest Territories, from 2000-2011. CLIMo was then run with and without the MODIS albedos integrated and compared against MODIS observed break-up dates. Simulations were also run under three difference snow cover scenarios (0%, 68%, and 100% snow cover). It was found that CLIMo without MODIS albedos performed better with the 0% snow cover scenario than with the MODIS albedos integrated in. Both simulations (with and without MODIS albedos) performed well with the snow cover scenarios. The MODIS albedo products slightly improved CLIMo break-up simulations when integrated up to a month in advance of actual lake ice break-up for Back Bay. With the MODIS albedo products integrated into CLIMo, break-up dates were simulated within 3-4 days of MODIS observed break-up. CLIMo without the MODIS albedos still performed very well simulating break-up within 4-5 days of MODIS observed break-up. It is uncertain whether this was a significant improvement or not with such a small study period and with the investigation being conducted at a single site (Back Bay). However, it has been found that CLIMo performs well with the original albedo parameterization and that MODIS albedos could potentially complement lake-wide break-up simulations in future studies.

## **Acknowledgements**

To my supervisor, Professor Claude Duguay, I would like to acknowledge the help and support you have provided throughout my academic career. Without your mentoring, guidance, and friendship, this would never have been possible. Thank you.

To Dr. Laura Brown, I would like to thank you for always being just an email away. I am sure that Fortran and Edlog would have defeated me long ago if it were not for you. Thank you to Josh King for assisting me in my field campaign. Thank you to Dr. Ellsworth LeDrew, Dr. Merrin Macrae, and Environment Canada for providing me with the required equipment to make this thesis possible. Thank you to Dr. LeeAnn Fishback and the Churchill Northern Studies Centre (CNSC) staff for providing accommodations and routinely checking my equipment for me.

The Natural Sciences and Engineering Research Council of Canada (NSERC) and the Ontario Graduate Scholarship (OGS) are also gratefully acknowledged for their financial support.

Thank you to my friends, who probably hindered my thesis completion more than anything... I will never forget our times together and here's to the good times yet to come.

Finally, thank you to my family. I cannot thank my Oma and Opa enough for their continued support. My Mother and Father's love, support, and patience know no bounds. Thank you for being there for me.

## Table of contents

List of Figures .....	ix
List of Tables .....	xi
List of Abbreviations .....	xiii
Nomenclature .....	xiv
Preface .....	xvi
Chapter 1 General introduction .....	1
1.1 Introduction .....	1
1.2 Problem statement .....	2
1.3 Research objectives .....	3
1.4 Thesis outline .....	3
Chapter 2 Background .....	4
2.1 Overview .....	4
2.2 Surface albedo and the surface energy budget .....	5
2.2.1 Albedo of snow .....	7
2.2.2 Albedo of lake ice .....	8
2.2.3 Cloud effects on snow and lake ice albedo .....	9
2.3 Importance of albedo in lake ice thermodynamics and phenology .....	10
2.4 Snow and ice albedo measurements .....	11
2.4.1 Ground-based measurements .....	12
2.4.2 Satellite estimates .....	14
2.4.2.1 Daily albedo products .....	14
2.4.2.2 16-day albedo product .....	16
2.5 Canadian Lake Ice Model .....	18
2.5.1 General description .....	18
2.5.2 Albedo parameterization scheme .....	21
2.6 Summary .....	22
Chapter 3 Evaluation of the Canadian Lake Ice Model albedo parameterization and MODIS albedo retrievals .....	23
3.1 Introduction .....	23
3.2 Data and methods .....	25
3.2.1 Study area .....	25
3.2.1.1 Malcolm Ramsay Lake .....	25

3.2.1.2 Malcolm Ramsay Lake <i>in situ</i> measurements .....	27
3.2.2 MODIS albedo products .....	29
3.2.2.1 MOD10A1/MYD10A1 daily albedo product .....	31
3.2.2.2 MCD43A3 16-day albedo product .....	32
3.2.3 CLIMo albedo parameterization .....	34
3.2.3.1 CLIMo simulations .....	36
3.2.4 Performance evaluation statistics .....	36
3.3 Results and discussion .....	37
3.3.1 CLIMo albedo values evaluated against <i>in situ</i> observations .....	37
3.3.2 MODIS retrieved albedo values evaluated against <i>in situ</i> observations .....	46
3.3.2.1 MODIS daily albedo products .....	46
3.3.2.2 MODIS 16-day albedo product .....	48
3.3.3 MODIS retrieved albedo values compared to CLIMo albedo values .....	51
3.3.3.1 Ice growth period .....	52
3.3.3.2 Break-up period .....	54
3.4 Summary and conclusions .....	57
Chapter 4 Integrating MODIS albedo within a lake ice model .....	60
4.1 Introduction .....	60
4.2 Study area .....	62
4.2.1 Yellowknife (Back Bay), Northwest Territories .....	62
4.3 MODIS snow albedo products and methods for integration .....	64
4.3.1 MxD10A1 daily snow product .....	66
4.3.2 MCD43A3 albedo product .....	67
4.4 Ice-off observations from MODIS .....	67
4.5 Canadian Lake Ice Model (CLIMo) .....	69
4.5.1 General description .....	69
4.5.2 Albedo parameterization and modifications .....	70
4.6 CLIMo simulations and atmospheric forcing .....	71
4.7 Results .....	75
4.7.1 Ice-off dates: Scenario 1, CLIMo with 0% snow .....	75
4.7.2 Ice off dates: Scenario 2, CLIMo with 68% snow .....	77
4.7.3 Ice off dates: Scenario 3, CLIMo with 100% snow .....	80
4.8 Discussion .....	81

4.8.1 MODIS albedo products and CLIMo's performance.....	81
4.9 Summary and conclusion .....	89
Chapter 5 General Conclusions.....	92
5.1 Summary .....	92
5.2 Limitations .....	94
5.3 Future work.....	95
Appendix A.....	96
A.1 Performance statistics .....	96
References.....	97

## List of Figures

Figure 2.1. A visual representation of the DHR and BHR. The broad arrow represents direct beam irradiance while the other arrows represent reflected and incident radiation fields. (Source: Martonchik <i>et al.</i> , 2000) .....	6
Figure 3.1. Location of the pyranometer stations and spatial coverage of the MODIS pixel on Malcolm Ramsay Lake.....	26
Figure 3.2. Daily minimum, maximum, and average temperatures (°C) from February 15 to June 09, 2012 for Churchill, Manitoba. ....	28
Figure 3.3. The photos (taken on February 12, 2012) depict the variable snow cover (a.) as well as the variability of bubble density/cracks (b. to d.) in the clear ice for Malcolm Ramsay Lake, Manitoba. ....	28
Figure 3.4. Boxplots of albedo for three <i>in situ</i> stations located on Malcolm Ramsay Lake (February 15 to April 25, 2012) .....	37
Figure 3.5. Daily albedo values for CLIMo with and without snow as well as Sites A, B, and C. Daily snowfall values reported at the Churchill Airport weather station are also included in this figure. ....	38
Figure 3.6. Site C on March 16, 2012 following snowfall events. ....	38
Figure 3.7. MAE for both CLIMo with and without snow for each of the stations as well as all stations averaged together (February 15 to April 25, 2012). ....	41
Figure 3.8. Snowfall amount from January 1 to March 9, 2012.....	41
Figure 3.9. Boxplots of the three <i>in situ</i> stations located on Malcolm Ramsay Lake (February 15 to March 9, 2012) .....	43
Figure 3.10. (Left) Section of clear ice used to find albedo values for clear ice and (Right) a section of snow ice used to find albedo values for snow ice on Malcolm Ramsay Lake. ....	44
Figure 3.11. MODIS retrieved and average <i>in situ</i> daily/16-day albedo values as well as snowfall amount for Malcolm Ramsay Lake from February 15th to April 25th, 2012. ....	46
Figure 3.12. Daily incoming shortwave radiation and average <i>in situ</i> albedo measurements for Site A on Malcolm Ramsay Lake from February 15 to April 25, 2012. ....	49
Figure 3.13. MODIS retrieved and CLIMo derived albedo values for Malcolm Ramsay Lake from February 15 <sup>th</sup> to April 25 <sup>th</sup> , 2012. ....	52
Figure 4.1. (Top) Map of Great Bear Lake and Great Slave Lake. (Bottom) A map that shows the location of Back Bay in relation to Yellowknife, NWT (Sources: Howell <i>et al.</i> , 2009; Ménard <i>et al.</i> , 2002).....	63

Figure 4.2. Location of the MODIS pixel near Back Bay (Yellowknife).....	65
Figure 4.3. Example of using MOD09GA to determine lake ice break-up on a portion of Great Slave Lake: true colour composite (left) and a NIR false colour composite (right) from June 5, 2007. ....	68
Figure 4.4. Flowchart illustrating MODIS albedo product integration into CLIMo.....	72
Figure 4.5. Observed and simulated break-up dates from 2000 to 2011 for S1 (CLIMo with 0% snow) over Back Bay. ....	77
Figure 4.6. Observed and simulated break-up dates from 2000 to 2011 for S2 (CLIMo with 68% snow) over Back Bay. ....	79
Figure 4.7. Observed and simulated break-up dates from 2000 to 2011 for S3 (CLIMo with 100% snow) over Back Bay. ....	80
Figure 4.8. Average snow-on-land and average snow-on-ice for Yellowknife and Back Bay from the 2002/2003 to 2010/2011 winter seasons ( <i>Ice Thickness Program Collection [2002-2012]</i> , 2012) ....	82
Figure 4.9. A comparison between MODIS surface albedo and CLIMo's surface albedo for the three snow cover scenarios for the years 2008 (Top) and 2010 (Bottom). Also indicated are the dates when the MODIS surface albedo data are integrated into CLIMo for the five different methods. ....	83
Figure 4.10. Average monthly temperatures for the winter seasons leading up to the 2006-2008 lake ice break-up date simulations.....	87
Figure 4.11. Mean air temperatures for Back Bay, GSL leading up to lake ice break-up in 2007. ....	87

## List of Tables

Table 2.1. Summary of recorded lake ice albedo collected from previous measurement studies. ....	13
Table 2.2. Summary of the validation studies performed for MOD10A1 and MYD10A1.....	15
Table 2.3. Summary of the validation studies performed for the MCD43 products. ....	17
Table 3.1. Historical monthly average temperature and snowfall (1971 to 2000) with the monthly average temperature and snowfall 2011-2012 for each month September through to May.....	27
Table 3.2. MODIS bands used in the generation of the albedo products of this study (Hall et al., 2009; Salomonson et al., 2006).....	30
Table 3.3. CLIMo derived albedo values evaluated against <i>in situ</i> albedo values for Malcolm Ramsay Lake from February 15 to April 25, 2012. ....	40
Table 3.4. CLIMo derived albedo values evaluated against <i>in situ</i> albedo values for Malcolm Ramsay Lake from February 15 to March 10, 2012. ....	42
Table 3.5. CLIMo derived albedo values evaluated against <i>in situ</i> albedo values for Malcolm Ramsay Lake from March 10 to April 25, 2012. ....	45
Table 3.6. MODIS daily albedo values evaluated with <i>in situ</i> observed albedo values for Malcolm Ramsay Lake from February 15 to April 25, 2012.....	47
Table 3.7. MODIS 16-day albedo product evaluated with daily observed albedo values for Malcolm Ramsay Lake for clear sky and cloudy sky days from February 15 to April 25, 2012. ....	50
Table 3.8. MODIS 16-day albedo product evaluated with daily observed albedo values for Malcolm Ramsay Lake from February 15 to April 25, 2012.....	50
Table 3.9. Descriptive statistics for MODIS retrieved and CLIMo derived albedo values for Malcolm Ramsay Lake from February 15th to April 25th, 2012. ....	53
Table 3.10. Difference statistics for MODIS retrieved and CLIMo derived albedo values for Malcolm Ramsay Lake from February 15th to April 25th, 2012. ....	53
Table 3.11. Difference statistics for MODIS retrieved and CLIMo derived albedo values for Malcolm Ramsay Lake from May 7th to June 9th, 2012.....	55
Table 4.1. MODIS bands used by the products in this study (Hall <i>et al.</i> , 2009; Salomonson <i>et al.</i> , 2006).....	64
Table 4.2. Dates when MODIS albedo data is integrated into CLIMo according to each method. ....	74
Table 4.3. Summary of the five methods for MODIS integration into CLIMo plus the three snow cover scenarios .....	75

Table 4.4. Error measure statistics to evaluate the performance of the simulated break-up dates to the observed break-up dates for S1 over Back Bay (2000-11). .....	76
Table 4.5. Error measure statistics to evaluate the performance of the simulated break-up dates to the observed break-up dates for S2 over Back Bay (2000-2011). .....	79
Table 4.6. Error measure statistics to evaluate the performance of the simulated break-up dates to the observed break-up dates for S3 over Back Bay (2000-2011). .....	81
Table 4.7. Error measure statistics to evaluate the performance of the simulated break-up dates to the observed break-up dates for S1, S2, and S3 over Back Bay, but with 2006-2008 removed (2000-2005, 2009-2011). .....	88

## **List of Abbreviations**

ARM	Atmospheric Radiation Measurement Program
BHR	Bi-hemispherical Reflectance
BRDF	Bidirectional Reflectance Distribution Function
BSA	Black Sky Albedo
CLIMo	Canadian Lake Ice Model
DHR	Directional-hemispherical Reflectance
MAD	Mean Absolute Difference
MAE	Mean Absolute Error
MBE	Mean Bias Error
MD	Mean Difference
MODIS	Moderate Resolution Imaging Spectroradiometer
NARR	North American Regional Reanalysis
NOAA	National Oceanic and Atmospheric Administration
RMSD	Root Mean Square Difference
RMSE	Root Mean Square Error
RTLSR	Ross Thick-Li Sparse Reciprocal
SGP	Southern Great Plains site
SURFRAD	Surface Radiation Budget Network
SZA	Solar Zenith Angle
TOA	Top of Atmosphere
WSA	White Sky Albedo

## Nomenclature

### Canadian Lake Ice Model (CLIMo)

#### Variables

<u>Symbol</u>	<u>Name</u>	<u>SI Unit</u>
$C_p(z, t)$	Specific heat capacity	$\text{J kg}^{-1} \text{K}^{-1}$
$F_0(t)$	Net downward heat flux absorbed at the surface	$\text{W m}^{-2}$
$F_{\text{lat}}(t)$	Downward latent heat flux	$\text{W m}^{-2}$
$F_{\text{lw}}(t)$	Downwelling longwave radiative energy flux	$\text{W m}^{-2}$
$F_{\text{sw}}(t)$	Downwelling shortwave radiative energy flux	$\text{W m}^{-2}$
$F_{\text{sens}}(t)$	Downward sensible heat flux	$\text{W m}^{-2}$
$h(t)$	Total thickness of slab, ice plus snow	m
$h_i(t)$	Ice thickness	m
$h_s(t)$	Snow thickness	m
$k(z, t)$	Thermal conductivity	$\text{W m}^{-1} \text{K}^{-1}$
$t$	Time	s
$T(z, t)$	Temperature within ice or snow	K
$\hat{T}(z)$	The estimated temperature prior to solving (2.1, 3.1, 4.1)	K
$T_{\text{mix}}(t)$	Lake mixed layer temperature	K
$z$	Vertical coordinate, positive downward	m
$\alpha(t)$	Surface albedo	dimensionless
$\rho(z, t)$	Density	$\text{kg m}^{-3}$

### Canadian Lake Ice Model (CLIMo):

#### Parameters

#### Symbol

$C_{\text{pi}}$	Specific heat capacity of ice, $2.062 \times 10^3 \text{ J kg}^{-1} \text{K}^{-1}$
-----------------	--

$c_1$	0.1 m
$c_2$	0.44 m
$c_3$	0.075 m
$d_{\text{mix}}$	Effective mixed layer depth (m)
$h_{\text{min}}$	Minimum ice thickness below which open water is assumed, 0.001 m
$I_0$	Fraction of shortwave radiation flux that penetrates the surface, equal to 0.17 if snow depth $\leq 0.01$ m, and equal to 0 if snow depth $> 0.1$ m
$L_{\text{fi}}$	Volumetric heat of fusion of freshwater ice, $3.045 \times 10^8 \text{ J m}^{-3}$
$L_{\text{fs}}$	Volumetric heat of fusion of snow, $1.097 \times 10^8 \text{ J m}^{-3}$
$T_{\text{f}}$	Freezing temperature of water, 273.15 K
$T_{\text{m}}$	Melting temperature at the surface, 273.15 K
$\alpha$	Surface albedo
$\alpha_{\text{i}}$	Ice albedo
$\alpha_{\text{ow}}$	Albedo of open water, 0.05
$\alpha_{\text{mi}}$	Albedo of melting ice, 0.55
$\alpha_{\text{s}}$	Albedo of snow
$\varepsilon$	Surface emissivity, 0.99
$K$	Bulk extinction coefficient for penetrating shortwave radiation, $1.5 \text{ m}^{-1}$
$\rho_{\text{w}}$	Density of water, $1000 \text{ kg m}^{-3}$
$\sigma$	Stefan-Boltzmann constant, $5.67 \times 10^{-8} \text{ W m}^{-2} \text{ K}^{-4}$

## Preface

In addition to general introduction/conclusions and a background chapter, the thesis contains two manuscripts that investigate the albedo parameterization of the Canadian Lake Ice Model (CLIMo) and the MODIS daily and 16-day albedo products (MOD10A1, MYD10A1, and MCD43A3). The first manuscript, to be submitted to *Hydrological Processes* (Special Issue of the 2013 Eastern Snow Conference) in June 2013, evaluates CLIMo's albedo parameterization and MODIS albedo products with *in situ* measurements of Malcolm Ramsay Lake near Churchill, Manitoba. The second manuscript is in preparation for submission in fall 2013 and investigates the direct integration of MODIS albedo products into CLIMo in support of the current albedo parameterization to see if there is a noticeable improvement in lake ice break-up simulations over Back Bay on Great Slave Lake.

The first manuscript is a result of direct collaboration with Prof. Claude Duguay, Dr. Laura Brown, Environment Canada, Prof. Ellsworth LeDrew, Joshua King and Dr. LeeAnn Fishback. Prof. Duguay provided guidance throughout the completion of the manuscript and aided in the design. Dr. Brown provided valued advice in setting up the equipment and provided data for the lake ice model CLIMo. Environment Canada and Prof. LeDrew generously provided a meteorological station, pyranometers, and data loggers to be deployed on Malcolm Ramsay Lake making the study possible. Joshua King helped design and set-up the stations installed on Malcolm Ramsay Lake. Dr. Fishback and the Churchill Northern Studies Centre (CNSC) staff provided accommodation and continually checked on the instrumentation throughout the field study.

The second manuscript is the result of direct collaboration with Prof. Claude Duguay and Dr. Laura Brown. Prof. Duguay's invaluable assistance and guidance throughout the completion of the manuscript can never be thanked enough. Dr. Brown provided data for the lake ice model as well as guidance in running CLIMo.

# Chapter 1

## General introduction

### 1.1 Introduction

The response of lakes to climate variability and change, and the role of lakes in the energy balance of Arctic, sub-Arctic, and high boreal environments have been the subject of several investigations (e.g., Brown and Duguay, 2010, 2011a, 2011b; Duguay *et al.*, 2003; Magnuson *et al.*, 2000; Ménard *et al.*, 2002; Rouse *et al.*, 2005, 2008a, 2008b). The thermal properties of water allow it to be a significant store of energy. Lakes are known to have an effect on the surrounding weather and climate of nearby regions (Brown and Duguay, 2010). The presence of lake ice combined with the high albedo of snow and ice severely limits the lake-atmosphere transfer of energy in the winter months. The Canadian Lake Ice Model (CLIMo), a one-dimensional (1-D) thermodynamic lake ice model, was developed to better understand the atmospheric forcing variables as well as the effect that climatic variability has on lake ice growth and phenology (Duguay *et al.*, 2003). There have been numerous studies performed for the evaluation of CLIMo (Brown and Duguay, 2011a, 2011b; Duguay *et al.*, 2003; Jeffries *et al.*, 2005a; Morris *et al.*, 2005; and Ménard *et al.*, 2002). However, none have focused on evaluation of the albedo parameterization of the lake ice model. Duguay *et al.* (2003) note that the albedo parameterization is unique to CLIMo compared to other existing lake, lake ice, and sea ice models (Ebert and Curry, 1993; Hostetler *et al.*, 1993; Mironov, 2008; Vavrus *et al.*, 1996).

The albedo is an important component of the surface energy balance as it represents how much incoming shortwave solar radiation is absorbed/reflected at the surface. The albedo of snow and lake ice is of particular interest due to their relatively high albedos (0.15-0.60 and 0.50-0.95, respectively) compared to the albedo of open water (0.05-0.10) (Bolsenga, 1977; Grenfell *et al.*, 1994; Heron and Woo, 1994; Serreze and Barry, 2005; Warren, 1982; Wiscombe and Warren, 1980). The high albedos of snow and lake ice have been shown to affect the timing of lake ice break-up making the accuracy of albedo simulations particularly important during that period (Martynov *et al.*, 2010; Vavrus *et al.*, 1996). Snow and lake ice albedo may vary on a day-to-day basis as the albedo is highly dependent on variables such as age, composition, surface type, presence of impurities, and the air temperature, which makes the modelling of snow and lake ice albedo and its decay challenging. Acquiring continuous *in situ* albedo measurements would be more accurate. However, the remote

locations of many northern lakes and the inherent danger of lake ice decay during the melt season make *in situ* albedo observations infeasible. As such, advances in remote sensing have allowed for the retrieval of surface albedo from space. Albedo products such as the Moderate Resolution Imaging Spectroradiometer (MODIS) daily (MOD10A1/MYD10A1) and 16-day (MCD43A3) albedo products are capable of capturing day-to-day variations in snow and lake ice albedo in areas not easily accessible (Klein and Stroeve, 2002; Schaaf *et al.*, 2002). These MODIS albedo products present the opportunity to evaluate CLIMo's albedo parameterization as well as the possibility to improve the simulation of lake ice break-up dates through the direct integration of satellite estimated albedo values into CLIMo. However, the MODIS albedo products MOD10A1, MYD10A1, and MCD43A3 must first be evaluated against *in situ* observations.

## 1.2 Problem statement

Determination of the radiation and energy balance at the surface of lake ice covers requires accurate measurements or estimates of surface albedo. The albedo parameterization of CLIMo, which provides daily estimates of surface albedo, has been devised based on *in situ* observations made in previous studies over Arctic lake ice and sea ice. The melting ice parameterization is based on observations made at a high Arctic lake near Resolute, Nunavut (Heron and Woo, 1994) as well as Langleben's (1971) study of sea ice near Tuktoyaktuk, Northwest Territories. The cold ice surface albedo parameterization of CLIMo is based on the work of Maykut (1982). Maykut (1982) derived his equation from sea albedo observations by Weller (1972) that were acquired during the Arctic Ice Dynamics Joint Experiment (AIDJEX). Sea ice albedo will be higher than lake ice albedo due to brine inclusions throughout the sea ice, creating higher volumetric scattering of the incident radiation (Grenfell and Perovich, 2004). Furthermore, CLIMo's albedo parameterization does not account for ice type (e.g. clear ice and snow ice) which is very important for the determination of lake ice albedo. An additional concern of CLIMo mentioned by Ménard *et al.* (2002) is that CLIMo does not take into account the decay of snow via metamorphism.

The MODIS albedo products provide retrievals that can capture daily variations in snow and lake ice albedo under clear-sky conditions. However, to date, there have been no evaluation efforts of the MOD10A1, MYD10A1, or MCD43A3 albedo products over lake ice. Also, the MODIS albedo products provide albedo retrievals over a pixel with a 500 m spatial resolution, whereas CLIMo is a 1-D lake ice model. The MODIS albedo retrievals estimate an albedo over a much larger area which may not be representative of the lake surface CLIMo is modelling, particularly if the surrounding lake

surface is heterogeneous (i.e. variable snow cover distribution over the lake ice surface). There are also concerns with the availability of MODIS albedo retrievals due to cloud cover interference.

### **1.3 Research objectives**

The overall goal of this research is to determine how important the accuracy of snow and lake ice albedo are in the simulation of lake ice break-up as well as to explore the potential for the integration of satellite estimated lake ice into a lake ice model (CLIMo). Satellite retrievals of snow and lake ice albedo are capable of providing accurate up-to-date estimates of changes occurring that are complex to model (e.g. snow metamorphism and the presence of impurities). The significance of this capability has yet to be determined. Specifically, the primary objectives are to: 1) evaluate CLIMo's albedo estimates and MODIS albedo products (MOD10A1, MYD10A1, and MCD43A3) against *in situ* observations during the ice growth period; 2) compare CLIMo's albedo estimates with MODIS retrievals during both the ice growth and the break-up periods; and 3) determine if the integration of MODIS albedo products in CLIMo significantly improves its simulation of break-up (ice-off) dates.

### **1.4 Thesis outline**

Chapter 2 provides a detailed background of surface albedo: the role of surface albedo in the surface energy budget; the factors that affect snow and lake ice albedo; existing lake ice albedo measurements and validation efforts for the MODIS albedo products MOD10A1, MYD10A1, MCD43AD; and a detailed description of CLIMo. Chapter 3 evaluates CLIMo's albedo parameterization and the MODIS albedo products (MOD10A1, MYD10A1, and MCD43A3) with *in situ* albedo measurements over Malcolm Ramsay Lake, near Churchill, Manitoba during the 2012 winter season. It also compares MODIS albedo products with CLIMo's albedo parameterization during the melt season. Chapter 4 explores the integration of MODIS albedo products (MOD10A1, MYD10A1, and MCD43A3) into CLIMo to determine if such integration improves the simulation of break-up dates for Back Bay, GSL near Yellowknife, Northwest Territories. Chapter 5 summarizes the key findings of the thesis and provides recommendations for further research concerning CLIMo's albedo parameterization and the MODIS albedo products.

# Chapter 2

## Background

### 2.1 Overview

Lakes are a dominant feature in the Northern Hemisphere. They play an important role in the energy and water balance of high-latitude regions. The presence or absence of lake ice affects local and regional climates (Brown and Duguay, 2010). When lake ice is absent, a lake is able to store and transfer energy into the atmosphere. In the cold winter months, ice forms over the lake and this severely restricts transfer of energy (i.e. conductive heat flow through the ice being the dominant transfer mechanism). The modelling of thermodynamic lake ice growth and phenology (i.e. freeze-up and break-up dates) is important for the understanding of regional climates in the Northern Hemisphere. An important variable of the surface energy balance is the surface albedo. Snow and lake ice have high surface albedos and thus reflect a large portion of the incoming shortwave radiation. As snow/ice albedo is known to affect the timing of ice break-up in the spring (Martynov *et al.*, 2010), accurate estimates of albedo is important in simulating lake ice phenology. Snow, a common feature on lakes in the winter, has an albedo of approximately 0.85 when fresh, but this value can decrease to as low as 0.50 when melting (Conway *et al.*, 1997; Serreze and Barry, 2005). Albedo can also vary on a day-to-day basis depending on factors such as fresh snowfall, temperature, presence of impurities, and the surface type.

This chapter provides a review of snow/ice surface albedo and its role in the surface energy budget; the factors that affect the albedo of snow and lake ice, and the influence of albedo on lake ice thermodynamics and phenology. Satellite remote sensing is capable of providing global albedo maps at high spatial (500-1000 m) and temporal resolutions (daily). There is therefore potential for the integration of satellite albedo (such as the Moderate Resolution Imaging Spectroradiometer [MODIS] albedo products) retrievals into lake ice models in order to determine if such data can help improve lake ice model predictions of ice phenology, particularly during the break-up period. However, to date, there have been no efforts for the evaluation of MODIS albedo products over lake ice. Therefore, this chapter also explores existing ground observations over lake ice as well as existing validation efforts for MODIS albedo products. Finally, this chapter also includes a description of the

Canadian Lake Ice Model (CLIMo) and its albedo parameterization since this is the candidate lake ice model selected for integration of the MODIS albedo products.

## 2.2 Surface albedo and the surface energy budget

Broadband albedo is a term often used and it represents albedo integrated over the entire solar spectrum (i.e., 0.3  $\mu\text{m}$  to 3.0  $\mu\text{m}$ ) (Massom and Lubin, 2006). Surface albedo is simply defined “as the ratio of reflected solar short-wave radiation from a surface to that incident upon it” (Struggnell and Lucht, 2001). The reflectance of a surface is dependent on the viewing as well as the illumination angle of a natural surface due to the fact that most natural surfaces are anisotropic (Wanner *et al.*, 1997). The bidirectional reflectance distribution function (BRDF) mathematically describes the reflectance of a surface based on the viewing and illumination angles of a surface (Nicodemus *et al.*, 1977; Schaepman-Strub *et al.*, 2006; Wanner *et al.*, 1997). With the spectral dependence omitted, the BRDF can be written as:

$$\text{BRDF} = f_r(\theta_i, \phi_i; \theta_r, \phi_r) = \frac{dL_r(\theta_i, \phi_i; \theta_r, \phi_r)}{dE_i(\theta_i, \phi_i)} [\text{sr}^{-1}] \quad (2.1)$$

where  $\theta_i$  is the incident zenith angle, in a spherical coordinate system (rad);  $\phi_i$  is the incident azimuth angle, in a spherical coordinate system (rad);  $\theta_r$  is the reflected zenith angle, in a spherical coordinate system (rad);  $\phi_r$  is the reflected azimuth angle, in a spherical coordinate system (rad);  $L_r$  is the reflected radiance ( $\text{W m}^{-2} \text{sr}^{-1}$ ); and  $E_i$  is the irradiance, incident flux density ( $\text{W m}^{-2}$ ). Surface albedo can be derived from the BRDF since it is a weighted integral over all angles in the upward hemisphere of the function (Nolan and Liang, 2000; Wanner *et al.*, 1997). Not to be confused with reflectance, which is “the ratio of the radiant exitance ( $M$  [ $\text{W m}^{-2}$ ]) with the irradiance ( $E$  [ $\text{W m}^{-2}$ ])” (Schaepman-Strub *et al.*, 2006), the ‘true’ surface albedo or directional-hemispherical reflectance (DHR) is “the direct beam irradiance at a specified angle and the reflected flux is integrated over the upward hemisphere” (diffuse reflection as opposed to specular reflection) (Figure 2.1) (Nicodemus *et al.*, 1977; Nolan and Liang, 2000; Schaepman-Strub *et al.*, 2006; Serreze and Barry, 2005).

$$\text{DHR} = \rho_{\text{ref}}(\theta_i, \phi_i, 2\pi) = \frac{d\Phi_r(\theta_i, \phi_i, 2\pi)}{d\Phi_i(\theta_i, \phi_i)} \quad (2.2)$$

where  $\rho_{\text{ref}}$  is the reflectance (dimensionless);  $\Phi_r$  is the reflected radiant flux (W); and  $\Phi_i$  is the incident radiant flux (W). However, irradiance at the Earth’s surface is influenced by refraction, scattering, absorption, and reflectance in the atmosphere (e.g. clouds and aerosols) as well as the surrounding surfaces before reaching the surface and this can alter the spectral distribution of the incident shortwave solar radiation (Henneman and Stefan, 1999; Nolan and Liang, 2000). Albedo

measurements made at the Earth's surface, therefore, may contain a significant diffuse component with the downward flux, which is termed the bi-hemispherical reflectance (BHR) (Figure 2.1) (Nicodemus *et al.*, 1977; Nolan and Liang, 2000; Schaepman-Strub *et al.*, 2006).

$$\text{BHR} = \rho_{\text{ref}}(\theta_i, \phi_i, 2\pi; 2\pi) = \frac{d\Phi_r(\theta_i, \phi_i, 2\pi; 2\pi)}{d\Phi_i(\theta_i, \phi_i, 2\pi)} \quad (2.3)$$

To avoid confusion, surface albedo will be referred to as  $\alpha$ .



**Figure 2.1. A visual representation of the DHR and BHR. The broad arrow represents direct beam irradiance while the other arrows represent reflected and incident radiation fields. (Source: Martonchik *et al.*, 2000)**

The surface energy budget consists of the radiation budget and non-radiative energy transfers. The non-radiative transfers of energy include sensible and latent heat fluxes as well as melt and conduction (Serreze and Barry, 2005). Albedo influences the surface energy budget via the radiation budget. The net radiation at the surface ( $F_{\text{net}}$ ) is the sum of the total upwelling and downwelling shortwave and longwave solar radiation:

$$F_{\text{net}} = F_{\text{sw}}(1 - \alpha) + F_{\text{lw}} - \varepsilon\sigma T_s^4 \quad (2.4)$$

where  $F_{\text{sw}}$  is the incoming shortwave radiation flux at the surface ( $\text{W m}^{-2}$ );  $\alpha$  is the surface albedo (dimensionless);  $F_{\text{lw}}$  is the incoming longwave radiation flux (i.e.  $4\mu\text{m}$  to  $300\mu\text{m}$ ) ( $\text{W m}^{-2}$ ); and  $\varepsilon\sigma T_s^4$  is the outgoing longwave radiation flux with  $\varepsilon$  representing the surface emissivity (dimensionless);  $\sigma$  is the Stefan Boltzmann constant ( $5.67 \times 10^{-8} \text{ W m}^{-2} \text{ K}^{-4}$ ); and  $T_s$  is the skin temperature (K) (Serreze and Barry, 2005). Albedo determines how much shortwave radiation is reflected by a natural surface. Snow and ice have high albedos and tend to reflect much of the incoming solar radiation back into the atmosphere. “Even a small change can dramatically modify the amount of incoming solar radiation absorbed, and thus the surface temperature and melt rate through the climate-albedo feedback process” (Massom and Lubin, 2006). For the ice-albedo feedback, if the surface albedo decreases, there is more absorption of solar radiation and the climate warms, which further reduces snow and ice in the Arctic. However, if the climate cooled, snow and ice would increase, which would then increase the surface albedo, and less solar radiation would be absorbed by the surface. This type of

feedback loop is a positive feedback loop meaning it is not a self-regulating system and warming or cooling would continue to increase (Serreze and Barry, 2005).

### **2.2.1 Albedo of snow**

Knowledge of the albedo of snow is essential when modelling the phenology of freshwater ice. The albedo of snow is very high and snow often covers (totally or partially) freshwater lakes in the Arctic and sub-Arctic. Snow is composed of ice crystals and can also have liquid water present during melt. The albedo of fresh snow ranges from 0.70 to 0.90, but as snow begins to melt, the albedo decreases to a range of 0.50 to 0.60 (Grenfell *et al.*, 1994; Grenfell and Perovich, 2004; Serreze and Barry, 2005; Warren, 1982; Wiscombe and Warren, 1980). The reflective properties of snow are determined by age, wetness, presence of impurities, density and composition, solar radiation incident angle, cloud cover, and surface roughness (Gardner and Sharp, 2010; Grenfell *et al.*, 1981; Henneman and Stefan, 1999). The surface albedo of snow is also wavelength dependent (see Section 2.2.3).

Most natural surfaces in nature are anisotropic. Snow tends to be more isotropically scattering than most other natural surfaces in nature, but it still has a strong forward scattering component (Nolin and Liang, 2000). Wiscombe and Warren (1980) found that the absorptive as well as forward scattering properties of snow increases with grain size and grain size increases as the snow ages. Snow is highly reflective in the ultraviolet and visible portions of the electromagnetic spectrum, but much less reflective and more variable/absorptive at near infrared wavelengths (Gardner and Sharp, 2010; Nolin and Liang, 2000; Wiscombe and Warren, 1980). The variability of albedo in the near infrared is also associated with the grain size of the snow (Wiscombe and Warren, 1980). In the near infrared portion of the electromagnetic spectrum, the albedo has the potential to fall by a factor of two or more for snow grains with radii between 50  $\mu\text{m}$  and 1000 $\mu\text{m}$  (Wiscombe and Warren, 1980). It is important to note that snow grains are not inherently spherical, but assuming the snow grains to be spherical in nature (optically equivalent spheres) allows for the Mie theory to be used to determine the single scattering properties (if the individual particles are separate) of snow and ice so long as one knows the radius of the sphere, the wavelength, and the complex refractive index of the medium (Gardner and Sharp, 2010; Grenfell *et al.*, 1994; Mullen and Warren, 1988; Nolin and Liang, 2000; Serreze and Barry, 2005; Warren, 1982; Wiscombe and Warren, 1980). Mugnai and Wiscombe (1980) showed that non-oriented spheroids had very similar scattering results (within 10%) when compared to the scattering results of spheres (Nolan and Liang, 2000). From the single scattering properties, multiple scattering can be determined using radiative transfer approaches such as the delta-Eddington approximation and the Henyey-Greenstein approximation (Aoki *et al.*, 2000;

Serreze and Barry, 2005; Gardner and Sharp, 2010; Wiscombe and Warren, 1980). The dimensionless optical single scattering properties required to determine multiple scattering include the “absorption efficiency; the scattering efficiency; and the asymmetry factor, which is the mean cosine of the scattering angle” (Gardner and Sharp, 2010). Single scattering properties can be used to determine the optical depths for snow and ice as well as the single scattering albedos, but the multiple scattering is needed to determine the broadband surface albedo with the solar zenith angle (Gardner and Sharp, 2010; Nolan and Liang, 2000).

Impurities such as soot or dust affect the albedo of snow and ice for wavelengths less than 0.9 $\mu$ m. This is the portion of the electromagnetic spectrum that is most reflective, which means that impurities will increase the chances of solar radiation being absorbed and, therefore, lower the overall surface albedo (Gardner and Sharp, 2010; Serreze and Barry, 2005). Conway *et al.* (1996) performed a study on the effect that impurities such as volcanic ash, hydrophobic soot (lampblack), and hydrophilic soot (Raven H<sub>2</sub>O) have on the albedo of natural snow. The study found that volcanic ash contributed to a 30-50% reduction in albedo depending on the amount applied and the hydrophilic soot resulted in a 20% albedo reduction. The hydrophobic soot also saw reductions in albedo. The findings of Conway *et al.* (1996) determined that a reduction of 30% in natural snow lead to a 50% increased ablation rate.

The solar zenith angle also influences the surface albedo of snow. As the solar zenith incident angle increases, so does the albedo of the snow (Serreze and Barry, 2005). Smaller zenith angles will increase the interaction of the incoming solar radiation with the snow grains and increase the chances of absorption, whereas larger zenith angles cause a higher likelihood for the solar radiation to be scattered upwards out of the snowpack (Serreze and Barry, 2005). “Surface roughness can also affect surface albedo by decreasing the angle of incidence relative to a flat surface” which is related to the solar zenith angle (Gardner and Sharp, 2010). A slope that is facing toward the sun will have a lower zenith angle and increase the chance of solar radiation being absorbed by the snow grains (Gardner and Sharp, 2010).

### **2.2.2 Albedo of lake ice**

Lake ice albedo is dependent on similar factors that affect snow albedo (i.e. surface roughness, solar radiation incident angle, impurities, and wetness), but the bubble content of ice, the absorption coefficient, ice composition, and the thickness of the ice bubble layer are additional factors that play a significant role in the spectral albedo of ice (Gardner and Sharp, 2010; Henneman and Stefan, 1999;

Mullen and Warren, 1988). The number and size of air bubbles are increasingly important when near the surface of the lake ice (Mullen and Warren, 1988).

The single scattering properties of ice can be found using Mie theory much like they are found for snow grains. The air bubbles within in the ice scatter the incoming shortwave radiation. However, since the air bubbles are contained within an absorbing medium (i.e., the ice), there is concern whether Mie theory is applicable or not (Mullen and Warren, 1988). It was determined that since ice is transparent in the visible spectrum, no absorption can be assumed for the scattering efficiency at shorter wavelengths. At longer wavelengths (greater than  $1.4\mu\text{m}$ ), ice absorbs more incoming solar radiation and Mie theory would produce incorrect results (Mullen and Warren, 1988). However, most light at the longer wavelengths is absorbed before it can be scattered by the bubbles and any reflection is due to specular reflection, but Mie theory is applicable so long as the inverse of the absorption coefficient is much greater than scattering mean free path (Gardner and Sharp, 2010; Mullen and Warren, 1988). As mentioned earlier, the single scattering properties are used to determine the optical depths as well as the single scattering albedo, which are then used to determine the spectral albedo of ice using radiative transfer models (Gardner and Sharp, 2010).

Unlike snow, where grain size had a large influence on albedo, and unlike sea ice, which has brine inclusions, lake ice albedo is governed by the size and distribution of air bubbles within the ice as well as cracks in the ice (Gardner and Sharp, 2010; Mullen and Warren, 1988). In lake ice, scattering is due to the presence of air and absorption by the ice, so information on the bubble size and concentration is required when determining the ice albedo (Mullen and Warren, 1988). Mullen and Warren (1988) found that ice with a bubble density less than  $0.3\text{ mm}^{-3}$  approached albedo values similar to bubble free ice, while bubble densities towards  $9\text{ mm}^{-3}$  began to demonstrate albedos similar to snow. The increase in size and distribution of bubbles in lake ice increases the albedo for shorter wavelengths. Solar radiation with longer wavelengths (greater than  $1\mu\text{m}$ ) is reflected at the surface and is, therefore, controlled by the solar zenith angle and surface roughness of the ice (Gardner and Sharp, 2010; Mullen and Warren, 1988).

### **2.2.3 Cloud effects on snow and lake ice albedo**

Cloud cover is a common feature in the Arctic and sub-Arctic that has an influence on the surface albedo and the amount of shortwave radiation that reaches the surface. The surface albedo and amount of shortwave radiation that reaches the surface is dependent on cloud thickness/cloud type and the cloud distribution (Henneman and Stefan, 1999). One reason why shortwave radiation is reduced as a result of cloud cover is because clouds, on average, have an albedo of 0.55 (Oke, 1978),

but their albedo can even be as high as 0.60 to 0.75 (e.g. for Arctic stratus clouds) (Serreze and Barry, 2005). Of the shortwave radiation that does reach the surface, only a small fraction is absorbed, but clouds do preferentially absorb near infrared radiation (Key *et al.*, 2001; Serreze and Barry, 2005). Since the clouds preferentially absorb the longer wavelengths, the radiation transmitted through the clouds is more diffuse (Serreze and Barry, 2005). Also, with snow cover especially, “attenuation of the downwelling flux by clouds is partially offset for high albedo surfaces due to multiple reflections from the surface to the clouds and back to the surface” (Serreze and Barry, 2005). It is important to remember that surface albedo is dependent on the wavelength and surface type (e.g. vegetation reflects most incoming near infrared radiation). Snow has a very high albedo, reflecting most visible radiation ( $>0.90$ ) compared to approximately 50% of near infrared radiation (Henneman and Stefan, 1999). The spectral reflectance of lake ice is similar to that of snow, but lake ice does not reflect as much incoming shortwave radiation (Grenfell and Perovich, 2004). If clouds are absorbing more near infrared radiation than visible radiation and snow/lake ice albedo reflect shortwave radiation in the visible portion more efficiently, the surface albedo will increase with cloud cover (Grenfell and Perovich, 2004; Key *et al.*, 2001). Key *et al.* (2001) found that cloud cover increased snow albedo by 5-6% when compared to snow albedo retrieved under clear-sky conditions. Grenfell and Perovich (2004) found that cloud cover increased snow albedo by up to 7.7%; deteriorated melting ice by 5.6%; undeteriorated melting ice by 3.7%; and what they described as “blue-green” by 3.6%.

## **2.3 Importance of albedo in lake ice thermodynamics and phenology**

The initial ice formation (freeze-up) is essential to the growth and development of lake ice, and eventual decay/break-up as the winter season progresses. Fresh water reaches maximum density at a temperature around 4°C ( $\sim 1.0 \text{ g cm}^{-3}$ ). Its density will decrease when it warms (or cools) above (or below) that temperature. Pure ice is less dense than water ( $\sim 0.92 \text{ g cm}^{-3}$  at 0°C) and will float on the surface (Oke, 1978, Patrenko and Whitworth, 1999). As water approaches its maximum density, it sinks creating a thermocline with water at its maximum density on the bottom of the lake, and a zone of mixing above the thermocline (Jeffries *et al.*, 2005b; Petrenko and Whitworth, 1999). When the water has become isothermal at 4°C, ice will begin to form at the surface free of a convective current (Barry and Maslanik, 1992; Jeffries *et al.*, 2005b; Gerard, 1990; Petrenko and Whitworth, 1999). In its early stage of formation, the ice is very thin, fragile, and can be easily broken down into small fragments by wind and wave action. When the ice is thin and fragile, it can also be influenced by the inclusion of snow (Jeffries *et al.*, 2005b; Gerard, 1990; Michel and Ramseier, 1971). A number of studies indicate that snow cover is an integral part of lake ice growth (Adams and Roulet, 1980;

Bengtsson, 1986; Duguay *et al.*, 2003; Ménard *et al.*, 2002; and others). Snow cover will insulate the underlying ice sheet, which will delay ice growth (Adams and Roulet, 1980; Bengtsson, 1986; Brown and Duguay, 2010; Ménard *et al.*, 2002). Snow is also capable of depressing the ice sheet below the hydrostatic water line, allowing for water to mix with the snow above the ice sheet, which, therefore, creates snow ice (Adams and Roulet, 1980; Brown and Duguay, 2010; Duguay *et al.*, 2003).

As ice grows, the latent heat of the freezing is conducted from the bottom of the ice sheet to the atmosphere. The lake ice will continue to thicken as long as “the conductive heat flux through the ice is greater than the heat flux from the water to ice” (Leppäranta, 2010). Thicker ice means that there will be a greater distance for the conduction of heat to travel and the ice growth rate will decrease (Leppäranta, 2010). With the ice growth, dissolved salts and gases are excluded from the ice and returned back into the water (Jeffries *et al.*, 2005b). Water has a nucleation level and when the gas content of the water is below the nucleation level, clear bubble-free ice forms. However, if the gas content of the water is above its nucleation level, then the gases are forced out of the solution, and air bubbles are formed in the ice (Jeffries *et al.*, 2005b). The presence of bubbles in the ice changes the optical properties and increases internal scattering. As a consequence, the inclusion of bubbles in lake ice increases albedo. On the other hand, the inclusion of impurities such as sediment or foreign objects decreases the albedo of lake ice (Petrenko and Whitworth, 1999).

As temperatures increase above freezing, the ice and snow begin to melt. Albedo is very important to the break-up process. As the ice becomes isothermal at 0°C, the melt occurs simultaneously at the ice-atmosphere interface and ice-water interface. If snow ice is present, it will be the first ice exposed to incident solar radiation upon the melting of the snow cover. Melt/decay of ice is influenced by the albedo. The albedo is affected by the variable ice crystal structure (Jeffries *et al.*, 2005b). Also, as temperatures increase, the albedo decreases due to the increase in water content and the subsequent absorption of incoming solar radiation. The increase in absorption of solar radiation then adds additional heat to the system and, therefore, increases the rate of melt. This is known as the ice-albedo feedback. Snow ice has a high albedo and can actually slow the break-up process (Jeffries *et al.*, 2005b).

## **2.4 Snow and ice albedo measurements**

Snow and ice comprise large portions of the Northern and Southern Hemisphere during the winter season. Therefore, the measurement of snow and ice albedo is essential to better understand the global energy budget. Surface albedo is very scale-dependent; meaning, a large area may be a heterogeneous surface containing more than one surface type (more than one surface albedo) (Serreze

and Barry, 2005). Ground-based observations of surface albedo are measured with upward and downward facing pyranometers. However, it is impractical to measure the global energy budget with just ground-based measurements. For this reason, advances have been made using satellite data (e.g. Advanced Very High Resolution Radiometer (AVHRR), Multi-angle Imaging SpectroRadiometer (MISR), and MODIS). Ground-based observations are, nonetheless, still required to validate the satellite albedo estimates. Ground-based networks such as the National Oceanic and Atmospheric Administration's (NOAA) Surface Radiation Budget Network (SURFRAD), which "provide long-term measurements of the surface radiation budget over the United States" (*Surface Radiation Budget Monitoring*, n.d.), do exist, but it is difficult to provide long-term measurements over lake ice due to melt, and therefore, radiation measurements over freshwater lake ice do not exist. Therefore, ground-based measurements of surface radiation over freshwater lake surfaces are still needed for the validation of satellite estimates. Also, satellite estimates of surface albedo can be used for more than just understanding the global surface energy budget. If integrated into lake ice models, the satellite estimates are capable of providing on-site albedo estimation over lake ice to assist with ice simulation. The following sections provide a review of ground-based measurements of snow and ice albedo (specifically over lake ice) and validation studies for the MODIS daily albedo products (MOD10A1 and MYD10A1), as well as the MODIS 16-day albedo product (MCD43A3).

### **2.4.1 Ground-based measurements**

Ground-based measurements are required to better understand the global surface energy budget and validate satellite estimates. Radiation measurements at the surface are made usually with pyranometers, but can be measured using field spectroradiometers that cover the shortwave portion of the electromagnetic spectrum (Grenfell and Perovich, 2004). By measuring upwelling and downwelling radiation flux (downward and upward facing pyranometers), the surface albedo can be obtained. A pyranometer measures the average flux density (irradiance if upward facing and radiant exitance if downward facing) in  $\text{W m}^{-2}$ . Surface albedo, expressed as a value between 0 and 1, is then calculated as radiant exitance divided by irradiance.

Snow, as mentioned earlier (Section 2.2.1), has very high albedos compared to other natural surfaces. The albedo of fresh snow ranges from 0.70 to 0.90, but as snow begins to melt, the albedo decreases to a range of 0.50 to 0.60. The albedo of lake ice has been found to vary depending on its composition. Heron and Woo (1994) acquired albedo observations on a high Arctic freshwater lake near Resolute, Nunavut and found that the albedo of bare ice increased from 0.15 to 0.50 due to increased surface porosity. A maximum ice albedo value of 0.56 was recorded "when the hydrostatic

**Table 2.1. Summary of recorded lake ice albedo collected from previous measurement studies.**

Location of <i>in situ</i> measurements	Lake ice albedo	Reference
Great Lakes	Snow ice: 0.39-0.46 Refrozen slush: 0.35-0.46	Bolsenga (1977)
Imikpuk Lake, near Barrow, Alaska	Bare ice albedo was ~0.30	Grenfell and Perovich (2004)
Freshwater lake near Minnesota	Lake ice albedo was 0.38 following snowmelt	Henneman and Stefan (1999)
Freshwater lake near Resolute, Nunavut	Bare ice albedo ranged from 0.15 to 0.50	Heron and Woo (1994)

water level was at its lowest beneath the surface of the ice, and when the surface ice reached minimum densities” (Heron and Woo, 1994). Heron and Woo (1994) also found in their study that the ice albedo decreased from 0.45 to 0.20 during melt and this was due to the removal of the c-axis vertical crystals. The c-axis is perpendicular to the basal plane of the ice-crystalline structure and Knight (1962) found that ice with a horizontal (to ice growth) c-axis was ‘darker’ or, in other words, had a lower albedo. With the horizontal c-axis crystals now exposed, internal melt began to occur and albedo values increased to 0.30 (Heron and Woo, 1994). On the Great Lakes, Bolsenga (1977) found snow ice to have albedo values between 0.39 and 0.46, while frozen slush had albedo values between 0.35 and 0.46 with the exception of a 0.58 value that was due to granular snow adhering to the surface of the ice. The albedo values in Bolsenga’s (1977) study ranged from 0.10 (clear ice) to 0.46 (snow ice). Snow ice was defined as milky-white in colour that has many bubbles of various sizes present (Bolsenga, 1977). The formation is due to snow cover on the surface of the ice and water seepage through stress cracks that wets the snow before being refrozen. The refrozen slush is formed by snow cover on the lake that becomes slush and is refrozen into a “snow-ice-like” substance (Bolsenga, 1977). Henneman and Stefan (1999) completed a study over a freshwater lake in Minnesota. They reported that the lake ice albedo was 0.38 once the snow had melted, which was a decrease from the average albedo of 0.83 after a new snowfall. Grenfell and Perovich (2004) acquired albedo over a snow-ice-land-ocean regime near Barrow, Alaska. Imikpuk Lake was one of the study sites where they collected albedo using a spectroradiometer. Spectral and wavelength-integrated albedos were measured along 200 m transects to gain knowledge of the spatial variability and average. Grenfell and Perovich (2004) noted that the structure of the lake ice was much different than that of sea ice due to the lack of submillimeter inhomogeneities caused by the brine inclusions in

the sea ice. The lack of brine inclusions in the lake ice decreased the volume scattering within the ice significantly and produced lower albedos over bare ice and thin snow cover (Grenfell and Perovich, 2004). There were portions of bare ice on Imikpuk Lake, due to wind scouring, which produced albedo values around 0.30 (Grenfell and Perovich, 2004).

## **2.4.2 Satellite estimates**

Surface albedo has been derived from various satellite missions (e.g. AVHRR Polar Pathfinder [APP-x], MISR, and Meteosat Visible and Infrared Imager [MVISI]); however, a specific focus is placed on the MODIS albedo products MOD10A1, MYD10A1, and MCD43A3, because they are products used in this thesis.

### **2.4.2.1 Daily albedo products**

MOD10A1 (Terra) and MYD10A1 (Aqua) snow cover daily L3 global 500 m gridded products provide daily albedo retrievals under clear sky conditions (Klein and Stroeve, 2002). Using bands 1 to 7 for MOD10A1 and bands 1 to 5, 7 for MYD10A1 (the detectors for band 6 on Aqua failed shortly after launch), the daily albedo algorithm performs a number of operations to retrieve snow albedo from the Earth's surface. Each pixel is determined to be cloud-free using the MODIS cloud mask (MOD35) and snow covered using a snow-mapping algorithm (MOD10) before albedo is retrieved (Ackerman *et al.*, 1997; Hall *et al.*, 2001). The anisotropic scattering for snow is corrected using a discrete-ordinate radiative transfer (DISORT) model (Klein and Stroeve, 2002; Stamnes *et al.*, 1988). Once the anisotropic scattering for snow is corrected, the spectral albedo measurements are converted from narrowband to broadband albedo using methods outlined by Liang (2000) (Hall and Riggs, 2007). The final product (albedo) is a linear combination of DHR (black sky albedo [BSA]) and BHR (white sky albedo [WSA]) (Stroeve *et al.*, 2006).

The MODIS daily albedo products have been validated over different snow-covered environments, but no validation studies have been performed over freshwater lake ice. Previous validation efforts for the MODIS daily albedo products are summarized in Table 2.2. The albedo algorithm developed by Klein and Stroeve (2002) was evaluated against *in situ* measurements part of the SURFRAD network located in Fort Peck, Montana. Initially, the MODIS daily products involved just the Terra satellite (MOD10A1) and many of the existing validation studies were done on only MOD10A1 (with the exception of Stroeve *et al.*, 2006). Klein and Stroeve (2002) found the maximum difference between MOD10A1 and *in situ* albedo measurements to be 15%. When

**Table 2.2. Summary of the validation studies performed for MOD10A1 and MYD10A1.**

Location of <i>in situ</i> measurements	Validation results	Reference
Fort Peck, MT	Maximum difference of 15% and 1-8% between ‘better’ retrievals (MOD10A1)	Klein and Stroeve (2002)
Greenland	RMSE of 0.067 (MOD10A1) and 0.075 (MYD10A1)	Stroeve <i>et al.</i> (2006)
Karasu basin, Turkey	Overestimated <i>in situ</i> measurements by 10% (MOD10A1)	Tekeli <i>et al.</i> (2006)
Karasu basin, Turkey	Overestimated <i>in situ</i> measurements by 10% (MOD10A1)	Şorman <i>et al.</i> (2007)
North Park, CO, USA and Namco, Tibetan Plateau, China	RMSE of 0.064 and MAE of 0.052 (MOD10A1)	Malik <i>et al.</i> (2011)

compared to what they considered the “best” albedo retrievals by MOD10A1, the differences compared with *in situ* measurements were between 1% and 8%. Over the Greenland ice sheet, Stroeve *et al.* (2006) found MOD10A1 to have a root mean square error (RMSE) of 0.067 and MYD10A1 to have an RMSE of 0.075 when evaluated with *in situ* measurements. Tekeli *et al.* (2006) and Şorman *et al.* (2007) both validated MOD10A1 against *in situ* albedo measurements acquired in the Karasu basin, Turkey (a mountainous region). Both studies found MOD10A1 to overestimate *in situ* snow albedo by 10%; both studies found better agreement between MOD10A1 and *in situ* measurements at higher elevations; and both studies believed discrepancies may have been attributed to the collection of *in situ* measurements at different times than the MOD10A1 acquisitions along with temperatures near the freezing temperature influencing snow albedo throughout the day (Şorman *et al.*, 2007; Tekeli *et al.*, 2006). The agreement between MOD10A1 albedo and higher elevation *in situ* albedo measurements was due to a more stable (cold) temperature at the higher elevations (Şorman *et al.*, 2007; Tekeli *et al.*, 2006). Although it was not the purpose of the study, Malik *et al.* (2011) did note MOD10A1 having an RMSE and a mean absolute error (MAE) of 0.064 and 0.052, respectively, when presenting their approach for estimating broadband albedo of snow. Malik *et al.* (2011) gathered *in situ* measurements in North Park, Colorado, USA and Namco, Tibetan Plateau, China. Both sites were said to be within areas of low relief with vegetation typical of prairie and tundra environments.

Although the methods for determining error varied between each validation study (e.g. difference (%), RMSE, MAE), the general consensus was that the MODIS daily products within

MOD10A1 and MYD10A1 were capable of retrieving within 0.10 of *in situ* measurements over different snow-covered environments. While there are some concerns on accuracy associated with the product's algorithm (see Stroeve *et al.*, 2006 for details), the errors associated with the retrieval of surface albedo via the MODIS daily products will be further developed in Chapters 3 and 4. The MODIS daily albedo products perform well over snow, but they have not been evaluated over lake ice in northern environments as of yet.

### 2.4.2.2 16-day albedo product

The MODIS BRDF/albedo L3 global product (MCD43) provides albedo maps as 500 m and 1 km spatial resolutions. MCD43 is derived from a combination of the MODIS sensors aboard the Terra and Aqua satellites. The MCD43A3 is a 16-day 500 m albedo product in a sinusoidal grid projection that provides updated albedo retrievals every eight days (Schaaf *et al.*, 2002). Like the MODIS daily products (MOD10A1/MYD10A1), MCD43A3 only retrieves albedo under clear sky conditions using the MODIS bands 1 to 7 (Schaaf *et al.*, 2002). The algorithm used by the MCD43 product is a kernel-driving Ross Thick-Li Sparse Reciprocal (RTLSR) BRDF model that describes the reflectance anisotropy (Schaaf *et al.*, 2002; Wang *et al.*, 2012). The MCD43A3 product provides the already derived albedo computations from the BRDF model needed to retrieve the albedo for a surface. MCD43 BRDF/albedo uses sequential multi-angle observations over 16 days to derive the estimates. Of the 16-day period, high quality full inversion retrieval requires at least seven cloud-free pixels that have been quality checked. Otherwise, a backup algorithm (magnitude inversion) is used (Schaaf *et al.*, 2002; Wang *et al.*, 2012). Unlike the MODIS daily products (MOD10A1/MYD10A1) which use a linear combination of BSA and WSA, the MCD43A3 provides BSA and WSA products separately. BSA is used in this thesis instead of the WSA, because the WSA simulates pure diffuse isotropic incident radiation, which is representative of thick cloud cover (Schaeppman-Strub *et al.*, 2006). Incoming shortwave radiation is influenced by the atmosphere, but it will be assumed that these influences are negligible and that the BSA (DHR) will accurately represent the surface albedo. The actual albedo could be calculated by combining the BSA and WSA, as seen with the MODIS daily products, but Stroeve *et al.* (2005) note that the appropriate atmospheric optical depth information should be obtained and these data were not available for this thesis.

There have been limited validation studies for MCD43 BRDF/albedo products over snow-covered areas (Stroeve *et al.*, 2005; Wang *et al.* 2012), but there have been numerous land surface validation studies over snow-free environments (Jin *et al.*, 2003; Liang *et al.*, 2002; Liu *et al.*, 2009; Salomon *et al.*, 2006; and Wang *et al.*, 2004, 2010). The validation studies performed over snow-free

environments include surface types such as grasslands, natural vegetation covers, diverse soils, crops, and man-made objects. When using the main full inversion algorithm, these studies usually fall within 5% of *in situ* measurements while retrievals with the backup magnitude inversion algorithm are less accurate, but still within 8-11%. These studies show that the MCD43 albedo retrievals are fairly accurate, but snow-covered environments produce much higher albedo values and have a strong forward scattering component. Snow-cover is arguably more homogenous than other surface types when depths are large enough as well, which would increase the accuracy of the evaluations since the large spatial areas covered by the MCD43A3 product would be more representative of the relatively small footprints of *in situ* measurements.

The available validation studies for the MCD43 products over snow are summarized in Table 2.3. Initially, the MCD43 products only utilized the Terra satellite and were labelled MOD43. The validation study done by Stroeve *et al.* (2005) used the MOD43B3 product. MOD43B3 is the Terra-only albedo product with a 1 km spatial resolution. Stroeve *et al.* (2005) evaluated the BSA and WSA against all sky and clear sky conditions for 20 different sites located throughout the Greenland ice sheet. The RMSE for the BSA and WSA evaluated against the *in situ* measurements for both all sky and clear sky were within 0.10. Stroeve *et al.* (2005) report the RMSE for clear sky BSA retrievals to be 0.07. The RMSE for the clear sky BSA retrievals using only the full inversion algorithm reduces to 0.04. Wang *et al.* (2012) performed their validation study using *in situ* albedo measurements from the Atmospheric Radiation Measurement Program (ARM) located on the North Slope of Alaska (over snow-covered tundra). The purpose of the validation study was to evaluate two new Direct Broadcast MCD43A BRDF/albedo products (MCD43 16-day daily and MCD43 1-day daily) presented in Shuai (2010), but they also evaluated a modified MCD43A1 BRDF/albedo product as well. The MCD43A1 utilizes both the Terra and Aqua satellites. Adding Aqua to the algorithm increases the number of observations available allowing the full inversion algorithm to be utilized more frequently (Salomon *et al.*, 2006). MCD43A1 has the same 500 m spatial resolution as

**Table 2.3. Summary of the validation studies performed for the MCD43 products.**

Location of <i>in situ</i> measurements	Validation results	Reference
Greenland	RMSE of 0.07 (0.04 without the backup algorithm) (MOD43B3)	Stroeve <i>et al.</i> (2005)
North Slope of Alaska	RMSE of 0.045 (MCD43A1*)	Wang <i>et al.</i> (2012)

**\*MCD43A1 was modified to use the solar zenith angle (SZA) at the end of the 16-day period.**

the MCD43A3 product, but the albedo needs to be computed separately. The modified aspect of the MCD43A1 product used in Wang *et al.* (2012) is that the solar zenith angle at the end of the 16-day period is used rather than at the beginning of the 16-day period to better represent the new products being introduced. Furthermore, Wang *et al.* (2012) used the actual (or Blue Sky) albedo which is a combination of the BSA and WSA. The modified MCD43A1 albedo retrievals evaluated against the *in situ* albedo measurements for snow over tundra had an RMSE of 0.045. Although the studies over snow have been limited, the MCD43A3 products have been shown to perform well in retrieving albedo over land and snow. Like the Daily albedo products, the MCD43 products have not been evaluated over lake ice.

## 2.5 Canadian Lake Ice Model

CLIMo simulates lake ice growth and phenology to examine the sensitivity of lake ice to climatic variability and change (Duguay *et al.*, 2003). Previous studies have found that CLIMo accurately simulates the growth and duration of lake ice (Brown and Duguay, 2011a, 2011b; Duguay *et al.*, 2003; Jeffries *et al.*, 2005a; Morris *et al.*, 2005; and Ménard *et al.*, 2002). Brown and Duguay (2011a) mention that the surface albedo parameterization does not currently take the albedo of snow ice into consideration and that the albedo parameterization is an area of the model that could be improved. The integration of the aforementioned MODIS albedo products into CLIMo could lead to an improvement of the representation of snow/ice albedo required for the modelling of lake ice. The following section provides a description of CLIMo and its albedo parameterization scheme.

### 2.5.1 General description

This description of the CLIMo illustrates the types of processes used to model lake ice, as well as how albedo is integrated into the computation. CLIMo (Duguay *et al.*, 2003) is a modification of the one-dimensional thermodynamic sea-ice model of Flato and Brown (1996). Flato and Brown (1996) based their model on a one-dimensional unsteady heat conduction equation presented by Maykut and Untersteiner (1971):

$$\rho C_p \frac{\partial T}{\partial t} = \frac{\partial}{\partial z} k \frac{\partial T}{\partial z} + F_{sw} I_0 (1 - \alpha) K e^{-Kz} \quad (2.5)$$

where  $\rho$  is the density ( $\text{kg m}^{-3}$ );  $C_p$  is the specific heat capacity ( $\text{J kg}^{-1} \text{K}^{-1}$ );  $T$  is the temperature (K) within the ice or snow;  $t$  is time (s);  $z$  is the vertical coordinate, positive downward (m);  $k$  is the thermal conductivity ( $\text{W m}^{-1} \text{K}^{-1}$ );  $F_{sw}$  is the downwelling shortwave radiative energy flux ( $\text{W m}^{-2}$ );  $I_0$  is the fraction of shortwave radiation flux that penetrates the surface ( $\text{W m}^{-2}$ );  $\alpha$  is the surface albedo

(dimensionless); and  $K$  is the bulk extinction coefficient for penetrating shortwave radiation (Duguay *et al.*, 2003). Equation (2.5) is subject to boundary conditions at the surface and ice underside. At the ice underside:

$$T(h, t) = T_f \quad (2.6)$$

where  $h$  is the total ice and snow thickness (m) and  $T_f$  is the freezing temperature of fresh water (273.15 K). This ensures that the ice-water interface is always at the freezing point (Duguay *et al.*, 2003). The upper surface boundary is defined by:

$$\begin{aligned} T(0, t) &= T_m & F_0 > 0, \hat{T}(0) \geq T_m \\ k \frac{\partial T}{\partial z} \Big|_{z=0} &= F_0 & \text{otherwise} \end{aligned} \quad (2.7)$$

where  $T_m$  is the melting temperature at the surface (also 273.15 K);  $F_0$  is the net heat flux absorbed at the surface ( $\text{W m}^{-2}$ ); and  $\hat{T}$  is the estimated temperature (K) prior to solving Equation (2.5). Equation (2.7) “states that the upper surface boundary condition is the net surface heat flux, obtained from the surface energy budget calculation (2.8) except when the surface is melting” (Duguay *et al.*, 2003). A generalized Crank-Nicholson, finite difference scheme is the numerical scheme used to solve for the heat conduction equations (2.5 to 2.7). A more in depth definition of the Crank-Nicholson, finite difference scheme can be found in Flato and Brown (1996).

The surface energy budget is expressed as:

$$F_0 = F_{lw} - \varepsilon \sigma T^4(0, t) + (1 - \alpha)(1 - I_o)F_{sw} + F_{lat} + F_{sens} \quad (2.8)$$

where  $\varepsilon$  is the surface emissivity;  $\sigma$  is the Stefan-Boltzmann constant ( $5.67 \times 10^{-8} \text{ W m}^{-2} \text{ K}^{-4}$ );  $F_{lw}$ ,  $F_{lat}$ , and  $F_{sens}$  are the downwelling longwave radiative energy flux ( $\text{W m}^{-2}$ ), the downward latent heat flux ( $\text{W m}^{-2}$ ), and the downward sensible heat flux ( $\text{W m}^{-2}$ ), respectively (Duguay *et al.*, 2003). With the exception of the downwelling longwave radiative energy flux, all terms in the surface energy budget (2.8) are dependent on the surface temperature (Duguay *et al.*, 2003). The surface temperature is found using a Newton-Raphson scheme (Duguay *et al.*, 2003).

For an annual cycle to occur where ice will completely melt away during the summer, a fixed-depth mixed layer is included in CLIMo (Duguay *et al.*, 2003). When ice is present, the mixed layer temperature is kept at the freezing point, and when the ice is absent, the temperature of the mixed layer is computed from the surface energy balance:

$$\rho_w C_{pw} d_{mix} \frac{\partial T_{mix}}{\partial t} = F_0 + F_{sw} I_0 (1 - \alpha) \quad (2.9)$$

where  $\rho_w$  is the density of water ( $1000 \text{ kg m}^{-3}$ );  $C_{pw}$  is the specific heat capacity of water ( $\text{J kg}^{-1} \text{ K}^{-1}$ );  $d_{mix}$  is the effective mixed layer depth (m); and  $T_{mix}$  is the mixed layer temperature (K) (Duguay *et al.*,

2003). Shallow lakes are often isothermal and well mixed, so  $d_{\text{mix}}$  can be designated as good approximating for the effect of lake depth leading up to freeze-up (Duguay *et al.*, 2003). Larger lakes are a bit more complex since the effective mixed layer depth usually ends at the thermocline instead of the lake bottom.

“Growth and melt at the ice underside are computed from the difference between the conductive heat flux into the ice and the heat flux out of the upper surface of the mixed layer” (Duguay *et al.*, 2003):

$$\left. \frac{\partial h_i}{\partial t} \right|_{z=h} = \left( k \left. \frac{\partial T}{\partial z} \right|_{z=h} - \int_h^\infty F_{\text{sw}} I_0 (1 - \alpha) K e^{-Kz} dz \right) \frac{1}{L_{\text{fi}}} \quad (2.10)$$

where  $h_i$  is the ice thickness (m) and  $L_{\text{fi}}$  is the volumetric heat of fusion of freshwater ice ( $3.045 \times 10^8 \text{ J m}^{-3}$ ). Any shortwave radiation that penetrates through the snow and ice is assumed to be absorbed by the mixed layer and then returned to the ice underside again to keep the temperature of the mixed layer equal to  $T_f$  (Duguay *et al.*, 2003).

“Melt at the upper surface is computed from the difference between the conductive flux and the net surface flux; any snow is melted first and the remaining heat is used to melt the ice” (Duguay *et al.*, 2003):

$$\left. \frac{\partial h_s}{\partial t} \right|_{z=0} = \left( F_0 - k \left. \frac{\partial T}{\partial z} \right|_{z=0} \right) \frac{1}{L_{\text{fs}}} \quad h_s > 0 \quad (2.11)$$

$$\left. \frac{\partial h_i}{\partial t} \right|_{z=0} = \left( F_0 - k \left. \frac{\partial T}{\partial z} \right|_{z=0} \right) \frac{1}{L_{\text{fi}}} \quad h_s = 0 \quad (2.12)$$

where  $h_s$  is the snow depth (m) and  $L_{\text{fi}}$  is the volumetric heat of fusion of snow ( $1.097 \times 10^8 \text{ J m}^{-3}$ ). Other factors that affect the ice thickness (e.g. the addition of snow ice) and a more detailed description of CLIMo and its parameterizations can be found in Duguay *et al.* (2003), Ebert and Curry (1993), and Flato and Brown (1996).

The atmospheric input variables required by CLIMo are mean daily air temperature, relative humidity, cloud amount, wind speed, and snowfall amount (Duguay *et al.*, 2003). These data can be collected from local meteorological stations with the exception of cloud cover which can be usually collected from airport stations. The daily output variables are energy balance components, snow depth, a temperature profile throughout the ice/snow (or water temperature in the absence of ice), and ice thickness (both clear and snow ice). Other output variables include the freeze-up (ice-on) date, break-up (ice-off) date, and end-of-season clear/snow/total ice thickness (Duguay *et al.*, 2003).

Albedo is important to the evaluation of the surface energy balance as well as for determining the timing of break-up. It is also required for modelling properly the energy exchange via insolation at the surface. The albedo parameterization scheme of CLIMo is described below.

## 2.5.2 Albedo parameterization scheme

Many of the parameterizations used in CLIMo can be found in Ebert and Curry (1993), and Duguay *et al.* (2003). For this study, interest is placed on the parameterization of surface albedo. The surface albedo parameterization takes the surface type (ice, snow, and open water), surface temperature, and ice thickness into account (Duguay *et al.*, 2003). The cold ice parameterization, i.e., temperatures below freezing, is taken from Maykut (1982), while the melting ice parameterization is based on ice observations from Heron and Woo (1994) (Duguay *et al.*, 2003). The surface albedo parameterization scheme is expressed as follows:

$$\alpha = \begin{cases} \alpha_{ow} & h_i < h_{min} \\ \min[\alpha_s, \alpha_i + h(\alpha_s - \alpha_i)/c_1] & h_i \geq h_{min} \quad h_i \leq c_1 \\ \alpha_s & h_i \geq h_{min} \quad h_s > c_1 \end{cases} \quad (2.13)$$

$$\alpha_i = \begin{cases} \max(\alpha_{ow}, c_2 h_i^{0.28} + 0.08) & T(0, t) < T_m \\ \min(\alpha_{mi}, c_3 h_i^2 + \alpha_{ow}) & T(0, t) = T_m \end{cases} \quad (2.14)$$

$$\alpha_s = \begin{cases} 0.75T(0, t) & < T_m \\ 0.65T(0, t) & = T_m \end{cases} \quad (2.15)$$

where  $\alpha$  is surface albedo;  $\alpha_{ow}$  is albedo of open water, equal to 0.06;  $\alpha_s$  is albedo of snow;  $\alpha_{mi}$  is the albedo of melting ice, equal to 0.55;  $h_{min}$  is minimum ice thickness below which open water is assumed, equal to 0.001 m;  $T(0, t)$  is the surface temperature (K) at the time (s);  $c_1$  is a constant equal to 0.1 m;  $c_2$  is a constant equal to 0.44 m; and  $c_3$  is a constant equal to 0.075 m. Equation (2.13) illustrates that the surface albedo is equal to the albedo of open water; a minimum function of the albedo of snow and a derived albedo value; or the albedo of snow depending on whether certain criteria are met. Equations (2.14) and (2.15) determine the values of ice albedo and snow albedo, respectively, depending on the temperature of the surface at a given time in relation to the parameter that represents the melting temperature at the surface.

## 2.6 Summary

Surface albedo is an important part of the surface energy balance in that it allows for the determination of how much shortwave radiation is absorbed and reflected. The surface albedos of snow and lake ice are affected by factors that are not easily modelled (e.g. impurities, and density and composition). Clouds also have an effect on snow and lake ice albedo due to albedo's spectral dependence. Lake ice is most affected by the high albedo of snow on top of the lake ice as well as the ice albedo itself, which are capable of delaying the break-up of lake ice during spring melt. These high albedos delay the melt process by reflecting incoming energy; however, the albedo of the snow and ice degrades during this warming trend as well and this degradation needs to be accounted for in the modelling of lake ice.

The integration of MODIS albedo products (MOD10A1, MYD10A1, and MCD43A3) presents an interesting prospect for the improvement of CLIMo simulations. Ground observations have found that the albedo of lake ice can vary greatly depending on the type of ice present (clear or snow ice) and whether snow is present or absent. Validation efforts need to be undertaken for the MODIS albedo products over lake ice before they can be used for integration in a lake ice model (Chapter 3); however, the products have been shown to perform well over snow-covered land retrieval albedo values within 0.10 of *in situ* observations. CLIMo was presented as a candidate model for the integration of the MODIS albedo products. This is explored in Chapter 4.

# Chapter 3

## Evaluation of the Canadian Lake Ice Model albedo parameterization and MODIS albedo retrievals

### Overview

*In situ* snow and ice albedo observations were taken over a partially snow covered freshwater lake near Churchill, Manitoba for the evaluation of Moderate Resolution Imaging Spectrometer (MODIS) albedo products (MOD10A1/MYD10A1 and MCD43A3) and albedo parameterization of the Canadian Lake Ice Model (CLIMo). Accurate simulations of freshwater lake ice are integral for the study of climatic variability in northern environments. Surface albedo has been shown to affect the timing of ice break-up during the melt season. Results show that the MODIS albedo products perform well when compared with *in situ* snow and ice albedo observations. Albedo products MOD10A1, MYD10A1, and MCD43A3 retrieved snow and ice albedo with root-mean-square-error (RMSE) values of 0.07, 0.08, and 0.06, respectively, compared to average *in situ* albedo observations. CLIMo's albedo compared well with *in situ* albedo observations retrieved over snow-covered ice with a RMSE of 0.07. CLIMo's cold ice parameterization, however, overestimated both clear and snow ice *in situ* albedo observations. The MODIS albedo products were then used to evaluate CLIMo's melting ice parameterization during the melt season. Results indicate that CLIMo's albedo estimates have an average difference of at least 0.14 compared with the MODIS albedo observations during melt. The quality of the albedo retrievals over lake ice from MODIS and the need for more accurate albedo simulations during the melt season suggest that direct insertion of the MODIS albedo products into CLIMo would be beneficial.

### 3.1 Introduction

The Canadian Arctic/sub-Arctic and other high latitude regions of the Northern Hemisphere are covered by numerous lakes. These lakes can range in size from small (shallow) lakes that cover a significant fraction of the landscape, to very large (deep) lakes. The latter are less abundant but have

been shown to have a significant impact on weather and climate at local and regional scales (Brown and Duguay, 2010; Schertzer, 1997). The thermal properties of water make lakes very important stores and transfers of energy and moisture. Water has a high specific heat capacity; therefore, large lakes are able to store large quantities of heat. Shallow lakes, however, have a much shorter thermal turnover than larger lakes on the magnitude of a couple weeks versus several months (Duguay *et al.*, 2003; Schertzer, 1997). The presence (or absence) of ice and snow on these lakes plays a very important role in their energy and water balances (Brown and Duguay, 2010). An important characteristic of snow and ice is their high albedo or their ability to reflect large portions of incoming shortwave radiation back to the atmosphere (Oke, 1978). Water has an albedo of 0.05 – 0.10 (that notably varies with zenith angle), whereas freshwater ice and snow have albedos ranging from 0.15 – 0.60 and 0.50 – 0.95, respectively (Bolsenga, 1977; Grenfell *et al.*, 1994; Heron and Woo, 1994; Serreze and Barry, 2005; Warren, 1982; Wiscombe and Warren, 1980). The range in albedo values depends on a number of factors such as zenith angle, age of the ice and snow, composition of the ice and snow, cloud cover, and impurities present (Gardner and Sharp, 2010; Serreze and Barry, 2005). One-dimensional thermodynamic lake ice models that simulate lake ice phenology incorporate snow and ice albedo into their derivations. However, existing lake ice models often simplify or neglect the aforementioned factors that affect snow and ice surface albedo in their parameterizations.

One-dimensional (1-D) lake models such as FLake (Mironov, 2008) and Hostetler *et al.* (1993) as well as 1-D lake ice models such as the lake ice model-numerical operational simulation (LIMNOS) (Vavrus *et al.*, 1996), a lake ice model developed by Launiainen and Cheng (1998), and the Canadian Lake Ice Model (CLIMo) (Duguay *et al.*, 2003) exist to “simulate lake ice growth and examine the sensitivity of ice phenology to climatic change [*sic*]” (Duguay *et al.*, 2003). Their albedo parameterizations are usually based on albedo observations obtained from previous studies and attempt to account for seasonal variations in albedo through changes in surface temperature and surface type. The one-dimensional thermodynamic lake ice model used in this study is CLIMo (Duguay *et al.*, 2003). CLIMo’s albedo parameterization depends on surface type (ice, snow, or open water), surface temperature (melting versus subfreezing), and ice thickness (Duguay *et al.*, 2003). This model uses a cold ice parameterization (Maykut, 1982) and a melting ice parameterization derived from high Arctic lake ice observations from Heron and Woo (1994) (Duguay *et al.*, 2003). With the recent development of remote sensing albedo products such as the MOD10A1/MYD10A1 daily snow albedo products (Klein and Stroeve, 2002; Riggs *et al.*, 2006) and the MCD43A3 16-day albedo product (Schaaf *et al.*, 2002), the potential to integrate remote sensing products in 1-D lake and lake ice models is emerging as an interesting prospect.

Previous efforts to validate the aforementioned MODIS albedo products have been made (Klein and Stroeve, 2002; Şorman *et al.*, 2007; Stroeve *et al.*, 2005; Stroeve *et al.*, 2006; Wang *et al.*, 2012), but no validation efforts have been performed over lake ice. This study focuses on the evaluation of CLIMo's albedo parameterization and MODIS retrieved albedo values with *in situ* albedo measurements collected over snow and ice on Malcolm Ramsay Lake near Churchill, Manitoba from February 15<sup>th</sup> to April 25<sup>th</sup>, 2012. CLIMo's albedo parameterization and the MODIS retrieved albedos are also compared against each other for the ice growth period as well as the ice break-up period to assess CLIMo's ability to simulate the temporal evolution of snow and ice albedo throughout an ice season on Malcolm Ramsay Lake.

## 3.2 Data and methods

### 3.2.1 Study area

#### 3.2.1.1 Malcolm Ramsay Lake

Malcolm Ramsay Lake is located near Churchill, Manitoba (58°45'N, 94°04'W) and is situated near the coast of Hudson Bay (Figure 3.1). The lake has a surface area of approximately 2.0 km<sup>2</sup> and a mean depth of 2.4 m with a maximum depth of 3.2 m (Duguay *et al.*, 2003). The mean annual air temperature (1971 to 2000) recorded for Churchill is -6.9°C with its coldest month being January (-26.7°C) and its warmest month being July (12.0°C). The average precipitation for each year is 432 mm with 44% falling as snow annually (<http://www.climate.weatheroffice.gc.ca/>). Malcolm Ramsay Lake is located at the northern limit of the tree-line and has a tundra-like landscape with areas of open forest, forest-tundra transition, and tundra, and is representative of the surrounding shallow lakes found throughout the Hudson Bay Lowlands (Duguay *et al.*, 2003). This lake was selected, because it is large enough to be seen in the MODIS products (which have a 500 m spatial resolution); it completely freezes over each year; and has been the subject of previous studies for the validation and evaluation of CLIMo (Brown and Duguay, 2011a; Duguay *et al.*, 2003).

At Malcolm Ramsay Lake, air temperatures (°C), relative humidity (%), wind speed (m s<sup>-1</sup>), and net shortwave radiation (both incoming/outgoing for shortwave/longwave radiation) (W m<sup>-2</sup>) were measured. The air temperature, relative humidity, and wind speed are some of the atmospheric forcing variables required as input for CLIMo (discussed in Section 3.2.3) and net shortwave radiation is required for the evaluation of the albedo parameterization and MODIS albedo products in this study.

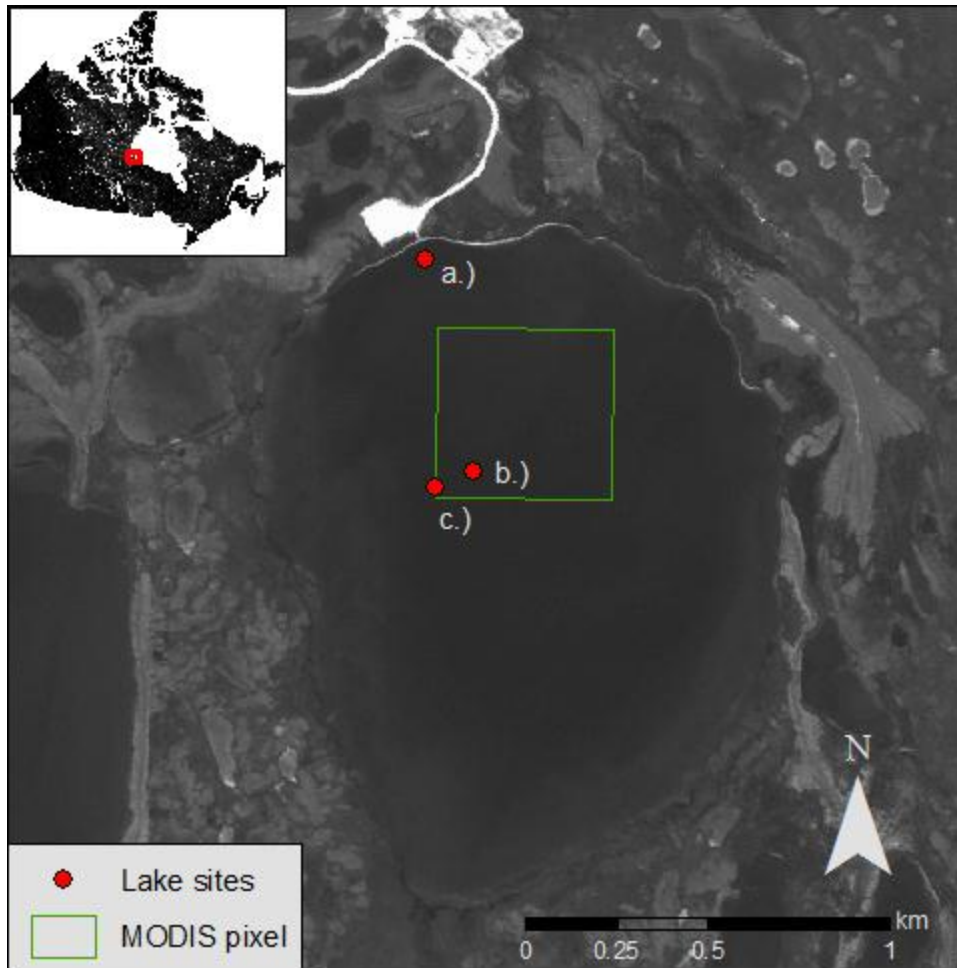


**Figure 3.1. Location of the pyranometer stations and spatial coverage of the MODIS pixel on Malcolm Ramsay Lake.**

From September through to May, historical climate records (1971 to 2000) show that Churchill has an average temperature of  $-12.5^{\circ}\text{C}$  and an average total snowfall of 187.5 cm. During the 2011-2012 winter (September to May), Churchill experienced an average temperature of  $-9.3^{\circ}\text{C}$  and a total snowfall amount of 100.5 cm. Table 3.1 shows a breakdown of the monthly average temperature and snowfall amount. During the winter of this study (2011-2012), monthly temperatures were above average in every month and snowfall was very low with the exception of January and March. The field season (February 15<sup>th</sup> to April 25<sup>th</sup>, 2012) took place during well below average snowfalls and should be noted in the interpretation of the results.

**Table 3.1. Historical monthly average temperature and snowfall (1971 to 2000) with the monthly average temperature and snowfall 2011-2012 for each month September through to May.**

	Sep	Oct	Nov	Dec	Jan	Feb	Mar	Apr	May
Historical Monthly average temperature (°C)	5.6	-1.7	-12.6	-22.8	-26.7	-24.6	-19.5	-9.7	-0.7
Monthly average temperature 2011-2012 (°C)	10.0	1.8	-9.1	-19.2	-24.3	-17.8	-16.2	-8.8	-0.3
Historical snowfall (cm)	6.0	28.7	37.0	24.2	19.8	18.3	18.3	19.8	15.4
Snowfall 2011-2012 (cm)	0.0	5.0	11.5	11.0	18.0	2.0	34.0	12.0	7.0

### 3.2.1.2 Malcolm Ramsay Lake *in situ* measurements

The field study began on February 15<sup>th</sup>, 2012 and ended on April 25<sup>th</sup>, 2012. The field season did not start until February 15<sup>th</sup> due to equipment and logistical issues, but the initial freeze-up of the lake is not affected by the albedo (Martynov *et al.*, 2010) and the winter season was still captured. Albedo has an effect particularly on the timing of break-up (Hostetler, 1991; Martynov *et al.*, 2010). April 25<sup>th</sup> was the end of the field season due to a warming trend in temperatures (Figure 3.2). The equipment was removed from the ice surface to avoid it falling into the lake. At the beginning of the field study, there had been little snowfall in the Churchill area and Malcolm Ramsay Lake was covered with patches of snow ranging from 1 to 21 cm in depth (Figure 3.3a). Clear ice and snow ice were encountered at various locations across the lake. The clear ice often had large cracks and bubbles of different size and density (Figure 3.3b, 3.3c, and 3.3d).

To measure the surface albedo of the lake ice and provide some of the required atmospheric forcing input for CLIMo, three separate stations were set up on Malcolm Ramsay Lake over snow, snow ice, and clear ice to represent the different surface types present (Figure 3.1). A meteorological station was set up at Site A near the northern shore that recorded air temperature (°C), relative humidity (%), wind speed (m s<sup>-1</sup>), and a combination of short and longwave radiation (W m<sup>-2</sup>). A Kipp and Zonen CNR1 net radiometer, that measures incoming/outgoing shortwave/longwave radiation separately, was mounted and leveled on the meteorological station 1.73 m above a clear ice surface in accordance with the World Meteorological Organization's (WMO) guide on instrumentation and observation that states the height of the pyranometer should be 1 to 2 m above the surface (WMO, 2008). The CNR1 uses two CM3 pyranometers, which have a spectral range of 305 to 2800 nm, for measuring incoming and outgoing shortwave solar radiation with  $\pm 5\%$  expected accuracy for daily sums. The incoming solar radiation from this site was used as the incoming solar

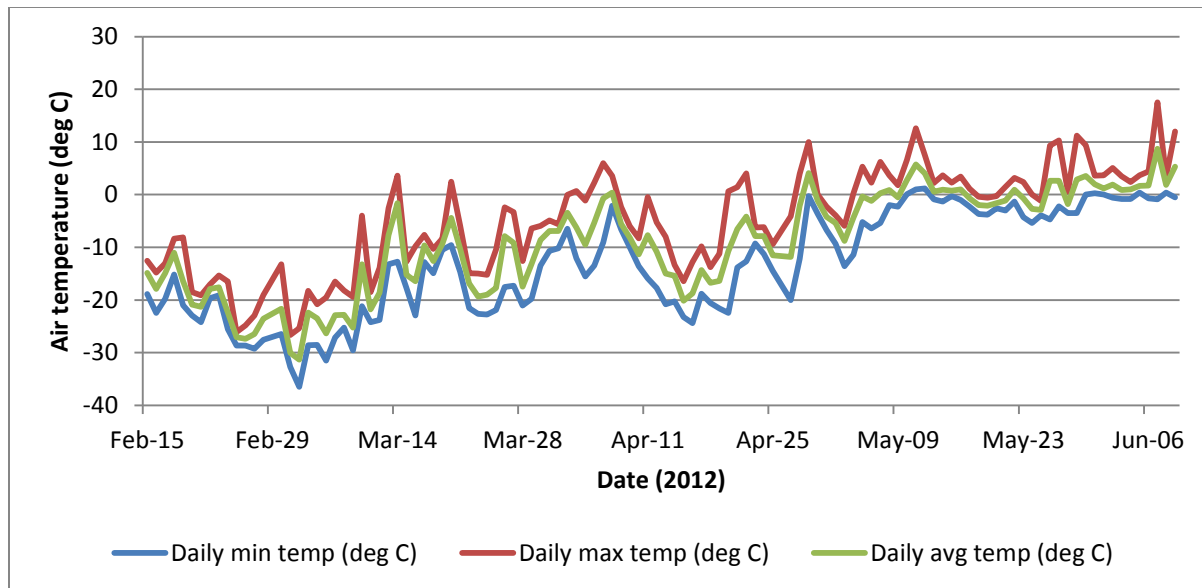


**Figure 3.2. Daily minimum, maximum, and average temperatures ( $^{\circ}\text{C}$ ) from February 15 to June 09, 2012 for Churchill, Manitoba.**



**Figure 3.3. The photos (taken on February 12, 2012) depict the variable snow cover (a.) as well as the variability of bubble density/cracks (b. to d.) in the clear ice for Malcolm Ramsay Lake, Manitoba.**

radiation for all sites. At Site B, a CM3 pyranometer was set up to measure reflected solar radiation near the centre of the lake. Metal tubing was frozen into the ice and the CM3 pyranometer was leveled and positioned 1.1 m above a snow covered surface. An Eppley Black and White pyranometer, model 8-48, was set up at Site C. The black and white pyranometer measures shortwave radiation ranging from 285 to 2800 nanometers with a  $\pm 3\%$  daily accuracy. This instrument was positioned 1.14 m above snow ice near the centre of the lake. The Eppley Black and White pyranometer had been calibrated prior to the field season. At the end of the field season, the CM3 pyranometers were placed beside the Eppley Black and White pyranometer and recorded incoming shortwave solar radiation for a two-week period. Shortwave solar radiation measurements of the CM3 pyranometers were found to be within  $\pm 4\%$  of the Eppley's shortwave solar radiation readings.

Prior to setting up the instrumentation, a section of snow ice and clear ice was swept clean (as was done in Bolsenga, 1977) and albedo measurements were taken to gain an understanding of what albedo values should be expected from the clear and snow ice recordings prior to comparing with CLIMo and MODIS.

Solar radiation (pyranometer) measurements ( $\text{W m}^{-2}$ ) were recorded on data loggers every minute and averaged every hour at each site for the duration of the field season. The pyranometers were periodically checked at each site to ensure that the lenses on the pyranometers were snow/ice free. In total, 70 daily average albedo values were calculated from the hourly records for the entire field season following the method presented in Henneman and Stefan (1999), where total reflected shortwave solar radiation is divided by the total incoming shortwave solar radiation during daylight hours. A fourth albedo value was included in which all three stations had their albedo observations averaged together. The MODIS albedo products have a 500 m spatial resolution and an average of the three stations would provide a more representative albedo for Malcolm Ramsay Lake. It is also useful to evaluate the CLIMo derived albedo values against the averaged albedo for the three stations to see if CLIMo's albedo parameterization is capable of capturing the average albedo of a lake and because the MODIS albedo products are evaluated against the averaged *in situ* observations.

### **3.2.2 MODIS albedo products**

The MODIS albedo products used in this study are the MOD10A1 and MYD10A1 daily albedo products and the MCD43A3 16-day albedo product. The spectral bands utilized for the generation of these products are shown in Table 3.2. The MOD10A1, MYD10A1, and MCD43A3 products have a 500 m spatial resolution. A pixel that covers Malcolm Ramsay Lake was carefully selected to ensure

**Table 3.2. MODIS bands used in the generation of the albedo products of this study (Hall et al., 2009; Salomonson et al., 2006).**

Band	Spectral Resolution ( $\mu\text{m}$ )	Spatial Resolution (m)	Product
1	0.620 – 0.670	250 by 250	MxD10A1* and MCD43A3
2	0.841 – 0.876	250 by 250	MxD10A1* and MCD43A3
3	0.459 – 0.479	500 by 500	MxD10A1* and MCD43A3
4	0.545 – 0.565	500 by 500	MxD10A1* and MCD43A3
5	1.230 – 1.250	500 by 500	MxD10A1* and MCD43A3
6	1.628 – 1.652	500 by 500	MOD10A1** and MCD43A3
7	2.105 – 2.155	500 by 500	MxD10A1* and MCD43A3

**\*MxD10A1 = MOD10A1 and MYD10A1**

**\*\*MYD10A1 (Aqua) band 6 excluded due to many inoperable detectors (Stroeve *et al.*, 2006)**

that land contamination was not an issue (see Figure 3.1). The pixel also includes two of the lake sites. Albedo values were retrieved from the pixel and evaluated against the averaged *in situ* measurements as well as compared to CLIMo predicted values. The *in situ* measurements from the three sites were averaged to provide a better spatial representation of Malcolm Ramsay Lake when evaluating the MODIS albedo products.

MODIS albedo products only retrieve albedo values under clear sky conditions. The shortwave radiation portion of the electromagnetic spectrum is used for the calculation of albedo, but clouds impede the ability of satellite remote sensing to gather the required information from the surface. It is important to note that the *in situ* observations conducted on Malcolm Ramsay Lake include all sky conditions. Key *et al.* (2001) found that snow and sea-ice albedo were on average 4-6% higher under cloud cover when compared to clear sky conditions and Grenfell and Perovich (2004) found that cloud cover could increase the albedo of snow by 7.7%. Clouds have an average albedo of 0.55 (Oke, 1978). Of the solar radiation that is not reflected back into the atmosphere by the clouds, little is absorbed in the visible portion of the electromagnetic spectrum, while clouds do absorb a significant portion of the shortwave infrared radiation (Key *et al.*, 2001). This means that more radiation in the visible portion will be transmitted through the clouds than from the shortwave infrared portion. Snow and ice tend to reflect more in the visible portion and absorb more in the infrared portion of the electromagnetic spectrum and this is why albedo is increased under cloudy conditions (Key *et al.*, 2001). This should be kept in mind when evaluating the MCD43A3 16-day albedo product which has an albedo value for every day during the study period. The MCD43A3 16-day albedo product will be discussed further in Section 3.2.2.2.

The MODIS albedo products do not provide daily average albedo values like the *in situ* observations. The MODIS albedo acquired is at the time when the satellite carrying the sensor is over the area of interest. This will have a slight effect on the albedo values retrieved, since albedo is affected by both solar zenith angle (SZA) and temperature changes throughout the day. However, since the timing of the albedo acquisition is not provided with the products, it will be assumed that the effect, when evaluated against daily albedo values, is negligible. The MODIS products are available at NASA's Earth Observing System Data and Information System (EOSDIS) (<http://reverb.echo.nasa.gov/>). For the study period, a total of 15 MCD43A3 and 114 MOD10A1/MYD10A1 image products were acquired.

### **3.2.2.1 MOD10A1/MYD10A1 daily albedo product**

The MOD10A1 (Terra) and MYD10A1 (Aqua) albedo products provide daily albedo information across the globe. MOD10A1/MYD10A1 provide daily albedo values at a 500 m spatial resolution in a sinusoidal grid. As indicated earlier, albedo is only recorded for clear sky conditions that are determined by the cloud mask product MOD35 (Hall et al., 2009; Klein and Stroeve, 2002). In order for albedo to be retrieved, the surface also has to be snow-covered (Klein and Stroeve, 2002). Lake ice is often covered by snow in the winter months, but Section 3.2.2.2 covers the unlikely event that the lake is completely absent of snow. Since lake ice is not forested, MOD10A1 accounts for anisotropic effects using the discrete-ordinate radiative transfer (DISORT) model developed by Stamnes *et al.* (1988). Albedo values are derived from the MODIS bands 1 to 7 (except for MYD10A1 due to unreliability issues with band 6 [Stroeve *et al.*, 2006]) that cover the visible to mid-infrared portion of the electromagnetic spectrum. A “narrowband reflectance is calculated for each of the seven MODIS bands and then combined into a spectrally integrated broadband albedo” (Hall et al., 2009; Klein and Stroeve, 2002).

Previous validation studies have been conducted on the MOD10A1/MYD10A1 snow albedo products. Klein and Stroeve (2002) found that MOD10A1 daily snow product albedo estimates have a maximum difference of 15% compared to *in situ* measurements from the SURFRAD site in Fort Peck, Montana. Stroeve *et al.* (2006) conducted a study using the Greenland Climate Network Automatic Weather Stations on the Greenland ice sheet and found MOD10A1 to have a RMSE of 0.067 and MYD10A1 to have a RMSE of 0.075. Şorman et al. (2007) and Tekeli *et al.* (2006) found that MOD10A1 overestimated albedo measurements by 10% when compared to their *in situ* measurements located in the Karasu Basin, Turkey (a mountainous region), but they contributed this difference to the fact that their *in situ* measurements were recorded at different times, with differences

in air temperature. Malik *et al.* (2011) found MOD10A1 to have a RMSE of 0.064 and a MAE of 0.052 when comparing the daily albedo product to *in situ* measurements in North Park, Colorado and Namco on the Tibetan Plateau.

### **3.2.2.2 MCD43A3 16-day albedo product**

MCD43A3 combines albedo retrievals from both the Terra and Aqua satellites. Using this combination, MCD43A3 provides a 16-day albedo product at a 500 m spatial resolution and is updated every 8 days (Schaaf *et al.*, 2002). The product makes use of the Ross Thick-Li Sparse Reciprocal (RTLSR) Bidirectional Reflectance Distribution Function (BRDF) model which is capable of deriving albedo based on the model's ability to describe reflectance anisotropy of each MODIS pixel (Wang *et al.*, 2012). At least seven cloud-free images over the desired area are required over the 16-day period, all of which are quality checked for outliers and poor angular sampling, to use the main algorithm with full inversion. Otherwise, a backup algorithm is used with a magnitude inversion applied (Schaaf *et al.*, 2002; Wang *et al.*, 2012). The MCD43A2 QA product for MCD43A3 determines whether the backup algorithm is used or not and if the albedo was recorded for a snow-covered pixel. MCD43A3 retrieves albedo year-round, but if the majority of the observations during the 16-day period are snow-covered, then only the snow-covered observations will be used in the algorithm and *vice versa* (Schaaf *et al.*, 2002). The output data include black sky albedo (BSA) (directional hemispherical reflection with no diffuse component) and white sky albedo (WSA) (bi-hemispherical reflection with no direct component and a diffuse component that is isotropic) with emphasis put on BSA for this study. Each albedo value, as in the MOD10A1/MYD10A1 products, is also taken under clear sky conditions. The WSA represents albedo under a pure diffused isotropic incident radiation (representative of thick cloud cover), which is why the BSA was used for this study (Schaeppman-Strub *et al.*, 2006). CLIMo accounts for cloud cover when calculating the shortwave radiation flux using a cloudy sky parameterization developed by Shine (1984).

The MCD43 products have been shown to provide robust albedo retrievals. MCD43 products refer to the MCD43B1 and MCD43B3 products which provide both the BRDF and albedo model parameters for 1 km and 500 m spatial resolutions in sinusoidal grids, respectively, and the MCD43A1 and MCD43A3 (aforementioned) which provide only the albedo model parameter for 1-km and 500 m spatial resolutions in sinusoidal grids, respectively. Prior to the combination of Aqua and Terra platform observations, the MCD43 products were known as the MOD43 products which utilized the Aqua platform observations (Salomon *et al.*, 2006). Stroeve *et al.* (2005) found, when comparing the MOD43 albedo product to *in situ* measurements observed in Greenland, that the

MOD43 albedo values had an average root-mean-square-error (RMSE) of 0.07. This value means that, on average, the MOD43 albedo values deviate approximately 7% from the *in situ* measurements. Wang *et al.* (2012) reported RMSE values that were less than 0.045 (or 4.5%) for albedo derived from the MCD43A1 (with a modified SZA) product over Alaskan tundra sites and Stroeve *et al.* (2005) mentioned a number of validation studies that reported snow albedo values to be accurate within 5% when using the main albedo algorithm. When there is a lack of sufficient data, the “backup algorithm” is used which has been found to be within 8 – 11% accurate (Stroeve *et al.*, 2005).

The temporal resolution of the MCD43A3 product is a concern, but when used in conjunction with the daily albedo products (MOD10A1/MYD10A1), there is much potential for this product. It is capable of filling in gaps in data when the daily albedo products experience a cloudy day. The albedo for MCD43A3, which is updated every eight days when the product itself is updated, will have the albedo for the subsequent days in between each product update set equal to the most recent albedo retrieved. Using this method, every day for the 114 day study period can be filled with albedo values that have a temporal resolution of eight days. For the evaluation of the MCD43A3 product against the *in situ* albedo observations, daily *in situ* albedo averages of all three stations were used to properly evaluate how the 16-day product compares to *in situ* observations. Comparison of the 16-day albedo product with daily *in situ* observations permitted the examination of how well the product captures daily variation in albedo. Prior to evaluating the MCD43A3 albedo product against *in situ* observations, the effect that clouds have on snow and ice albedo was checked to ascertain that clouds do increase the albedo of snow and ice. Loosely following the method of Key *et al.* (2001), the total incoming shortwave solar radiation for each day was used to determine whether cloud cover was present (i.e. days with noticeably lower total incoming shortwave radiation). Due to variability in surface conditions and changes in SZA throughout the season, the albedo for each cloudy day could only be compared to the clear-sky albedo values directly before and/or after a day with cloudy sky conditions. Key *et al.* (2001) chose to monitor consecutive cloudy periods followed by consecutive clear-sky periods for each day. The method of Key *et al.* (2001) was modified for this study from consecutive cloudy periods followed by consecutive clear-sky periods each day to consecutive cloudy days followed by consecutive clear-sky days carefully determined by incoming solar radiation measurements at Site A on Malcolm Ramsay Lake.

### 3.2.3 CLIMo albedo parameterization

The following description of CLIMo illustrates the types of processes used to predict and model lake ice, as well as how albedo is integrated into the computation. CLIMo (Duguay et al., 2003) is a modification of the one-dimensional thermodynamic sea-ice model by Flato and Brown (1996). Flato and Brown (1996) based their model on a one-dimensional unsteady heat conduction equation presented by Maykut and Untersteiner (1971), which can be seen in Equation (3.1):

$$\rho C_p \frac{\partial T}{\partial t} = \frac{\partial}{\partial z} k \frac{\partial T}{\partial z} + F_{sw} I_0 (1 - \alpha) K e^{-Kz} \quad (3.1)$$

where  $\rho$  is the density ( $\text{kg m}^{-3}$ );  $C_p$  is the specific heat capacity ( $\text{J kg}^{-1} \text{K}^{-1}$ );  $T$  is the temperature (K) within the ice or snow;  $t$  is time (s);  $z$  is the vertical coordinate, positive downward (m);  $k$  is the thermal conductivity ( $\text{W m}^{-1} \text{K}^{-1}$ );  $F_{sw}$  is the downwelling shortwave radiative energy flux ( $\text{W m}^{-2}$ );  $I_0$  ( $\text{W m}^{-2}$ ) is the fraction of shortwave radiation flux that penetrates the surface;  $\alpha$  is the surface albedo; and  $K$  is the bulk extinction coefficient for penetrating shortwave radiation (Duguay et al., 2003).

The surface energy budget is:

$$F_0 = F_{lw} - \varepsilon \sigma T^4(0, t) + (1 - \alpha)(1 - I_0)F_{sw} + F_{lat} + F_{sens} \quad (3.2)$$

where  $F_0$  ( $\text{W m}^{-2}$ ) is the net downward heat flux absorbed at the surface;  $\varepsilon$  is the surface emissivity;  $\sigma$  is the Stefan-Boltzmann constant ( $5.67 \times 10^{-8} \text{ W m}^{-2} \text{K}^{-4}$ );  $F_{lw}$  ( $\text{W m}^{-2}$ ) is the downwelling longwave radiative energy flux;  $F_{lat}$  ( $\text{W m}^{-2}$ ) is the downward latent heat flux; and  $F_{sens}$  ( $\text{W m}^{-2}$ ) is the downward sensible heat flux (Ménard et al., 2002).

The atmospheric input variables required for CLIMo are daily mean values of air temperature ( $^{\circ}\text{C}$ ), relative humidity (%), cloud amount (tenths), and wind speed ( $\text{m s}^{-1}$ ) as well as the daily total snowfall (m) (Duguay et al, 2003). These data can be collected from local meteorological stations. The daily output variables are energy balance components, on-ice snow depth, a temperature profile throughout the ice/snow (or surface water temperature in the absence of ice), and ice thickness (both clear and snow ice). Other output variables include the freeze-up date (ice-on), break-up date (ice-off), and end-of-season clear/snow/total ice thickness (Duguay et al., 2003).

Albedo is important to the evaluation of the surface energy balance and it is required to appropriately measure and predict energy exchange via insolation at the surface. CLIMo's surface albedo parameterization takes the surface type (ice, snow, and open water), surface temperature, and ice thickness into account (Duguay et al., 2003). As mentioned earlier, the cold ice parameterization

(i.e. temperatures below freezing) is taken from Maykut (1982), while the melting ice parameterization is based on ice observations from Heron and Woo (1994) (Duguay et al., 2003). The surface albedo parameterization is expressed as:

$$\alpha = \begin{cases} \alpha_{ow} & h_i < h_{min} \\ \min[\alpha_s, \alpha_i + h(\alpha_s - \alpha_i)/c_1] & h_i \geq h_{min} \quad h_i \leq c_1 \\ \alpha_s & h_i \geq h_{min} \quad h_s > c_1 \end{cases} \quad (3.3)$$

$$\alpha_i = \begin{cases} \max(\alpha_{ow}, c_2 h_i^{0.28} + 0.08) & T(0, t) < T_m \\ \min(\alpha_{mi}, c_3 h_i^2 + \alpha_{ow}) & T(0, t) = T_m \end{cases} \quad (3.4)$$

$$\alpha_s = \begin{cases} 0.75 & T(0, t) < T_m \\ 0.65 & T(0, t) = T_m \end{cases} \quad (3.5)$$

where  $\alpha$  is surface albedo;  $\alpha_{ow}$  is albedo of open water, equal to 0.05;  $\alpha_s$  is albedo of snow;  $\alpha_{mi}$  is the albedo of melting ice, equal to 0.55;  $h$  is the total thickness of slab, ice plus snow (m);  $h_i$  is ice thickness (m);  $h_{min}$  is minimum ice thickness below which open water is assumed, equal to 0.001 m;  $h_s$  is snow thickness (m);  $T(0, t)$  is the temperature within ice or snow at the vertical coordinate 0 at the time (s);  $T_m$  is melting temperature at the surface, equal to 273.15 K;  $c_1$  is equal to 0.1 m;  $c_2$  is equal to 0.44 m; and  $c_3$  is equal to 0.075 m. The parameters  $c_1$ ,  $c_2$ , and  $c_3$  are derived from field observations found in various studies by Maykut (1982). Equations (3.4) and (3.5) determine the albedo of ice and snow, respectively, based on whether certain criteria, mainly involving melting temperature at the surface, are met. Equation (3.3) determines which albedo value to use based on ice and snow thicknesses.

Maykut (1982) based his observations on the observations of Weller (1972) who took radiation measurements over sea water, multiyear sea ice, natural and artificial refreezing leads, hummocks/ridges, and snow cover on central Arctic ice over the ocean. Grenfell and Perovich (2004) noted that sea ice will have significantly [*sic*] different surface albedo values than freshwater lake ice due to the brine inclusions that cause an increase in volumetric scattering and therefore higher surface albedo. The melting ice parameterization, however, was taken from Heron and Woo (1994) who retrieved their albedo observations over a high-Arctic freshwater lake near Resolute, Nunavut.

It is important to note that the cold ice and melting ice parameterizations do not take ice type (clear ice or snow ice) into account and neither Maykut (1982) nor Heron and Woo (1994) specify the ice type that the albedo observations were retrieved from.

### 3.2.3.1 CLIMo simulations

The daily mean air temperature, relative humidity, and wind speed values were retrieved for 2010 to 2012 from a meteorological station that is set up on the north shore of Malcolm Ramsay Lake (Brown and Duguay, 2011a). During the study period (February 15<sup>th</sup> to April 25<sup>th</sup>, 2012), the daily air temperature, relative humidity, and wind speed values that were inputted into the model were taken from the meteorological station set up at Site A. Unfortunately, the meteorological station set up on the north shore had a malfunctioning snow depth sensor so values had to be retrieved from the nearby meteorological station at the Churchill airport. The data are provided by the National Climate Data and Information Archive (<http://www.climate.weatheroffice.gc.ca/>). Cloud amount data were provided by Environment Canada by request and from the netCDF files of the North American Regional Reanalysis (NARR) (<http://www.esrl.noaa.gov/psd/data/gridded/data.narr.html>).

Due to the variable snow cover present on Malcolm Ramsay Lake, CLIMo was run once with recorded snow depths and once without snow (i.e. bare ice surface) for evaluation and comparison. The mixing depth for the lake was set to 2 metres for both model runs.

### 3.2.4 Performance evaluation statistics

The statistical error measures used to compare *in situ* with estimated albedo values (CLIMo and MODIS) were the mean absolute error (MAE), root mean square error (RMSE), and mean bias error (MBE). The MAE provides an absolute measure of the average magnitude of errors between the modelled (or estimated) and observed values. If the MAE between the modelled (or estimated) and observed values was 0, that would indicate that there was no error. The closer the MAE is to 0, the better. However, the MAE does not indicate whether the modelled values are over- or underestimating the observed values. Much like the MAE, the RMSE provides information on the deviation of the modelled (or estimated) values from the observed. The RMSE is squared before being averaged and will not provide information on over- or underestimation of the modelled/estimated values compared to the observed (Ménard *et al.*, 2002). The values returned by the RMSE will always be greater than or equal to the MAE and since it is squared, it is more susceptible to extreme values. If the RMSE is much larger than the MAE, it is an indication that outliers exist within the data (Legates and McCabe, 1999). The MBE is a statistical error measure capable of providing information on the over- or underestimation of modelled/estimated values compared to observed values. Again, the closer the MBE is to 0, the better; however, the MBE is not an absolute measure; is not squared before being average; and is, therefore, capable of a negative

outcome. If the value is negative, the CLIMo modelled or MODIS estimated albedo is being underestimated by that number and vice versa. The MAE, RMSE, and MBE are reported in albedo values between 0 and 1. When comparing CLIMo against MODIS estimated albedo values, the same performance statistics were calculated but are referred to as the mean difference (MD), mean absolute difference (MAD), and root mean square difference (RMSD) since albedo values from both CLIMo and MODIS are estimates.

### 3.3 Results and discussion

#### 3.3.1 CLIMo albedo values evaluated against *in situ* observations

Sites A, B, and C were initially located over clear ice, snow, and snow ice, respectively. Site B, as expected, had a higher, less variable, and a lower range of albedo values over the entire field season due to the location over snow (Figure 3.4). Sites A and C appear to have captured two albedo seasons. During the month of March, the albedo values recorded for Sites A and C reflected a dramatic increase (Figure 3.5). Following snowfall events starting on March 10, 2012, the albedo stations recorded a notable rise in albedo values. The higher recorded albedo values are believed to be due to snowfall events that began on March 10 causing drifts to form in front of the pyranometer sites (Figure 3.6). For this reason, a full study period as well as two separate segments of the study period (before and after March 10<sup>th</sup>) are evaluated in this study. CLIMo produced albedo values that are less variable than the observed albedo values for each site (Figure 3.5 and Table 3.3).

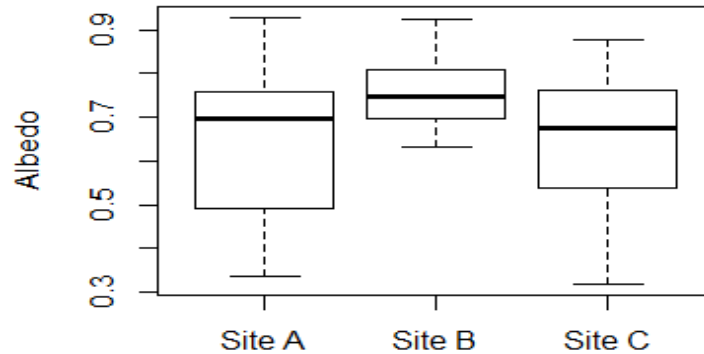


**Figure 3.4. Boxplots of albedo for three *in situ* stations located on Malcolm Ramsay Lake (February 15 to April 25, 2012)**

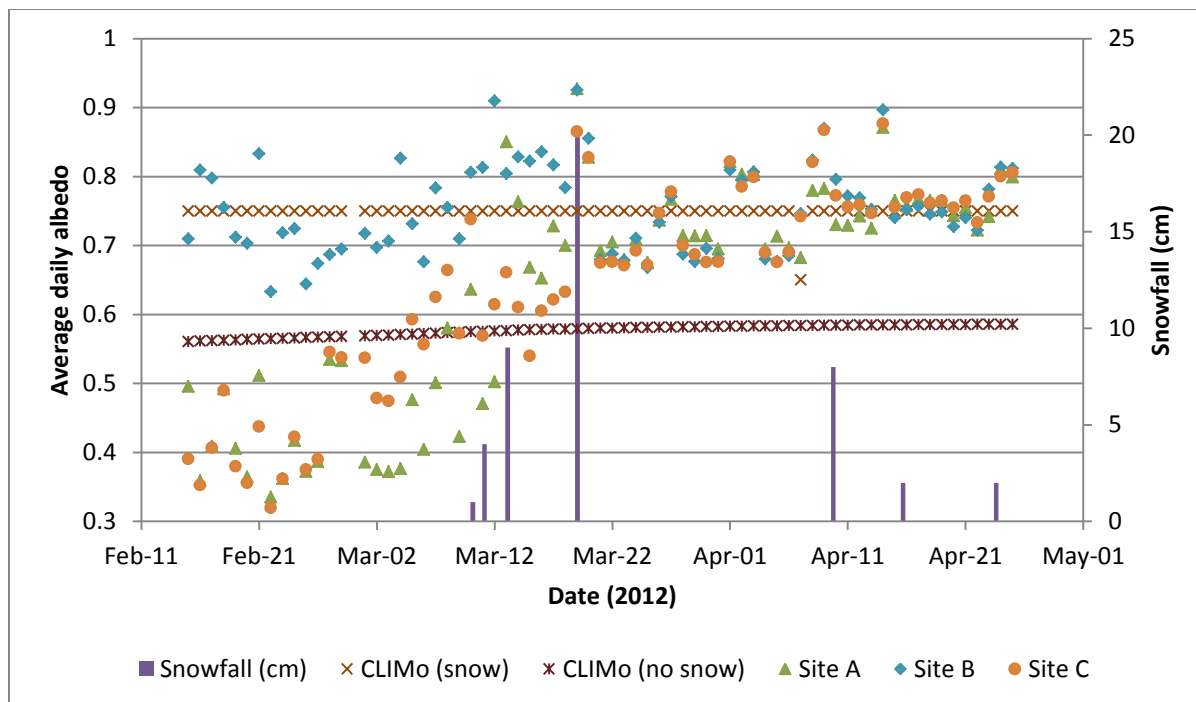


**Figure 3.5. Daily albedo values for CLIMo with and without snow as well as Sites A, B, and C. Daily snowfall values reported at the Churchill Airport weather station are also included in this figure.**



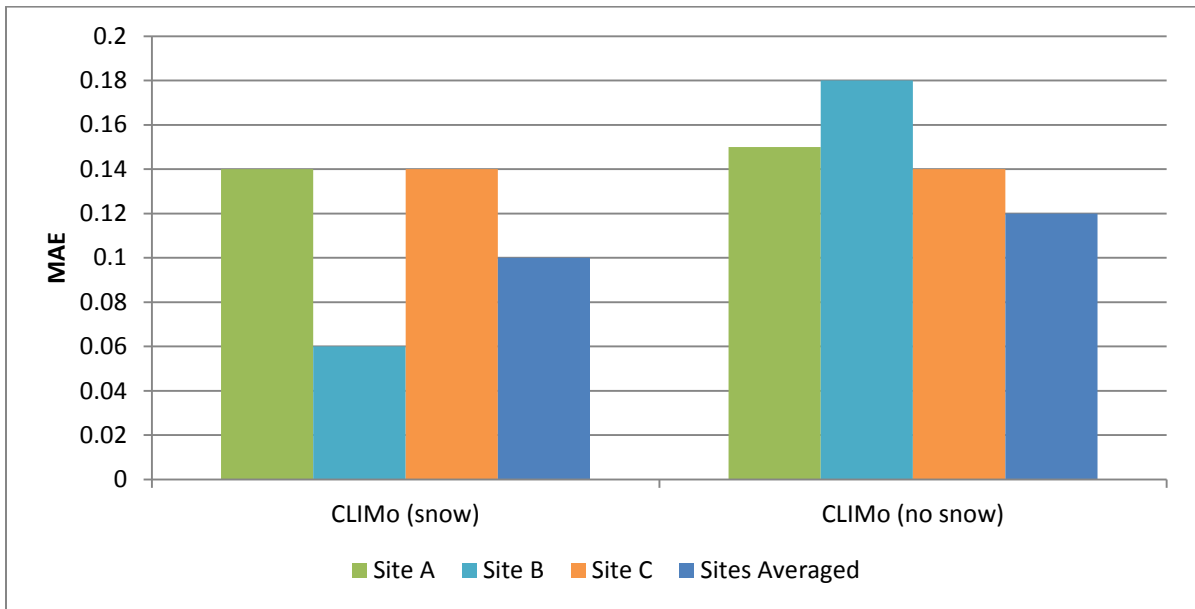
**Figure 3.6. Site C on March 16, 2012 following snowfall events.**

Each of the lake stations were evaluated against the albedo values derived from CLIMo's albedo parameterization. A fourth evaluation was included in which all three stations had their albedo observations averaged together. Table 3.3 summarizes the comparison between the modelled and observed values on Malcolm Ramsay Lake for the entire field season. The mean of Site C was 0.01 higher than Site A while Site B's mean was 0.12 and 0.11 higher than Site A and C, respectively. The standard deviations of Site A (0.16) and Site C (0.15) were higher than Site B (0.07). This was due to the shift to higher albedo values following snowfall events starting on March 10 (Figure 3.5). The mean of CLIMo with snow added to the model was equal to Site B, but its standard deviation was much lower with a value of 0.01. The albedo for CLIMo with snow was 0.75 for every day except for April 7 where the albedo of snow was determined to be 0.65 since the surface temperature was determined to be equal to melting. While the maximum temperature did rise above 0°C multiple times throughout the study period (Figure 3.3), April 7 was the only time the daily mean temperature rose above 0°C. The average albedo for CLIMo without snow added to the model was 0.58, which is below all other average albedo values for CLIMo with snow and for each of the pyranometer stations. When the observed values were evaluated with CLIMo albedo values (with and without snow), CLIMo with snow compared well with albedo observed at Site B. The RMSE and MAE of CLIMo with snow indicate that the albedo values only differed by 0.07 and 0.06, respectively, from observed values at that station. The MBE was -0.01, indicating that CLIMo underestimated observed albedos by 0.01. Site B was initially located over snow, which shows that the albedo parameterization for snow performs fairly well during the cold season. When comparing Site B observations with CLIMo without snow, the model did not perform well having RMSE and MAE values of 0.19 and 0.18, respectfully, and underestimating observed values by 0.18. Again, Site B was initially located over snow, while CLIMo without snow recorded ice albedo values derived from the albedo parameterization. These larger errors were expected since the albedo of ice is lower than the albedo of snow. As was seen with CLIMo without snow evaluated against Site B, CLIMo (with and without) snow did not perform as well against the other stations (Figure 3.7). CLIMo (with and without snow) had RMSE and MAE values greater than 0.10 for Site A, C, and the averaged observations. The MBE values indicate that CLIMo without snow only underestimated albedo values by 0.06 and 0.07 for Sites A and C, respectively. Sites A and C were initially located over clear ice and snow ice and it was expected that CLIMo with snow would not perform well, but CLIMo without snow added to the model should have reproduced albedo values with less error when compared to observations for Sites A and C. This is likely due to the shift in albedo values following snowfall events starting March 10<sup>th</sup>, 2012 and snow drifts forming beneath the sensors. The first half of the

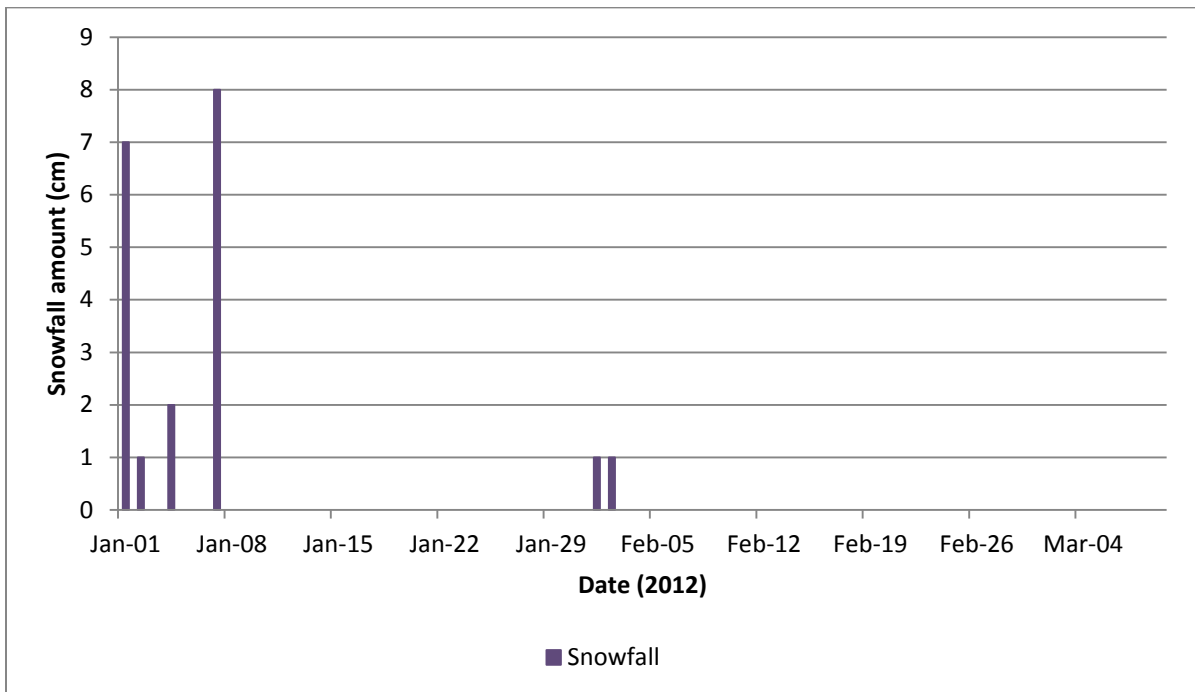
**Table 3.3. CLIMo derived albedo values evaluated against *in situ* albedo values for Malcolm Ramsay Lake from February 15 to April 25, 2012.**

Albedo stations	Statistic	Observed	CLIMo (snow)	CLIMo (no snow)
Site A (Clear ice)	Sample size, n	70	70	70
	Mean	0.63	0.75	0.58
	Standard deviation	0.16	0.01	0.01
	RMSE		0.20	0.16
	MAE		0.14	0.15
	MBE		0.11	-0.06
Site B (Snow)	Sample size, n	70	70	70
	Mean	0.75	0.75	0.58
	Standard deviation	0.07	0.01	0.01
	RMSE		0.07	0.19
	MAE		0.06	0.18
	MBE		-0.01	-0.18
Site C (Snow ice)	Sample size, n	70	70	70
	Mean	0.64	0.75	0.58
	Standard deviation	0.15	0.01	0.01
	RMSE		0.18	0.15
	MAE		0.14	0.14
	MBE		0.11	-0.07
Sites averaged together	Sample size, n	70	70	70
	Mean	0.68	0.75	0.58
	Standard deviation	0.11	0.01	0.01
	RMSE		0.13	0.14
	MAE		0.10	0.12
	MBE		0.07	-0.10

field season (before March 10<sup>th</sup>) was during a period of little to no snowfall. There had been snow fall events early in the season, at the beginning of January, and two small snowfall events at the beginning of February, but very little precipitation had fallen a month before the start of the field season on February 15<sup>th</sup>, 2012 (Figure 3.8). As seen in Figure 3.3, snow presence on Malcolm Ramsay Lake was highly variable and low precipitation prior to the field season may have attributed to this. To see how this shift in albedo values affected the results, the study period was split into two separate seasons. The first season is from February 15<sup>th</sup> to March 9<sup>th</sup>, 2012 and the second season from March 10<sup>th</sup> to April 25<sup>th</sup>, 2012.



**Figure 3.7.** MAE for both CLIMo with and without snow for each of the stations as well as all stations averaged together (February 15 to April 25, 2012).



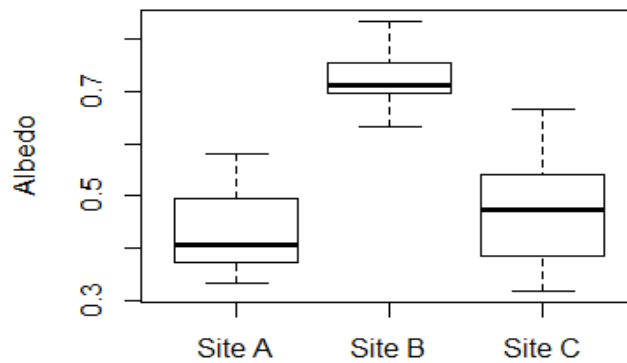
**Figure 3.8.** Snowfall amount from January 1 to March 9, 2012.

Table 3.4 summarizes the CLIMo albedo values evaluated against observed albedo values for the first part of the field season from February 15<sup>th</sup> to March 9<sup>th</sup>, 2012. At the beginning of the field season, Site B recorded albedo values similar to those recorded for the entire season and the variability of albedo values was still low as well (Figure 3.9). The mean albedo recorded for all the station observations averaged together for that period was 0.54, which was lower than the averaged observed mean for the entire season (0.68) (Table 3.3 and 3.4). For Sites A and C, the albedo values recorded at these sites were lower and have a lower range of values when compared to the albedo values recorded for the entire season (Figures 3.4 and 3.9). The mean values for Sites A and C were 0.43 and 0.47 respectively, which are much lower than the mean albedo values recorded by Sites A and C for the entire season (0.63 and 0.64, respectively) (Table 3.3 and 3.4). A larger difference was expected to be found between Sites A and C. Clear ice was found to have albedo values of 0.33, 0.32, and 0.30; while snow ice had albedo values of 0.62, 0.63, and 0.65 when measurements were taken

**Table 3.4. CLIMo derived albedo values evaluated against *in situ* albedo values for Malcolm Ramsay Lake from February 15 to March 10, 2012.**

Albedo stations	Statistic	Observed	CLIMo (snow)	CLIMo (no snow)
Site A (Clear ice)	Sample size, n	23	23	23
	Mean	0.43	0.75	0.57
	Standard deviation	0.07	0.01	0.01
	RMSE		0.33	0.15
	MAE		0.32	0.14
	MBE		0.32	0.13
Site B (Snow)	Sample size, n	23	23	23
	Mean	0.73	0.75	0.57
	Standard deviation	0.05	0.00	0.004
	RMSE		0.06	0.17
	MAE		0.05	0.16
	MBE		0.02	-0.16
Site C (Snow ice)	Sample size, n	23	23	23
	Mean	0.47	0.75	0.57
	Standard deviation	0.10	0.00	0.004
	RMSE		0.30	0.14
	MAE		0.28	0.11
	MBE		0.28	0.10
Sites averaged together	Sample size, n	23	23	23
	Mean	0.54	0.75	0.57
	Standard deviation	0.06	0.00	0.004
	RMSE		0.22	0.06
	MAE		0.21	0.05
	MBE		0.21	-0.08

from areas swept clean just before the start of the field season. These areas, however, were picked to be perfect representations of clear ice and snow ice (i.e. clear ice with no bubbles present and snow ice that was hard to differentiate from snow) (Figure 3.10). Snow ice albedo values were found to range from 0.39 to 0.46 in Bolsenga (1977). Heron and Woo (1994) observed that the albedo for bare ice ranged from 0.15 to 0.5 with a maximum albedo of 0.56. The snow ice albedo values observed for this study were on the high side of freshwater ice albedo values. CLIMo without snow added to the model calculated a mean albedo of 0.57 for the study period from February 15<sup>th</sup> to March 10<sup>th</sup>, 2012. The albedo parameterization for bare ice in CLIMo has produced values that are over at least 0.10 higher than recorded means at Site A and C for the same period. CLIMo's mean for bare ice is also above the maximum ice albedo observed by Heron and Woo (1994). Site C had snow ice (Figure 3.6), but it was not as pure as the snow ice albedo observed prior to the field season (Figure 3.10). Site C's mean albedo for the beginning of the season was higher than Site A's mean albedo by 0.05 and was representative of Bolsenga's (1977) findings.



**Figure 3.9. Boxplots of the three *in situ* stations located on Malcolm Ramsay Lake (February 15 to March 9, 2012)**

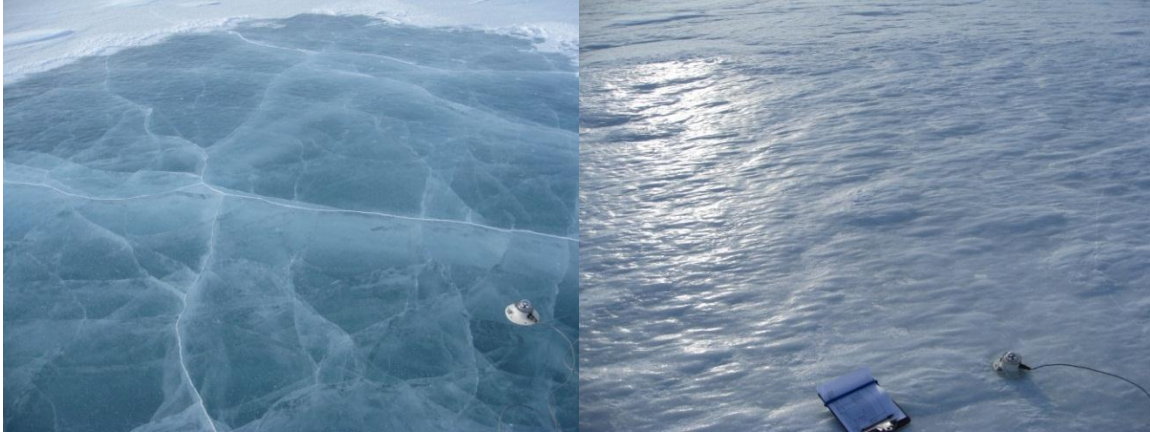


**Figure 3.10. (Left) Section of clear ice used to find albedo values for clear ice and (Right) a section of snow ice used to find albedo values for snow ice on Malcolm Ramsay Lake.**

For CLIMo with snow, Site B improved slightly with a RMSE equal to 0.06 and a MAE equal to 0.05, but remained unaffected by the snowfall events that began on March 10<sup>th</sup> (Table 3.4). Removing snow from CLIMo did not improve the bare ice observations at Site A and C as expected. Instead, the model went from underestimating the site observations to overestimating the observations with MBE values of 0.13 and 0.10 for Site A and C, respectively. The sites averaged together had a RMSE of 0.06 and MAE of 0.05, indicating that the observed albedo values averaged together were often within 0.05 and 0.06 of modelled values for CLIMo without snow. These were the only findings that showed a great improvement for CLIMo being run without snow which suggests that it is better suited to capturing lake ice albedo with variable snow cover.

Once the snowfall events occurred (see Figure 3.8), snow drifts formed in front of the bare ice sites (Site A and C) and albedo values rose and resembled snow albedo values for the rest of the field season. Table 3.5 summarizes the evaluation of CLIMo's modelled albedo values against the observed albedo values for the period from March 10<sup>th</sup> to April 25<sup>th</sup>, 2012. CLIMo with snow produced a mean albedo of 0.75 for this time period. The mean albedo values for each site were within 0.02 of the modelled mean for CLIMo with snow. The standard deviations were 0.06 to 0.07 higher than the modelled standard deviation for CLIMo with snow. CLIMo without snow, however, had a mean albedo of 0.58 and was much lower than the observed means (Table 3.5).

For every site, as well as the sites averaged together, the RMSE and MAE when evaluated against the modelled results for CLIMo without snow were 0.15 or greater. CLIMo without snow produced MBE results which suggest that the modelled values underestimated the observed values by at least 0.15 as well. On the other hand, CLIMo with snow evaluated against each station performed very well. Site A had a RMSE of 0.08 and a MAE of 0.05; Site B had a RMSE of 0.07 and a MAE of

**Table 3.5. CLIMo derived albedo values evaluated against *in situ* albedo values for Malcolm Ramsay Lake from March 10 to April 25, 2012.**

Albedo stations	Statistic	Observed	CLIMo (snow)	CLIMo (no snow)
Site A (Clear ice)	Sample size, n	47	47	47
	Mean	0.73	0.75	0.58
	Standard deviation	0.08	0.01	0.003
	RMSE		0.08	0.17
	MAE		0.05	0.16
	MBE		0.01	-0.15
Site B (Snow)	Sample size, n	47	47	47
	Mean	0.77	0.75	0.58
	Standard deviation	0.07	0.01	0.003
	RMSE		0.07	0.20
	MAE		0.06	0.19
	MBE		-0.02	-0.19
Site C (Snow ice)	Sample size, n	47	47	47
	Mean	0.73	0.75	0.58
	Standard deviation	0.08	0.01	0.003
	RMSE		0.08	0.16
	MAE		0.06	0.15
	MBE		0.02	-0.15
Sites averaged together	Sample size, n	47	47	47
	Mean	0.74	0.75	0.58
	Standard deviation	0.06	0.01	0.003
	RMSE		0.06	0.17
	MAE		0.05	0.16
	MBE		0.005	-0.16

0.06; Site C had a RMSE of 0.08 and a MAE of 0.06; and the observations averaged together had a RMSE of 0.06 and a MAE of 0.05. The MBE values with snow had MBE values between -0.02 and 0.02 for all the sites indicated that modelled values either under- or overestimated observed albedo values by just 0.02. With snow added CLIMo calculated snow albedo values that were within at least 0.08 of observed values for each site.

CLIMo's ice albedo parameterization overestimated bare ice observations when evaluated against observed albedo values on Malcolm Ramsay Lake. The snow albedo parameterization, however, performed very well when evaluated against the observations made on Malcolm Ramsay Lake. With the exception of the sites averaged together, each observation provides a 1-D albedo

value which was evaluated against a 1-D model. The following section explores how MODIS albedo products perform against the *in situ* observed albedo.

### 3.3.2 MODIS retrieved albedo values evaluated against *in situ* observations

The MODIS albedo products (MOD10A1, MYD10A1, and MCD43A3) all have spatial resolutions of 500 m. Therefore, the three *in situ* stations on Malcolm Ramsay Lake were averaged before being used to evaluate the MODIS albedo products. Unlike the albedo values calculated by CLIMo, the MODIS retrieved albedo values tend to follow the trends observed in the *in situ* observations (Figure 3.11). Like the *in situ* observations, the MODIS albedo products are able to retrieve information directly from the site and do not rely on ancillary data for inputs as with CLIMo. The albedos retrieved from the MODIS albedo products reliably capture surface changes throughout the season and do not require further evaluation in sub-sections during the field season like the albedo parameterization for CLIMo.

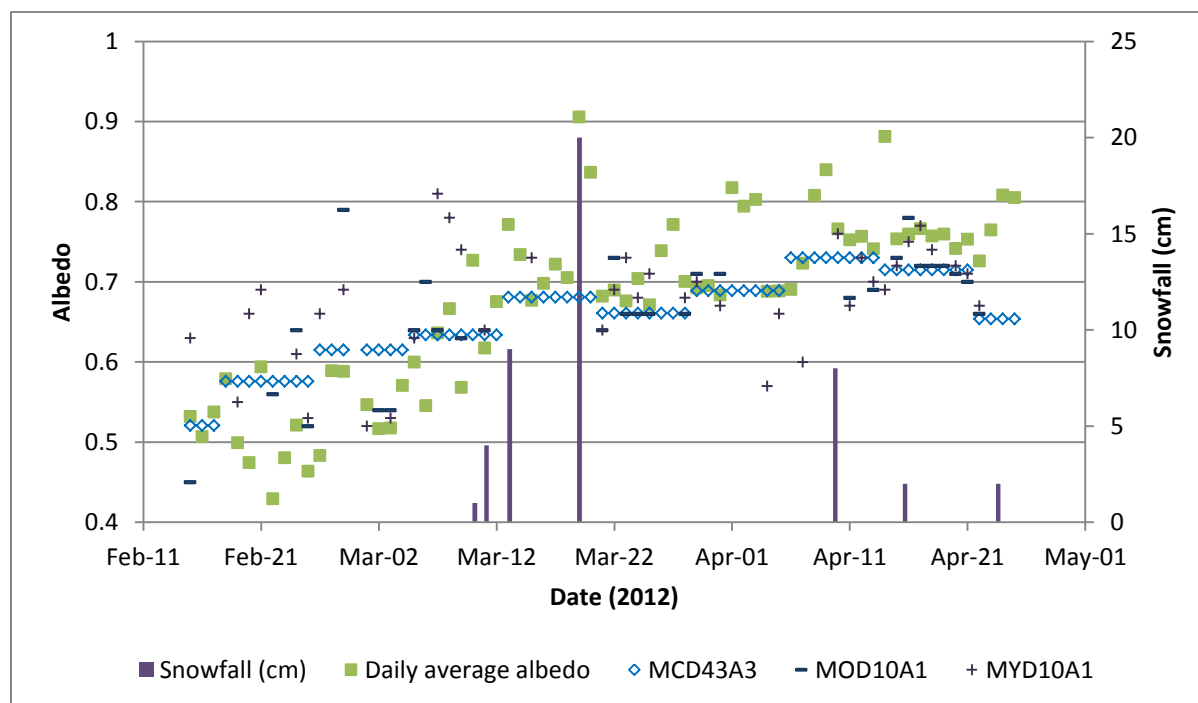


**Figure 3.11. MODIS retrieved and average *in situ* daily/16-day albedo values as well as snowfall amount for Malcolm Ramsay Lake from February 15th to April 25th, 2012.**

#### 3.3.2.1 MODIS daily albedo products

The MODIS daily products MOD10A1 (Terra) and MYD10A1 (Aqua) are recorded each day under clear-sky conditions. Each product is generated from two separate satellites (Terra and Aqua) that

pass over the field site on a daily basis, but at varying times throughout the day. Therefore, each daily albedo product has a different number of observations due to varying cloud cover throughout the day. From February 15 to April 25, 2012, Terra (MOD10A1) was able to retrieve 30 albedo observations and Aqua (MYD10A1) 39 albedo observations from the 70 images acquired. Table 3.6 summarizes the MODIS daily products evaluated against the *in situ* observations made over Malcolm Ramsay Lake during the field season. The MOD10A1 and MYD10A1 daily products have very similar means and standard deviations when compared to *in situ* albedos at Malcolm Ramsay Lake. The mean of MOD10A1 when compared to the *in situ* mean is 0.01 higher and MYD10A1 has a mean 0.02 higher than the observed values. The standard deviation for MOD10A1 and MYD10A1 are both slightly lower than the standard deviations for the *in situ* albedos, which suggest that the products are a little less variable in nature. The RMSE for MOD10A1 and MYD10A1 are 0.07 and 0.08, respectively, which fall within the RMSE values found by previous studies that were close to 0.10 (Klein and Stroeve, 2002; Şorman *et al.*, 2007; Stroeve *et al.*, 2006). Stroeve *et al.* (2006) found the MOD10A1 to have a lower RMSE (0.07) than the RMSE for the MYD10A1 (0.08) for the Greenland ice sheet study and these RMSE values match the RMSE values found in this study. Both the MOD10A1 and MYD10A1 products overestimate the *in situ* albedo values, but only by 0.01 and 0.02, respectively.

The daily MODIS albedo products evaluated against the averaged *in situ* observations perform very well having low RMSE and MAE percentages that just slightly overestimate albedo values when retrieved. There is the issue of cloudy periods where only values for 30 of 70 days were retrieved for MOD10A1 and 39 of days were retrieved for MYD10A1. The MCD43A3 16-day product, however, updates every 8 days and the average value can be used to fill in gaps in data due to clouds. The following section evaluates the performance of MCD43A3 to the observe albedo values on Malcolm Ramsay Lake.

**Table 3.6. MODIS daily albedo values evaluated with *in situ* observed albedo values for Malcolm Ramsay Lake from February 15 to April 25, 2012.**

Statistic	MOD10A1	MYD10A1
Sample size, n	30	39
Observed mean (standard deviation)	0.65(0.10)	0.66(0.10)
MODIS mean (standard deviation)	0.66(0.08)	0.68(0.07)
RMSE	0.07	0.08
MAE	0.05	0.06
MBE	0.01	0.02

### 3.3.2.2 MODIS 16-day albedo product

The only period during the study to have poor quality flags occurred from March 5<sup>th</sup> to March 11<sup>th</sup>, 2012, which means the backup algorithm was used. Wang *et al.* (2012) make note that the backup algorithm still performs well under normal situations. Unlike the MODIS daily products, MCD43A3 averages the retrieved albedo values for the previous 16 days and is updated every 8 days. However, the albedo can only be retrieved under clear sky conditions and, therefore, does not always include a full 16-day average. If the albedo values are to be compared with days that are dominated by cloud cover, it is useful to look at these cloudy days and clear-sky days separately when comparing the *in situ* albedo observations with the MCD43A3 albedo product. Once it has been determined how the MCD43A3 product performs under cloudy and clear-sky conditions, MCD43A3 retrieved albedo values evaluated against the daily *in situ* observations will be able to determine if the product is able to accurately represent daily albedo values.

As mentioned earlier, the MODIS albedo products are retrieved only under clear sky conditions. Key *et al.* (2001) reported findings that suggest the albedo of snow and sea ice were increased by 5-6% under cloud cover, while Grenfell and Perovich (2004) found cloud cover to increase snow albedo up to 7.7%. Throughout the field season for this study, 24 cloudy days were identified after carefully observing incoming solar radiation values from the meteorological station at Site A for each date. It is possible that there were clear sky periods in a cloudy day, but the main aspect that was taken into consideration was that there was a noticeable decrease in total incoming shortwave radiation for the day, meaning that each designated cloudy day was affected by cloud cover to some degree. The *in situ* albedo values for cloudy days when compared to the previous or subsequent clear sky *in situ* albedo values found that the albedo of freshwater ice and snow were, on average, 7.7% higher under cloudy conditions with a range of -4% to 20%. The wide range between albedo values was probably due to different cloud types/cloud amount and changes in surface conditions. Changes in surface condition are believed to be the reason for three cloudy days that had observed albedo values lower than clear sky albedo values. These three days were only slightly lower than the clear sky albedo values that they were compared against. The 7.7% average higher albedo for cloudy sky conditions agrees with the findings of Key *et al.* (2001) and matches perfectly with Grenfell and Perovich's (2004) findings for snow. Figure 3.12 illustrates how lower incoming shortwave radiation may have affected the daily albedo observed at Site A. When evaluating MCD43A3 against the all sky averaged *in situ* albedo observations, it should be noted that RMSE values may be increased due to albedo observations recorded during days with cloud cover. This

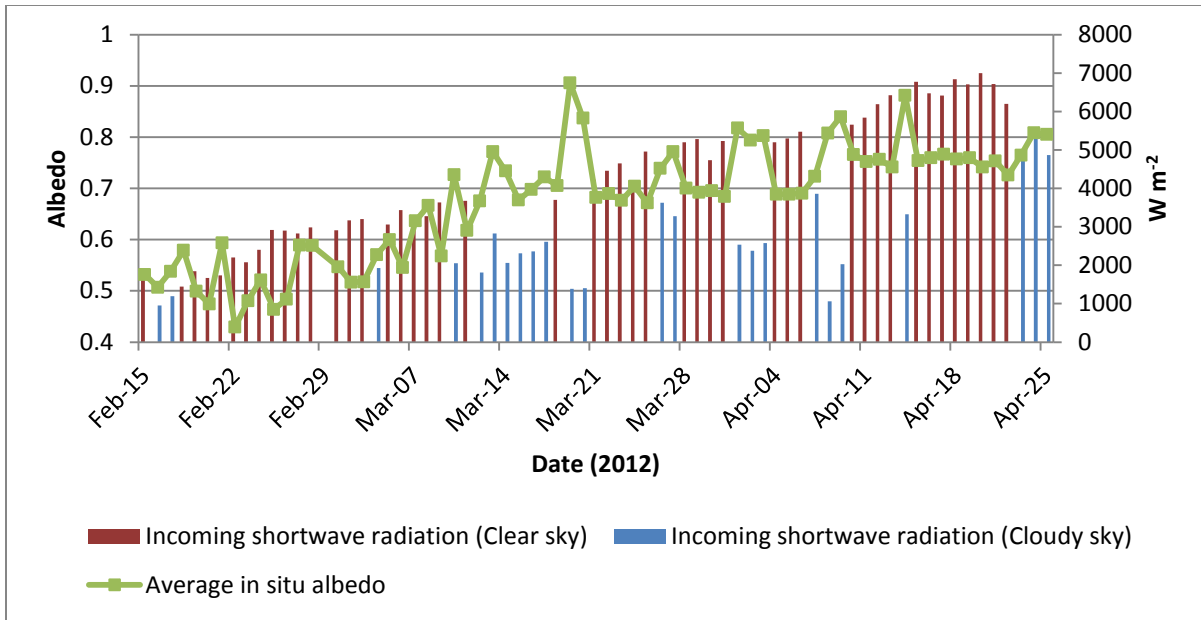


**Figure 3.12. Daily incoming shortwave radiation and average *in situ* albedo measurements for Site A on Malcolm Ramsay Lake from February 15 to April 25, 2012.**

change in albedo should not affect CLIMo's outputs since cloud amount is taken into account by CLIMo (see Section 3.2.2.2). The cloudy sky parameterization in place in CLIMo was developed by Shine (1984) who states that, "replacing the spectrally varying albedo by a spectrally constant albedo with the correct value for the given cloud thickness generated errors no greater than 1.5%, indicating that the spectral variation, *per se*, is not critical for surface flux determination".

The next step involved determining how well MCD43A3 retrieved albedos performed under clear-sky and cloudy days. Table 3.7 summarizes MCD43A3 retrieved albedos against *in situ* observations for these clear and cloudy sky days. For the 24 days determined to have cloud cover for much of the day, the mean *in situ* albedo observed at the three stations on Malcolm Ramsay Lake was 0.75, which is 0.09 higher than the mean albedo retrieved from the MCD43A3 product. The mean *in situ* albedo observed for the clear sky days throughout the study period was 0.64, which is 0.01 lower than the mean albedo retrieved from the MCD43A3 product. The RMSE and MAE for dates with cloudy conditions suggest that MCD43A3 has an average error of 0.10 and 0.09, respectively, when compared to *in situ* observations and MCD43A3 underestimates the *in situ* observations by 0.08. Since cloud cover was found to increase the albedo at the *in situ* stations by 7.7% or 0.077, these findings show that MCD43A3 does in fact underestimate snow and ice albedo under cloudy conditions near the observed amount. The RMSE and MAE for clear sky conditions were more accurate with average errors of 0.06 and 0.04, respectively, and MCD43A3 was found to overestimate the *in situ* observations by 0.01. The validation study by Stroeve *et al.* (2005) was done under clear

**Table 3.7. MODIS 16-day albedo product evaluated with daily observed albedo values for Malcolm Ramsay Lake for clear sky and cloudy sky days from February 15 to April 25, 2012.**

Statistic	Cloudy sky		Cleary sky	
	Observed	MCD43A3	Observed	MCD43A3
Sample size, n	24	24	46	46
Mean	0.75	0.66	0.64	0.65
Standard deviation	0.10	0.05	0.10	0.06
RMSE		0.10		0.06
MAE		0.09		0.04
MBE		-0.08		0.01

sky conditions, so the findings in this study have a lower average error than the 0.07 reported over Greenland. Wang *et al.* (2012) reported an average error less than 0.047, which matches closely the findings in this study. When comparing the MCD43A3 product to *in situ* observations, the presence of clouds increases the average albedo by 4-5% or 0.04-0.05. Evaluating the MCD43A3 product against the entire season of averaged *in situ* observations will be influenced by the amount of cloud cover throughout the season.

Table 3.8 provides a summary of the MCD43A3 retrieved albedos evaluated against the daily *in situ* albedo observations. As mentioned before, MCD43A3 is produced every 8 days and the albedo for each subsequent day is set equal to that updated albedo value until the next update. Using this method, the full 70 day study period can be filled with MCD43A3 albedo values. Using a MCD43A3 retrieved albedo for each day is not an exact albedo and it does not capture sharp changes in albedo (e.g. related to temperature or surface changes), but it does represent the gradual change seen in albedo over the season.

**Table 3.8. MODIS 16-day albedo product evaluated with daily observed albedo values for Malcolm Ramsay Lake from February 15 to April 25, 2012.**

Statistic	Daily averaged albedo	
	Observed	MCD43A3
Sample size, n	70	70
Mean	0.68	0.66
Standard deviation	0.11	0.05
RMSE		0.08
MAE		0.06
MBE		-0.02

The daily mean albedo for MCD43A3 of 0.66 for Malcolm Ramsay Lake from February 15<sup>th</sup> to April 25<sup>th</sup>, 2012, was only 0.02 lower than the *in situ* daily mean albedo. The standard deviation for the MCD43A3 retrieved albedos was lower than the observed standard deviation which was expected, since the albedo remains constant until the next albedo retrieval. The RMSE and MAE values for the MCD43A3 retrieved albedos evaluated against the *in situ* albedos were 0.08 and 0.06, respectively. These values indicate that the average error of the MCD43A3 retrieved albedo values are within 0.10 of the observed *in situ* albedo values. The MCD43A3 16-day albedo product has the same average error as the MYD10A1 daily product and an average error 0.01 higher than the MOD10A1 daily product for both the RMSE and MAE. The MCD43A3 albedo product under all sky conditions reported RMSEs within 0.10, which match the findings of Stroeve *et al.* (2005). However, the MCD43A3 error values reported in this study are higher than error values found in other validation studies. Previous validation investigations have reported the RMSE for MCD43 products to be within 0.05 of observed albedo values (Stroeve *et al.*, 2005; Wang *et al.*, 2012). Although the findings are very close to being within 0.05 average error, the difference can be attributed the all sky conditions where clouds would have an impact on these errors. Still, these findings perform well, being within a 0.10 average error and closely matching the RMSE and MAE values of MOD10A1 and MYD10A1 found in this study.

### **3.3.3 MODIS retrieved albedo values compared to CLIMo albedo values**

The *in situ* observation period on Malcolm Ramsay Lake ended on April 25<sup>th</sup>, 2012 due to warming temperatures leading to unstable lake ice. Therefore, the melting ice and snow albedo parameterization of CLIMo could not be evaluated against *in situ* albedo observations. The lack of *in situ* albedo observations over lake ice provides the opportunity for the MODIS albedo products to help “evaluate” CLIMo’s melting ice albedo parameterization, by comparing the albedo values against each other, and demonstrate MODIS’ ability to retrieve albedo values in environments not easily accessible for observation. There is also potential for the MODIS albedo products to be integrated into CLIMo and this comparison demonstrates the need for integration into the model or not. It has been shown, in sections 3.3.1 and 3.3.2, how CLIMo derived and MODIS retrieved albedos perform when evaluated against *in situ* observations made on Malcolm Ramsay Lake from February 15<sup>th</sup> to April 25<sup>th</sup>, 2012, but CLIMo and MODIS record albedo values very differently. CLIMo’s albedo parameterization is part of a 1-D model and only derives an albedo value for a single point on the surface where atmospheric forcing variables are collected. The albedo parameterization for CLIMo is based on previous observations made in high-latitude climates. MODIS, on the other

hand, retrieves albedo values from information contained within a pixel that has a 500 m spatial resolution after it has been corrected for any atmospheric effects and correction for anisotropic reflection at the surface (Klein and Stroeve, 2002). Due to these differences in surface albedo representation, it is useful to first compare CLIMo and MODIS derived albedo values during the ice growth season since these have both been evaluated against *in situ* ground observations. The main reason for the comparison is to assess if CLIMo's albedo parameterization accurately captures the temporal evolution of albedo during both the ice growth and break-up (melt) period. In the following sections, the MODIS albedo products are compared with CLIMo derived albedos for the ice growth (field season), February 15<sup>th</sup> to April 26<sup>th</sup>, 2012, and the break-up periods, May 7<sup>th</sup> to June 6<sup>th</sup>, 2012.

### 3.3.3.1 Ice growth period

The albedo values for the MODIS products and CLIMo derived albedos both with and without snow included in the model are plotted against each other in Figure 3.13. The figure illustrates that CLIMo with snow added into the model appears to overestimate MODIS retrieved albedo values while CLIMo without snow added into the model appears to underestimate MODIS retrieved albedos. The mean values seen in Table 3.9 where the mean albedo values for CLIMo with and without snow are 0.75 and 0.58, respectively and all three MODIS albedo products have means that fall in between

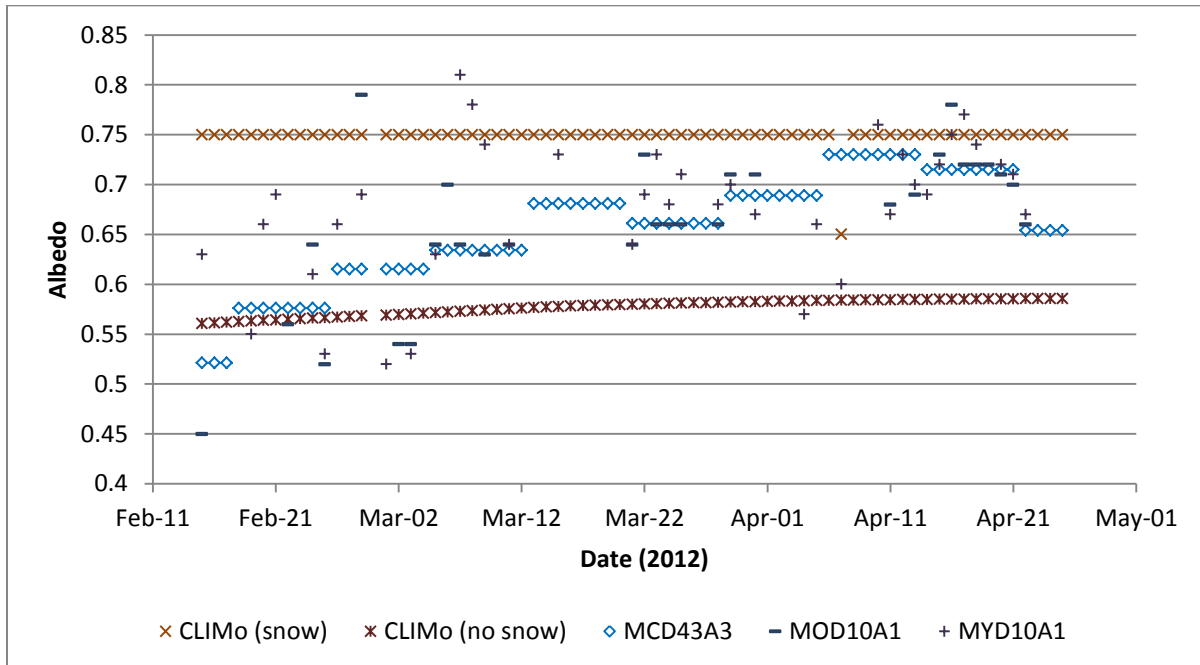


**Figure 3.13. MODIS retrieved and CLIMo derived albedo values for Malcolm Ramsay Lake from February 15<sup>th</sup> to April 25<sup>th</sup>, 2012.**

those two means (see Table 3.9). The standard deviations for the MODIS albedo products are higher than the CLIMo standard deviations indicating that there is more variation within the MODIS albedo products than CLIMo's albedo parameterization. As discussed earlier, MODIS is capable of retrieving albedo values that follow trends in surface changes for the 500 m<sup>2</sup> pixel whereas CLIMo's albedo parameterization has trouble with this aspect. When comparing the MODIS albedo products with both model runs of CLIMo, RMSD, MAD, and MD values were as expected after visual inspection of the data (Table 3.10). The RMSD values for MOD10A1, MYD10A1, and MCD43A3 against CLIMo with snow were 0.12, 0.10, and 0.11, respectively. The RMSD values for MOD10A1, MYD10A1, and MCD43A3 were 0.11, 0.12, and 0.09, respectively. These values indicate that the MODIS albedo products and CLIMo albedo parameterization have an average difference that is 0.10. The MD values for MOD10A1, MYD10A1, and MCD43A3 confirm that the MODIS albedo values are lower than those estimated by CLIMo with snow added to the model (negative MD values) and higher without snow added to the model (positive MD values). Even though the MODIS albedo products represent a gridded product, it would still be useful to integrate them into the 1-D model CLIMo, because they are able to capture changes to the surface better than the CLIMo albedo parameterizations as was seen in section 3.3.2. It is important to have the correct albedo on a daily basis, because it determines how much shortwave radiation is being absorbed or reflected at the surface.

**Table 3.9. Descriptive statistics for MODIS retrieved and CLIMo derived albedo values for Malcolm Ramsay Lake from February 15th to April 25th, 2012.**

Statistic	CLIMo (snow)	CLIMo (no snow)	MOD10A1	MYD10A1	MCD43A3
Mean (Standard Deviation)	0.75(0.01)	0.58(0.01)	0.66(0.08)	0.68(0.07)	0.66(0.06)

**Table 3.10. Difference statistics for MODIS retrieved and CLIMo derived albedo values for Malcolm Ramsay Lake from February 15th to April 25th, 2012.**

Model version	Statistic	MOD10A1	MYD10A1	MCD43A3
CLIMo (snow)	RMSD	0.12	0.10	0.11
	MAD	0.09	0.08	0.09
	MD*	-0.09	-0.07	-0.09
CLIMo (no snow)	RMSD	0.11	0.12	0.09
	MAD	0.10	0.11	0.08
	MD*	0.08	0.10	0.08

**\*Positive (Negative) values indicate that MODIS albedos are, on average, higher (lower) than CLIMo derived albedos.**

### 3.3.3.2 Break-up period

Thus far, the MODIS albedo products and cold ice and cold snow albedo parameterizations of CLIMo have been evaluated against *in situ* observations. However, *in situ* observations ended on April 25<sup>th</sup>, 2012 to ensure that the equipment did not fall into Malcolm Ramsay Lake. This leaves CLIMo's melting ice and melting snow parameterizations unevaluated. Since there were no *in situ* albedo observations made after the end of April 2012, the MODIS albedo products were compared with the melting ice/snow parameterizations to assess their general performance. The break-up period began on May 7<sup>th</sup>, 2012 and reached predicted open water conditions for CLIMo with snow and CLIMo without snow on June 5<sup>th</sup> and June 9<sup>th</sup>, respectively, at the location of the MODIS 500-m<sup>2</sup> pixel (see Figure 3.1). MODIS retrieved albedo values were not available following June 9<sup>th</sup> for the daily products (cloud interference) and MCD43A3 retrieved albedos that resembled open water values (less than 0.05).

The MODIS albedo products performed very well retrieving albedo over lake ice when evaluated against the *in situ* observations during the cold winter season (within 0.10). The albedo values for the albedo products MOD10A1, MYD10A1, and MCD43A3 as well as the albedo values for CLIMo run with and without snow can be seen in Figure 3.14. CLIMo with snow added to the model has a constant albedo of 0.65 at the beginning of the melt season before dropping suddenly on May 12<sup>th</sup>. The melting snow albedo parameterization comes into effect when the surface temperature is above the melting temperature at the surface (0°C or 273.15K). The coverage of the MODIS daily albedo products (MOD10A1 and MYD10A1) is sporadic due to cloud cover, but it can be seen, in Figure 3.14 that MODIS albedo products are similar to the melting ice parameterization in CLIMo at the beginning of the melt season, but do not retrieve albedos as low as CLIMo simulates as the season progresses. The MCD43A3 16-day product was not able to retrieve an albedo value before lake ice break-up, but it also reported similar albedo values to the daily MODIS products.

The performance statistics can be seen in Table 3.11. The mean retrieved albedo values for MOD10A1, MYD10A1, and MCD43A3 are 0.41, 0.36, and 0.39, respectively, when compared to the same days used for CLIMo derived albedo values with snow included in the model and 0.40, 0.36, and 0.39, respectively, when compared to the same days used for CLIMo derived albedos without snow in the model. The reason for the slight difference in means for MOD10A1 is due to the difference break-up dates simulated by CLIMo with and without snow included the model. The average albedo retrievals made by the MODIS products agree with observations made by Henneman and Stefan (1999) where they found average minimum surface albedo of a freshwater lake during melt to be  $0.38 \pm 0.033$ . The mean albedo values for CLIMo with and without snow are 0.28 and

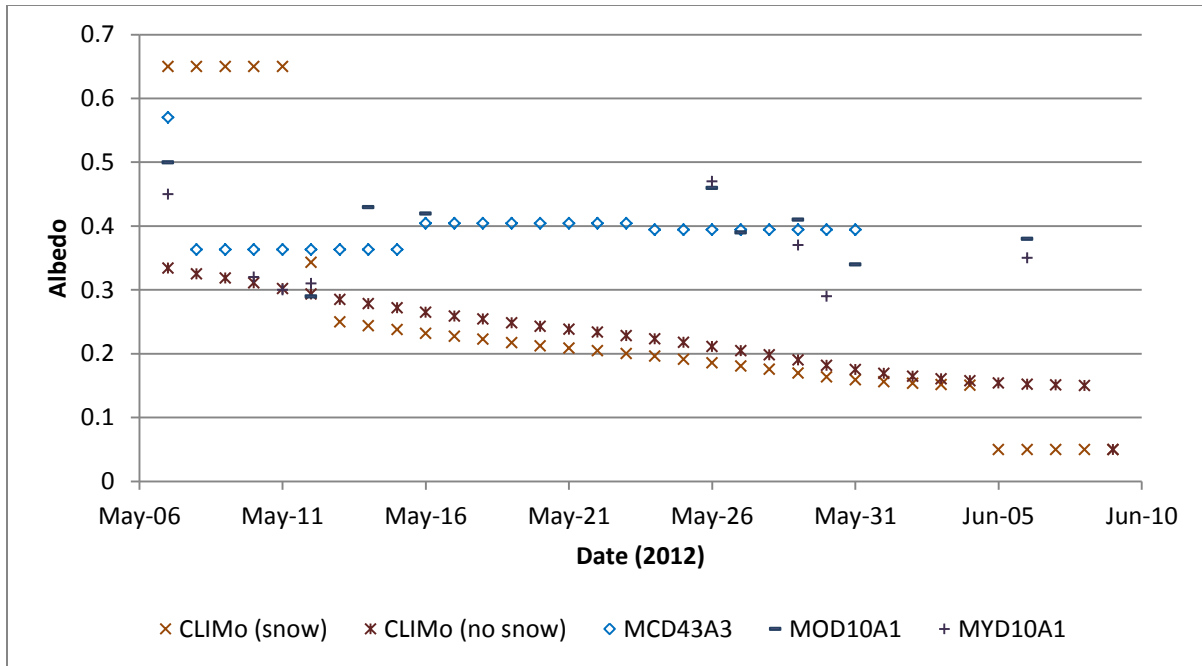


**Figure 3.14. MODIS retrieved and CLIMo derived albedo values for Malcolm Ramsay Lake from May 7<sup>th</sup> to June 9<sup>th</sup>, 2012.**

**Table 3.11. Difference statistics for MODIS retrieved and CLIMo derived albedo values for Malcolm Ramsay Lake from May 7th to June 9th, 2012.**

Statistic	CLIMo (snow)	MOD10A1	MYD10A1	MCD43A3
Sample size, n	29	8	7	25
Mean	0.28	0.41	0.36	0.39
Standard deviation	0.18	0.07	0.07	0.04
RMSD		0.20	0.24	0.20
MAD		0.19	0.22	0.19
MD*		0.13	-0.04	0.10
	CLIMo (no snow)	MOD10A1	MYD10A1	MCD43A3
Sample size, n	33	9	8	25
Mean	0.23	0.40	0.36	0.39
Standard deviation	0.06	0.06	0.07	0.04
RMSD		0.18	0.14	0.15
MAD		0.17	0.11	0.14
MD *		0.17	0.11	0.14

**\*Positive (Negative) values indicate that MODIS albedos are, on average, higher (lower) than CLIMo derived albedos.**

0.23, respectively, which are lower than the mean albedos seen by the MODIS albedo products. The mean albedo for CLIMo with snow is larger than CLIMo without snow due to the melting snow albedo parameterization at the beginning of the break-up period (melt). The high albedo values of the melting snow albedo parameterization also accounts for CLIMo with snow's higher standard deviation (0.18) when compared to the other albedo retrieval products (see Table 3.11). The RMSD for the comparison between CLIMo with snow derived albedos and the MOD10A1, MYD10A1, and MCD43A3 retrieved albedos are 0.20, 0.24, and 0.20, respectively. The MAD for the comparison between CLIMo with snow derived albedos and the MOD10A1, MYD10A1, and MCD43A3 retrieved albedos are 0.19, 0.22, and 0.19, respectively. These differences are much larger than MODIS albedo products and CLIMo comparisons during the ice growth period. It is difficult to report the MD for CLIMo with snow due to a high range in albedo values (e.g. the melting snow parameterization produces an albedo equal to 0.65). This can be specifically seen for MYD10A1, which had three of its seven retrievals during the melting snow parameterization. The MD between CLIMo derived albedos with snow in the model and MYD10A1 are negative which indicates that CLIMo derived albedos are, on average, 0.04 lower than MYD10A1 retrieved albedo values over lake ice which is opposite of what is seen when comparing CLIMo to MOD10A1 and MCD43A3 (see Table 3.11). CLIMo derived albedos without snow present in the model did not have the melting snow parameterization at the beginning of the melt season to influence the comparison with the MODIS albedo products. The RMSD for the CLIMo without snow in the model compared to MOD10A1, MYD10A1, and MCD43A3 retrieved albedos are 0.18, 0.14, and 0.15, respectively. The MD for CLIMo without snow in the model compared to MOD10A1, MYD10A1, and MCD43A3 retrieved albedos are 0.17, 0.11, and 0.14, respectively. These differences, while still large, are closer to the MODIS albedo products and CLIMo derived albedos during the cold weather field season. These MD values are not influenced by the melting snow parameterization in CLIMo and, therefore, we can confidently say that the MODIS albedo products retrieved albedo values larger than albedo values simulated by CLIMo's melting ice albedo parameterization. Based on these difference results, it can be concluded that the melting ice parameterization for CLIMo underestimates albedo when compared to those values retrieved by MODIS. The MODIS albedo values have been shown to have an average error within 0.10 of *in situ* albedo observations over lake ice. However, for this particular melt season in Churchill, the amount of clear-sky days that were required for the MODIS albedo products to make albedo retrieval were very sparse (i.e. small number of days for comparison). Integrating MODIS albedo values directly into CLIMo could benefit ice-off date simulations, but there is still a large reliance on the melting snow and melting ice parameterizations during the lake ice

simulations. Further study on melting ice and snow parameterizations is required before being able to make any solid conclusions.

### 3.4 Summary and conclusions

This study evaluated CLIMo's albedo parameterization and the MODIS albedo products MOD10A1, MYD10A1, and MCD43A3 against *in situ* albedo observations made on Malcolm Ramsay Lake, Churchill, Manitoba during the winter of 2012. The study also compared CLIMo's albedo parameterization with the MODIS albedo products during the ice growth period as well as the ice break-up period (melt).

The model performed well simulating albedo, but had difficulty simulating bare ice albedo. CLIMo albedo simulations were performed with and without snow integrated into the model and evaluated against *in situ* albedo observations recorded over clear ice (Site A), snow (Site B), and snow ice (Site C). It was noted that Site A and C experienced a change in surface conditions partway through the ice growth season due to snowfall events. The snowfall events resulted in snow being present underneath the pyranometers recording albedo at Sites A and C. CLIMo's snow albedo simulations for the entire ice growth season evaluated against snow albedo observations recorded at Site B had a RMSE equal to 0.07 and a MAE equal to 0.06. Following the change in surface type under Site's A and C, CLIMo's snow albedo simulations evaluated against Site's A and C recorded albedo observations had RMSE values equal to 0.08 for both and MAE values equal to 0.05 and 0.06, respectively. When snow cover was present at the *in situ* stations, CLIMo consistently simulated snow albedo values with an average error within 0.10 of *in situ* observations. The bare ice simulations calculated using CLIMo's cold ice albedo parameterization did not perform as well as the snow albedo simulations. Evaluating CLIMo's bare ice simulations against Site A (clear ice) and Site C (snow ice) showed that CLIMo overestimated bare ice albedo with MBE values equal to 0.13 and 0.10, respectively. With snow removed from CLIMo, the albedo parameterization still overestimated bare ice *in situ* albedo observations, but did perform well when the *in situ* observations were averaged together having a RMSE equal to 0.06. The cold ice albedo parameterization has shown that it overestimates bare ice observations and underestimates snow albedo, but it works well when evaluated against an average albedo of surface types. The cold ice parameterization appears to overestimate bare ice albedo in all situations except for very pure snow ice examples. The snow albedo parameterization does not capture variation due to surface changes and other factors that affect snow albedo, but it does provide an albedo that is representative of the albedo of snow.

MODIS albedo products were also evaluated against the average *in situ* albedo observations recorded on Malcolm Ramsay Lake. The MOD10A1, MYD10A1, and MCD43A3 products reported RMSE values equal to 0.07, 0.08, and 0.08, respectively, when evaluated against daily *in situ* albedo averages. The RMSE values for the daily MODIS products, MOD10A1 and MYD10A1, agree with previous validation studies performed on the products. MCD43A3 RMSE values were slightly higher than previous validation studies, but this was due to the evaluation against cloudy sky days as well. Cloudy conditions were found to increase snow and ice albedo by 0.07 (7.7%) on average. The MODIS products performed about as well as CLIMo's snow albedo parameterization. However, it is important to note that the MODIS albedo products were able to capture the apparent surface change that was observed by Site's A and C during the snowfall events in March. The MODIS albedos are capable of providing accurate albedo retrievals over a 500 m by 500 m area.

Without *in situ* measurements during the break-up (melt) period, CLIMo's albedo parameterization could not be evaluated against ground observations. However, knowing that the MODIS albedo products retrieved albedo values with an average error of 0.10 during the field season meant that the MODIS albedo products could be compared with CLIMo's albedo parameterization to gain a basic understanding of how CLIMo performed during lake ice break-up. Since both CLIMo and the MODIS products were evaluated against *in situ* observations, the comparison was done during the ice growth period (field season) as well. During the ice growth period, the comparison between the MODIS albedo retrievals and CLIMo simulated albedo values had an average difference around 0.10. It was found that MODIS retrieved albedo values were lower than CLIMo with snow in the model having MD values for MOD10A1, MYD10A1, and MCD43A3 equal to -0.09, -0.07, and -0.09, respectively. MOD10A1, MYD10A1, and MCD43A3 retrieved albedo values higher than CLIMo without snow with MD values equal to 0.08, 0.10, and 0.08 respectively. CLIMo without snow was found to overestimate *in situ* bare ice albedo measurements and underestimate *in situ* snow albedo measurements so the MD results after the comparison with MODIS albedo products were expected. MODIS retrieves surface albedo over a 500 m<sup>2</sup> surface area which would capture the variable surface cover (bare ice and snow) during the ice growth season for Malcolm Ramsay Lake. During the break-up period, the MODIS albedo products retrieved albedos that were higher, on average, than the CLIMo albedo simulations. The MD for the MODIS albedo products compared to CLIMo with snow was difficult to interpret due to the stark contrast in albedo values between the melting snow and melting ice albedo parameterization in CLIMo. The RMSD and MAD values for the comparison between MODIS albedo products and CLIMo with snow were at least 0.19 or greater for each MODIS product, which is a fairly large difference. For the comparison between the MODIS

albedo products and CLIMo without snow, the RMSD and MAD values were similar but not as large. The RMSD for MOD10A1, MYD10A1, and MCD43A3 compared to CLIMo without snow were equal to 0.18, 0.14, and 0.15, respectively. The MAD for MOD10A1, MYD10A1, and MCD43AD were equal to 0.17, 0.11, and 0.14, respectively. The MD for the comparison between the MODIS albedo products and CLIMo without snow was easier to interpret due to the absence of the melting snow parameterization. The MD for MOD10A1, MYD10A1, and MCD43A3 compared with CLIMo without snow were equal to 0.17, 0.11, and 0.14, respectively. CLIMo simulations were low overall when simulating albedo during break-up. These conclusions should be taken lightly since MODIS albedo retrievals are approximations. Also, the MODIS daily products (MOD10A1/MYD10A1) had low sample sizes due to cloud interference.

Satellite remote sensing is capable of retrieving observations in environments that are not easily accessible and/or in environments where atmospheric forcing variables are hard to measure. The integration of MODIS albedo products into CLIMo could provide daily albedo measurements that represent the surface conditions over a 500 m<sup>2</sup> area and improve the simulation of lake ice break-up. However, MODIS albedo acquisitions are limited to clear-sky conditions and this limited the number of observations made during the break-up period. Also, the fact that the MODIS albedo products have a 500 m spatial resolution had to be evaluated as well, because CLIMo is a 1-D lake ice model. CLIMo's albedo parameterization calculates albedo at a single point and does replicate an albedo value that is representative of an entire lake surface. The MODIS albedo products have been shown to retrieve freshwater lake snow and ice albedo accurately when compared to *in situ* measurements. CLIMo's albedo parameterization performed well simulating snow albedo when compared to *in situ* observations, but the cold and bare ice parameterizations have shown that the parameterization does need some improvement. In future studies, the integration of the MODIS albedo products MOD10A1, MYD10A1, and MCD43A3 into CLIMo will be investigated to see if capturing variation in surface albedo over freshwater lakes improves the simulated break-up dates.

# Chapter 4

## Integrating MODIS albedo within a lake ice model

### Overview

Moderate Resolution Imaging Spectrometer (MODIS) albedo products (MOD10A1, MYD10A1, and MCD43A3) were integrated directly into the Canadian Lake Ice Model's (CLIMo) albedo parameterization to see if there was an improvement in the simulation of break-up (ice-off) dates for Back Bay on Great Slave Lake near Yellowknife, Northwest Territories. The high albedo of snow and lake ice has been shown to affect the timing of break-up. Therefore, the surface energy balance parameterization of CLIMo requires accurate albedo values when modelling the phenology of lake ice. The albedo of snow and lake ice can vary from day-to-day and the MODIS albedo products are capable of capturing these variations. Three different snow cover scenarios (0%, 68%, and 100% snow cover) were used to reproduce a wide range of possible ice conditions for each winter. CLIMo with and without the MODIS albedo products performed better when snow cover was included into the model. When integrated up to a month prior to lake ice break-up for Back Bay, CLIMo with MODIS albedos reported accurate RMSE and MAE values of 3-4 days when compared to MODIS observed break-up dates. However, CLIMo using the original albedo parameterization also performed well reporting RMSE and MAE values of 4-5 days. While the MODIS albedo products do not greatly improve break-up simulations for CLIMo, they are able to produce break-up dates as well as CLIMo. CLIMo's albedo parameterization has been shown to perform adequately in simulating albedo during the melt period for Back Bay. However, the MODIS albedo products are still useful for capturing albedo in remote locations as well as capturing daily variations in albedo. MODIS albedo products could still benefit CLIMo's lake ice break-up simulations in future work via data assimilation techniques.

### 4.1 Introduction

At high latitudes, lakes can cover 15% to 40% of the landscape, making them an important part of the cryosphere for several months of the year (Duguay et al., 2003). The hydrologic cycle in the North is

heavily influenced by the presence or absence of ice. Earlier ice break-up dates lead to greater incoming solar radiation being absorbed rather than reflected by lakes while later freeze-up dates allow for “more evaporative moisture to be transferred into the atmosphere” into the fall to early winter period (Duguay et al., 2003). Duguay et al. (2003) developed the Canadian Lake Ice Model (CLIMo) for the purpose of improving our understanding of the response of lake ice to climate and the effect of lake ice presence or absence on high-latitude weather and climate. CLIMo has previously been evaluated in its simulation of lake ice phenology (freeze-up and break-up), thickness and composition (clear ice and snow ice), and surface temperature in Arctic, sub-Arctic, and high-boreal forest environments (e.g. Brown and Duguay, 2010; Brown and Duguay 2011a; Duguay et al., 2003; Kheyrollah Pour *et al.*, 2012; Ménard *et al.*, 2002). Snow and ice albedos are two components parameterized in CLIMo that are particularly important to simulate during the break-up period. Snow and freshwater ice have relatively high albedos (0.50 to 0.90 and 0.15 to 0.60, respectively) when compared to open water (0.06 to 0.10) (Bolsenga, 1977; Grenfell *et al.*, 1994; Herron and Woo, 1994; Serreze and Barry, 2005; Warren, 1982; Wiscombe and Warren, 1980). Surface albedo is defined as the ratio of upwelling (reflected) to downwelling (incident) radiative flux at the surface; therefore, surface albedo is the part of the surface energy balance that determines how much incoming shortwave solar radiation is reflected or absorbed by a surface (Hostetler, 1991).

CLIMo, the lake ice model of interest in this study, utilizes a number of parameterizations for the computation of lake ice phenology and growth. Martynov et al. (2011) found that altering the albedos of lake models that include an ice cover component, such as CLIMo, had a direct effect on the timing of break-up (ice-off) dates. In the particular case of CLIMo, the albedo parameterization is comprised of a cold ice parameterization taken from Maykut (1982) and a melting ice parameterization that is based on observations made by Heron and Woo (1994). Currently, the surface albedo in CLIMo evolves with surface temperature and is also dependent on the surface type (i.e. ice, snow, or open water) and ice thickness. Surface temperature and surface type are important determining factors of surface albedo, but the albedo of snow and freshwater ice are also controlled by other factors as well. Snow albedo is affected by the presence of impurities, density, composition, age, solar zenith angle (SZA), wetness, and surface roughness (Gardner and Sharp, 2010; Grenfell *et al.*, 1981; Henneman and Stefan, 1999). Freshwater ice albedo is affected by similar factors that affect snow. Other factors that affect freshwater ice albedo include the bubble content (especially near the surface), absorption coefficient, and ice composition (Gardner and Sharp, 2010; Henneman and Stefan, 1999; Mullen and Warren, 1988). Clouds also have an effect on the snow and ice albedo where the presence of clouds will raise the albedo of snow and ice by several percent (Key et al.,

2001). Many of the different factors affect the albedo of snow and ice and the albedo can change on a day-to-day basis. Integrating satellite remote sensing surface albedo products into models are beginning to be investigated to capture these daily changes and improve model outputs (Malik et al., 2012).

The goal of this study is to determine if the integration of Moderate Resolution Imaging Spectroradiometer (MODIS) daily snow albedo products and a MODIS 16-day albedo product into CLIMo leads to a significant improvement in the estimation of break-up dates. Lake ice break-up periods for 12 years (2000 to 2011) on Back Bay, Great Slave Lake (near Yellowknife, Northwest Territories) are the focus of this investigation.

## **4.2 Study area**

### **4.2.1 Yellowknife (Back Bay), Northwest Territories**

Back Bay (62°21'45.00"N, 114°20'40.22"W) is located near Yellowknife, Northwest Territories on the north end of Great Slave Lake's (GSL) central basin (Figure 4.1). The main basin of GSL has a mean depth of 41 m and a maximum depth of 163 m, while the eastern arm has a mean depth of 249 m and a maximum depth of 614 m (Howell et al., 2009). According to Ménard et al. (2002), Back Bay has a mean depth of approximately 10 m. Back Bay was selected for this study for three reasons: (1) it is protected by surrounding land from the dynamic break-up processes encountered in more opened and deeper sections of GSL (e.g., central basin) (Figure 4.1), hence ice break-up is mainly thermodynamically driven (i.e. *in situ* melt); (2) it is large enough to be seen in the MODIS albedo products without any land contamination; and (3) the site has been the subject of previous investigations involving the verification of CLIMo in its determination of freeze-up and break-up dates, and ice/snow thickness (Brown and Duguay, 2011; Ménard et al., 2002).

CLIMo was forced using data obtained from the nearby Yellowknife airport meteorological station over 12 years (2000 to 2011). Vegetation in the vicinity of the meteorological station is typical of the taiga found on the Precambrian Shield (Ménard et al., 2002). Yellowknife experiences temperatures ranging from 7.1°C to 16.8°C in the summer and -17.3°C to -26.8°C in the winter months. Historically, annual precipitation is 280.7 mm with 151.8 cm falling as snow.

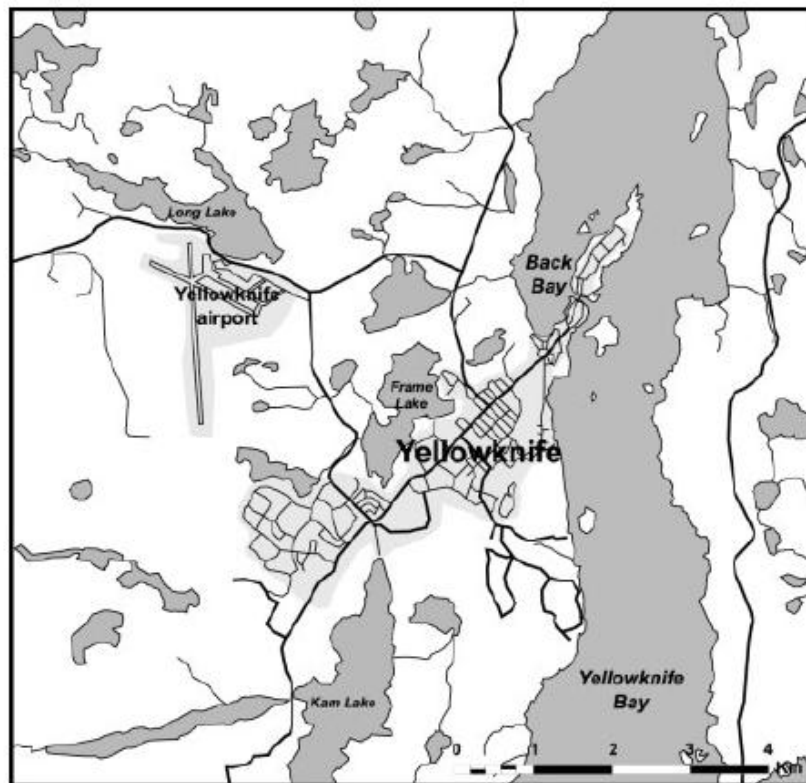
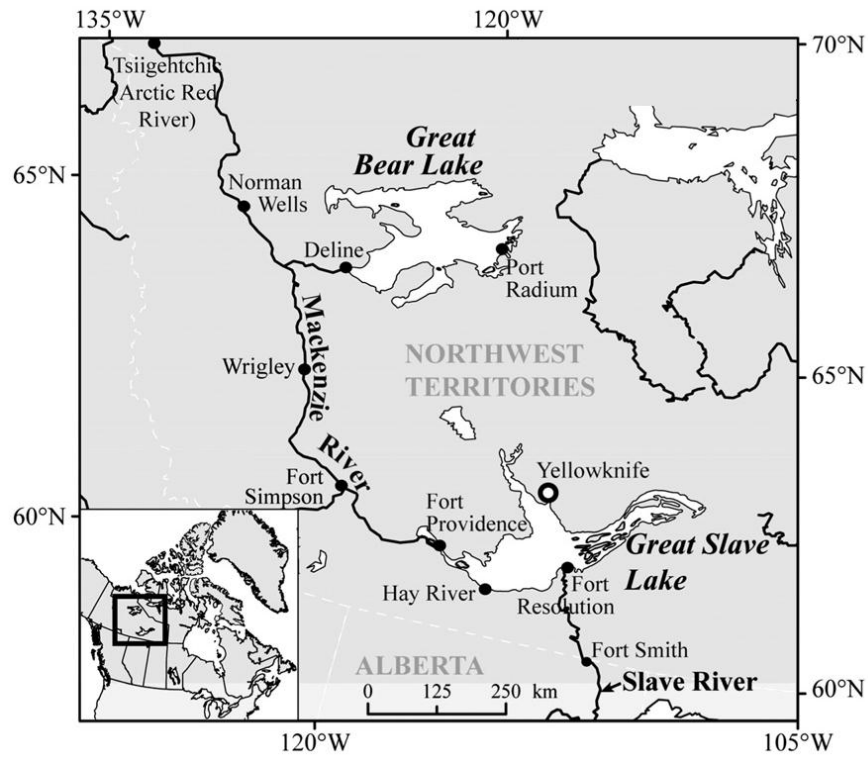


**Figure 4.1. (Top) Map of Great Bear Lake and Great Slave Lake. (Bottom) A map that shows the location of Back Bay in relation to Yellowknife, NWT (Sources: Howell *et al.*, 2009; Ménard *et al.*, 2002).**

### 4.3 MODIS snow albedo products and methods for integration

The MODIS sensor was designed to view the entire globe every 1 to 2 days. MODIS has 36-channels ranging from the visible spectrum to the thermal infrared spectrum (0.405 to 14.385  $\mu\text{m}$ ) with bands 1 and 2 at a 250 m spatial resolution; bands 3 to 7 with a 500 m spatial resolution, and bands 8 to 36 with a 1000 m spatial resolution (Salomonson *et al.*, 2006). The MODIS sensor is onboard NASA's Earth Observation System (EOS) satellites Terra and Aqua and has a near-polar orbit (Hall *et al.*, 2009; Salomonson *et al.*, 2006). Terra was launched in December of 1999 and Aqua was launched in May of 2002 (Hall *et al.*, 2009; Salomonson *et al.*, 2006).

The MODIS albedo products used in this study are the MOD10A1/MYD10A1 (MxD10A1 from now on) daily snow products, and the MCD43A3 albedo product. The bands utilized by these MODIS products are shown in Table 4.1. Each of the snow products only retrieves albedo values under clear sky conditions. Cloud cover is a source of error in this study. The MCD43A3 product retrieves albedo from the previous 16 days collected over a specific location. MCD3A3 is used to fill in gaps when daily albedo values from MxD10A1 are not available. While MCD43A3 is not the albedo for a specific date, it does represent recent albedo conditions observed at a location and is reliably updated every eight days. However, if daily albedo is missing for a specific day, there is a good chance that this is due to cloud cover. Key *et al.* (2004) found cloud cover to increase surface albedo of snow and ice up to 4-6% on average. In Chapter 3, it was reported that cloud cover increased surface albedo by 7.7% on average. This means that MCD43A3 albedo measurements used on cloudy days could underestimate the surface albedo actually experienced at the surface on cloudy days. It will be assumed that the difference is negligible, but should still be kept in mind when interpreting the results of this study.

**Table 4.1. MODIS bands used by the products in this study (Hall *et al.*, 2009; Salomonson *et al.*, 2006).**

Band	Spectral Resolution ( $\mu\text{m}$ )	Spatial Resolution (m)	Product
1	0.620 – 0.670	250 by 250	MxD10A1 and MCD43A3
2	0.841 – 0.876	250 by 250	MxD10A1 and MCD43A3
3	0.459 – 0.479	500 by 500	MxD10A1 and MCD43A3
4	0.545 – 0.565	500 by 500	MxD10A1 and MCD43A3
5	1.230 – 1.250	500 by 500	MxD10A1 and MCD43A3
6	1.628 – 1.652	500 by 500	MxD10A1 and MCD43A3
7	2.105 – 2.155	500 by 500	MxD10A1 and MCD43A3

Another source of error is high SZAs experienced in the winter at high latitudes. High SZAs are known to increase the surface albedo of snow and ice (Gardner and Sharp, 2011). Stroeve et al. (2006) found erroneous albedo values in their study of the MODIS daily products MxD10A1. These values include impossible albedo values equal to 100% albedo and many that exceed an albedo of 90%. The errors were attributed to high SZAs. Riggs et al. (2006) attempted to eliminate these errors in MxD10A1 by including SZA as a scoring factor in the algorithm and choosing observations made closest to local solar noon when the SZA would be lowest. Still, these erroneous values were present regardless of the changes (Riggs et al., 2006). These erroneous values were also observed in this study for both the daily albedo products as well as the 16-day product, MCD43A3. The SZA for the MCD43 products are limited to being less than  $75^\circ$ , but any SZA above  $70^\circ$  are considered unreliable (Stroeve et al., 2005; Wang et al., 2012). Due to the high latitude location of Back Bay (above  $60^\circ$  N), SZAs during the winter are generally high and are likely to be the cause of the impossible albedo values. In order to ensure that only accurate albedo values are being integrated into CLIMo, several different selection methods (discussed in further detail in section 4.6) are used in this study to determine when to start integrating MODIS albedo values.

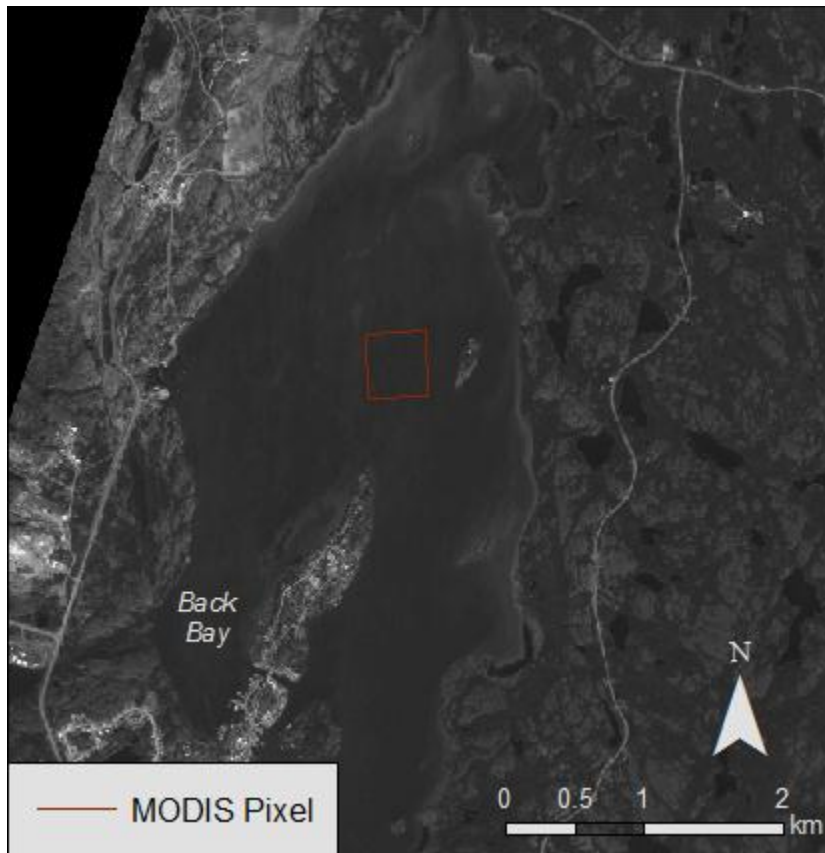


**Figure 4.2. Location of the MODIS pixel near Back Bay (Yellowknife).**

Both the MODIS daily and 16-day albedo products have 500 m spatial resolutions. A pixel, in close proximity to Back Bay (Yellowknife), was carefully selected to ensure that the acquired albedo represented only snow and lake ice (i.e. without land contamination). All albedo data retrieved from the MODIS albedo products were taken from the spatial segment illustrated in Figure 4.2. It is important to note that albedo retrieved from the MODIS products represent one satellite pass during a day and not the daily average albedo. Unfortunately, determining the time of each acquisition for each day is a complicated process and not included in the MODIS albedo products (Stroeve et al., 2006). While CLIMo produces an average albedo for each day, it was determined in Chapter 3 that the retrievals from a satellite overpass still accurately represent the albedo for that day.

### **4.3.1 MxD10A1 daily snow product**

The MxD10A1 daily snow product is a tile of the data gridded in the sinusoidal projection by MOD10\_L2G. MOD10A1 utilizes images acquired from the Terra satellite, while MYD10A1 uses images acquired from the Aqua satellite. These daily snow products are level 3 products. This means that they are geophysical products that have been altered temporally or spatially and put into a grid. Each tile is approximately 1200 by 1200 km and has a 500 m nominal resolution. Within the snow product is a snow albedo output science dataset (SDS) (Riggs et al., 2006). The term ‘daily’ does not mean that these products provide daily albedo averages. The albedo value produced “is the ‘best’ single observation in a day” (Stroeve *et al.*, 2006). Daily refers to the albedo value being selected once per day based on factors such as cloud presence as well as viewing and illumination angles (Stroeve *et al.*, 2006). For the snow albedo SDS, a “narrowband reflectance is calculated for each of the seven MODIS bands seen in Table 4.1 and then combined into a spectrally integrated broadband albedo” (Hall et al., 2009). MOD10A1 is calculated under clear sky conditions which are determined by the MOD35 cloud mask product (Hall et al., 2009; Klein and Stroeve, 2002). However, Klein and Stroeve (2002) did report some difficulties with the cloud mask product where it incorrectly classified dates with cloud cover when *in situ* measurements determined otherwise. This is a problem that cannot be overcome and it is assumed that all measurements from the MOD10A1/MYD10A1 products are accurate and classified correctly.

Past validation studies for MxD10A1 have compared the daily snow product albedo estimates to ground-based observations acquired over snow and the Greenland ice sheet. MxD10A1 products were found to be within 10% of these ground-based observations (Klein and Stroeve, 2002; Stroeve et al., 2006). In Chapter 3, it was found that the MxD10A1 products compared to ground-based

observations from lake ice near Churchill, Manitoba, displayed similar accuracies that were also within 10%.

### **4.3.2 MCD43A3 albedo product**

The MODIS albedo product MCD43A3 combines the Terra and Aqua satellites to produce a 16-day level 3 product that produces an albedo map every eight days at a 500 m nominal resolution in a sinusoidal grid. Its outputs consist of a black sky albedo (BSA) (directional hemispherical reflection with no diffuse component) and a white sky albedo (WSA) (bi-hemispherical reflection with no direct component and a diffuse component that is isotropic) (Schaaf, 2004). The MCD43 products use the Ross Thick-Li Sparse Reciprocal (RTLSR) Bidirectional Reflectance Distribution Function (BRDF) that is capable of deriving surface albedo values. This study utilizes the BSA since its albedos “are computed for the local noon SZA for each location” and that was deemed to be adequate (Schaaf et al., 2002).

MCD43A3 utilizes a full model inversion or a backup magnitude inversion to create the BRDF dependent on whether certain conditions are met (Schaaf et al., 2002). MODIS makes frequent overpasses at high latitudes due to its near-polar orbit. For the full model inversion to be run, seven cloud-free observations of the surface are required during the 16-day period (Schaaf et al., 2002). If there is not a sufficient amount of cloud-free observations, the backup magnitude inversion method is used where a priori information (static field-based BRDFs) is used in conjunction with any observations made (Schaaf et al., 2002).

Stroeve et al. (2005) performed a validation study on the MCD43 product with *in situ* observations in Greenland and found MCD43 to have an average root mean square error (RMSE) of 0.07. In Chapter 3, MCD43A3 was found to have an average RMSE of 0.08 when compared *in situ* ground observations over lake ice near Churchill, Manitoba. The slightly higher RMSE value was attributed to the product being compared against all-sky conditions. Under clear sky conditions, an average RMSE of 0.06 was obtained when comparing the MCD43A3 product to *in situ* observations over lake ice.

## **4.4 Ice-off observations from MODIS**

CLIMo defines its break-up (ice-off) date as the first date of the year when the thickness of lake ice is equal to zero. To match CLIMo, the observed break-up date was determined to be when ice is no longer visibly present. Ground observations for lake ice break-up were not available for Back Bay from 2000 to 2011. Instead, the use of satellite imagery for the determination of lake ice break-up

dates over Back Bay was explored. Duguay et al. (2003) utilized airborne and satellite observations of break-up dates for their study and determined that they “provide a better, more objected means of evaluating the ability of CLIMo to simulate lake-ice phenology spatially at a regional scale.” MODIS imagery at 500 m spatial resolution pixel was therefore used to determine break-up dates. Two MODIS daily products were used for this purpose: MxD10A1 daily snow albedo and the MOD09GA and MYD09GA (MxD09GA from now on) daily surface reflectance products. Rather than provide a surface albedo value for open water, the MODIS daily products indicate the presence of open water when the snow and lake ice have completely melted away. Using the first day of open water or when the pixel is consistently open water is one method of determining the break-up date. The MxD09GA daily surface reflectance product contains the seven bands shown in Table 4.1. Using combinations of these bands, it is possible to make true and false colour composite images that can be used to assess the presence of lake ice (Figure 4.3). Band 5 is located in the near-infrared (NIR) portion of the electromagnetic spectrum. NIR is almost completely absorbed by liquid water. Snow and ice are not great reflectors of NIR, but they do reflect more incoming NIR than water. Using true colour composite imagery and NIR bands, one can determine the break-up in Back Bay with confidence. The presence of cloud cover is a source of error when using this method, because clouds prevent the observation of surface conditions. This means that there can be periods of several days when observations cannot be made. This almost always results in a slight overestimation (later) of the break-up date for lake ice although it is possible for underestimations to occur as well. For this study, only the break up date for 2001 was subject to an extended period of cloudy conditions. The break-up date for 2001 may be anywhere from one to seven days earlier than recorded.

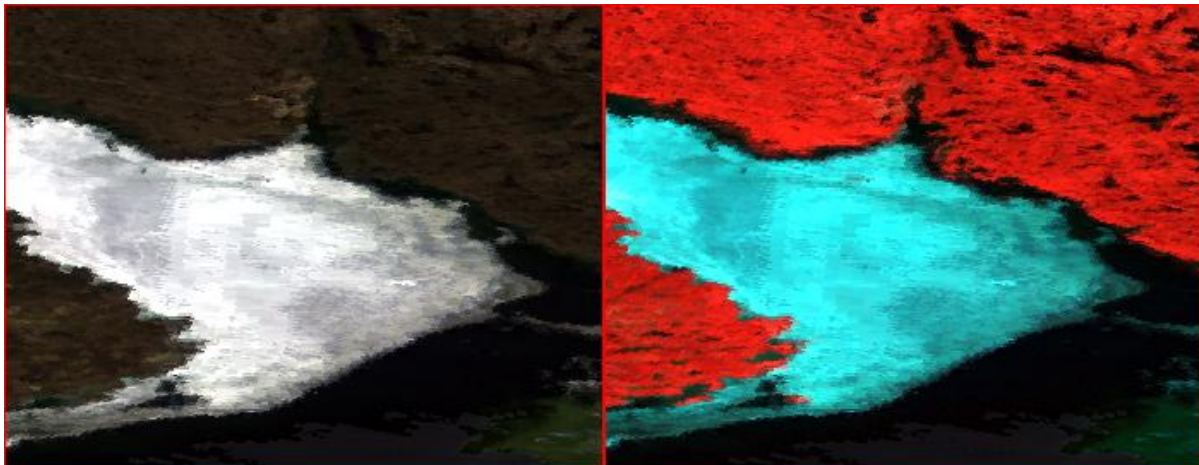


**Figure 4.3. Example of using MOD09GA to determine lake ice break-up on a portion of Great Slave Lake: true colour composite (left) and a NIR false colour composite (right) from June 5, 2007.**

## 4.5 Canadian Lake Ice Model (CLIMo)

### 4.5.1 General description

CLIMo (Duguay et al., 2003) is a modification of the one-dimensional thermodynamic sea-ice model by Flato and Brown (1996). Flato and Brown (1996) based their model on a one-dimensional unsteady heat conduction equation presented by Maykut and Untersteiner (1971), which can be seen in Equation (4.1):

$$\rho C_p \frac{\partial T}{\partial t} = \frac{\partial}{\partial z} k \frac{\partial T}{\partial z} + F_{sw} I_0 (1 - \alpha) K e^{-Kz} \quad (4.1)$$

where  $\rho$  is the density ( $\text{kg m}^{-3}$ );  $C_p$  is the specific heat capacity ( $\text{J kg}^{-1} \text{K}^{-1}$ );  $T$  is the temperature (K) within the ice or snow;  $t$  is time (s);  $z$  is the vertical coordinate, positive downward (m);  $k$  is the thermal conductivity ( $\text{W m}^{-1} \text{K}^{-1}$ );  $F_{sw}$  is the downwelling shortwave radiative energy flux ( $\text{W m}^{-2}$ );  $I_0$  is the fraction of shortwave radiation flux that penetrates the surface, equal to 0.17 if snow depth is  $\leq 0.1$  m, and equal to 0.0 if snow depth is  $>0.1$  m.;  $\alpha$  is the surface albedo; and  $K$  is the bulk extinction coefficient for penetrating shortwave radiation, equal to  $1.5 \text{ m}^{-1}$  (Duguay et al., 2003). Equation (4.1) is subject to boundary conditions at the ice underside and at the upper surface. At the ice underside:

$$T(h, t) = T_f \quad (4.2)$$

where  $h$  is the total thickness (snow and ice) (m) and  $T_f$  is the freezing temperature of fresh water, equal to 273.15 K (Duguay et al., 2003). The boundary at the upper surface is defined as

$$\begin{aligned} T(0, t) &= T_m & F_0 > 0, \hat{T}(0) &\geq T_m \\ k \frac{\partial T}{\partial z} \Big|_{z=0} &= F_0 & \text{otherwise} \end{aligned} \quad (4.3)$$

where  $T_m$  is the melting temperature at the surface, equal to 273.15 (K);  $F_0$  is the net heat flux that is absorbed at the surface ( $\text{W m}^{-2}$ ); and  $\hat{T}$  is the estimated temperature that is calculated before solving for equation (4.1) (K) (Duguay et al., 2003). Equation (4.2) states that the temperature at the ice underside is constantly at the freshwater freezing temperature (Duguay et al., 2003). Equation (4.3) states that the upper surface boundary condition is the net surface heat flux, obtained from the surface energy budget calculation (described in more detail in Duguay et al (2003) and Flato and Brown (1996), except when the surface is melting (Duguay et al., 2003). A generalized Crank-Nicholson, finite difference scheme is the numerical scheme used to solve for the heat conduction equations (4.1 to 4.3). A more in depth definition of the Crank-Nicholson, finite difference scheme can be found in Flato and Brown (1996).

A fixed-depth mixed layer is included in the model to allow for an annual cycle where the ice completely melts away (Duguay et al., 2003). When ice is present, the mixed layer is assumed to be constant at the freezing point. When ice is absent, the temperature of the mixed layer is determined by the surface energy budget (Duguay et al., 2003).

The growth and melt at the ice underside is determined by finding the difference between conductive heat flux into the ice and the heat flux out of the upper surface of the mixed layer (Duguay et al., 2003). Conversely, melt at the upper surface of the ice or snow is determined by the difference between the conductive flux and the net surface flux (Duguay et al., 2003). Snow is melted away first followed by the ice.

The following section focuses on CLIMo's albedo parameterization and the modifications made to it in order to integrate MODIS albedo products into the model. For a more in depth look into the CLIMo and the parameterizations associated with the model, please refer to Duguay et al. (2003), Ebert and Curry (1993), and Flato and Brown (1996).

## 4.5.2 Albedo parameterization and modifications

Surface albedo is the ratio of incoming and outgoing shortwave radiation at the surface. An important component of CLIMo, surface albedo is required to calculate the surface energy budget which, in turn, is required to determine essential components of CLIMo (e.g. the net surface heat flux). The surface albedo parameterization takes into account the surface type, surface temperature, and ice thickness (Duguay et al., 2003). However, the surface albedo parameterization does not take into account snow and ice composition, age, surface roughness, and other important factors in determining surface albedo. CLIMo uses a cold ice parameterization, taken from Maykut (1982), and a melting ice parameterization taken from Heron and Woo (1994) (Duguay et al., 2003). The surface albedo parameterization takes the following form:

$$\alpha = \begin{cases} \alpha_{ow} & h_i < h_{min} \\ \min[\alpha_s, \alpha_i + h(\alpha_s - \alpha_i)/c_1] & h_i \geq h_{min} \quad h_i \leq c_1 \\ \alpha_s & h_i \geq h_{min} \quad h_s > c_1 \end{cases} \quad (4.4)$$

$$\alpha_i = \begin{cases} \max(\alpha_{ow}, c_2 h_i^{0.28} + 0.08) & T(0, t) < T_m \\ \min(\alpha_{mi}, c_3 h_i^2 + \alpha_{ow}) & T(0, t) = T_m \end{cases} \quad (4.5)$$

$$\alpha_s = \begin{cases} 0.75 & T(0, t) < T_m \\ 0.65 & T(0, t) = T_m \end{cases} \quad (4.6)$$

where  $\alpha$  is surface albedo;  $\alpha_{ow}$  is albedo of open water, equal to 0.05;  $\alpha_s$  is albedo of snow;  $\alpha_{mi}$  is the albedo of melting ice, equal to 0.55;  $h_i$  is ice thickness (m);  $h_{min}$  is minimum ice thickness below

which open water is assumed, equal to 0.001 m;  $h_s$  is snow thickness (m);  $T(0,t)$  is the surface temperature (K);  $T_m$  is melting temperature at the surface, equal to 273.15 K;  $c_1$  is a constant equal to 0.1 m;  $c_2$  is a constant equal to 0.44 m; and  $c_3$  is a constant equal to 0.075 m. Equation (4.4) determines if the albedo of open water, ice, or snow should be used based on the depths of the ice and snow at the time. The albedo values of ice and snow are determined in equations (4.5) and (4.6), respectively. Whether the surface temperature is above or below the melting temperature of ice and snow will determine how the surface albedo will be calculated for both equations.

In order to allow for the integration of the MODIS albedo products into the parameterization, the parameterization itself needed to be altered. Daily albedo values retrieved from remote sensing products such as the MODIS albedo products can be read into CLIMo each day. Figure 4.4 details a simplified decision process on how the MODIS albedo products are integrated into CLIMo. The modified albedo parameterization gives priority to the daily albedo products (MxD10A1). First, the availability of MOD10A1 and MYD10A1 is checked for each date. If both daily products are available, then the average of the two products is used as the albedo for that day. If only MOD10A1 (or MYD10A1) is available, then that albedo will be integrated into CLIMo for that day. If neither of the daily products is available, then the most recent MCDD43A3 16-day albedo is integrated into CLIMo for that day. If the MODIS albedo products were not able to retrieve an albedo for a particular day, then CLIMo's original albedo parameterization is used.

## 4.6 CLIMo simulations and atmospheric forcing

The atmospheric forcing variables used as inputs for CLIMo are surface air temperature ( $^{\circ}\text{C}$ ), relative humidity (%), percent cloud cover (tenths), wind speed ( $\text{m s}^{-1}$ ), and snowfall amount (m) (Duguay et al., 2003). These data were collected from the Yellowknife airport meteorological station ( $62^{\circ}27'46.00''$  N,  $114^{\circ}26'25.00''$  W). Additionally, albedo (a dimensionless value between 0 and 1) was added as an input for this study to accommodate the integration of the MODIS albedo products. The atmospheric forcing data were retrieved from the Weather Office's historical climate records (<http://weatheroffice.gc.ca>) and the MODIS images were downloaded from NASA's Earth Observing System Data and Information System (EOSDIS) (<http://reverb.echo.nasa.gov/>).

CLIMo provides daily output variables on energy balance components; snow depth; a temperature profile throughout the ice/snow (or water temperature in the absence of ice); and ice thickness. Freeze-up (ice-on) dates, break-up (ice-off) dates, and end-of-season clear/snow/total ice thickness are also outputs of CLIMo (Duguay et al., 2003). For this study, we are most interested in

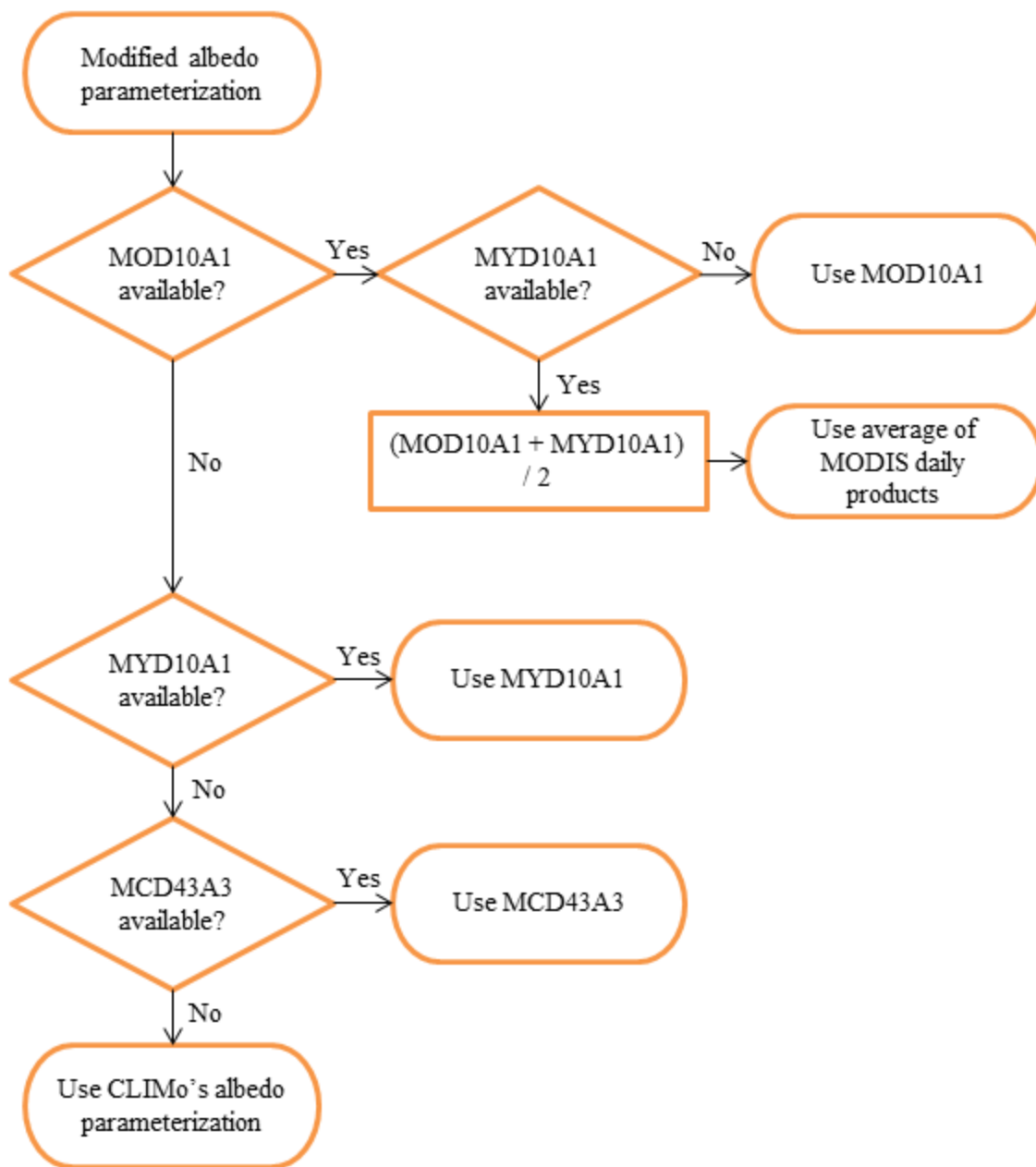


**Figure 4.4. Flowchart illustrating MODIS albedo product integration into CLIMo**

the break-up (ice-off) dates and how they are affected by the integration of the MODIS albedo products.

As mentioned earlier, erroneous values were observed in this study for both the daily ( $> 0.90$ ) and 16-day MODIS albedo products. These erroneous values are likely due to high SZAs, since the issue has been noted in previous studies and the impossible values cease later in the winter season when SZAs are lower during the day (Riggs et al., 2006; Stroeve et al., 2006). Fortunately, this study is mainly concerned with how surface albedo affects the timing of lake ice break-up in the spring when SZAs are lower during the day. Therefore, this study explores (1) the  $0^{\circ}\text{C}$  isotherm and (2) implementation of a set date for each year when SZAs are no longer a source of error.

The  $0^{\circ}\text{C}$  isotherm has been explored in previous studies for observing trends and variability in climate for northern Canada (Bonsal and Prowse, 2003; Duguay et al., 2006). The  $0^{\circ}\text{C}$  spring isotherm is defined as “the date when mean daily temperature rises above  $0^{\circ}\text{C}$ ” (Bonsal and Prowse, 2003). Both Bonsal and Prowse (2003) and Duguay et al. (2006) noted a relationship between spring and autumn  $0^{\circ}\text{C}$  isotherm dates and freshwater ice break-up and freeze-up dates, respectively (especially for break-up dates). Average daily temperatures tend to rise above and below  $0^{\circ}\text{C}$  on multiple occasions during the spring. To rectify this issue, Bonsal and Prowse (2003) applied a filter to the average daily temperatures by using an 11-, 21-, and 31-day running mean. They found that the temperatures rarely crossed the  $0^{\circ}\text{C}$  threshold more than once when using the 31-day running mean (Bonsal and Prowse, 2003). However, the albedo of snow and ice can change very rapidly as soon as the temperature is consistently above  $0^{\circ}\text{C}$  due to melt. Using a running mean on average daily temperatures would mean that the integration of MODIS albedo values would miss the beginning of these melt periods, especially with the 31-day running mean. This study therefore uses the 11- and 31-day  $0^{\circ}\text{C}$  isotherm, but also explores another option on when to start integrating MODIS albedo data into CLIMo in order to try and capture the very onset of melt.

The second method for when to integrate MODIS data into CLIMo involves implementing a set date when SZAs are no longer a source of error. After observing the MODIS data, erroneous albedo values cease to be present towards the end of March for each year when SZAs are lower (below  $70^{\circ}$ ) near local solar noon. However, since break-up occurs at a different date each year, instead of integrating the MODIS products at the beginning of April annually, the MODIS albedo products were integrated into CLIMo 15, 30, and 45 days prior to each observed break-up date for MxD09GA. This ensured that MODIS albedo products were integrated into CLIMo prior to ice break-up on a consistent basis. The first day the maximum daily temperature or the first day the average daily temperature exceeded  $0^{\circ}\text{C}$  were considered as points to integrate the MODIS albedo

products into CLIMo. Due to the variable nature of weather (e.g. freeze/thaw cycles, warming trends followed by snow precipitation, etc.), it was decided that set intervals prior to break-up for each year would better represent the break-up period of lake ice.

Using the methods described above, we were able to determine when to begin integrating MODIS data into CLIMo for each year of the study (Table 4.2). The 11-day 0°C isotherm will be referred here onward as Method 1 (M1); the 31-day 0°C isotherm as Method 2 (M2); integrating the MODIS products 15 days before the break-up date for a specific year as Method 3 (M3); integrating the MODIS products 30 days before the break-up date for specific year as Method 4 (M4); and integrating the MODIS products 45 days before the break-up date for that year as Method 5 (M5). Table 4.3 summarizes the aforementioned methods. The only year where MODIS albedo data is integrated into CLIMo before April is 2006 and it is done on the last day of March.

**Table 4.2. Dates when MODIS albedo data is integrated into CLIMo according to each method.**

Year	Observed BU* dates (DOY)	MODIS integration dates (DOY)				
	MxD09GA	M1	M2	M3	M4	M5
2000	May-20 (141)	Apr-27 (118)	May-11 (132)	May-05 (126)	Apr-20 (111)	Apr-05 (96)
2001	Jun-02 (153)	May-04 (124)	May-16 (136)	May-18 (138)	May-03 (123)	Apr-18 (108)
2002	Jun-07 (158)	May-16 (136)	May-31 (151)	May-23 (143)	May-08 (128)	Apr-23 (113)
2003	May-30 (150)	Apr-22 (112)	May-11 (131)	May-15 (135)	Apr-30 (120)	Apr-15 (105)
2004	Jun-08 (160)	May-25 (146)	Jun-03 (155)	May-24 (145)	May-09 (130)	Apr-24 (115)
2005	May-27 (147)	May-12 (132)	May-18 (138)	May-12 (132)	Apr-27 (117)	Apr-12 (102)
2006	May-15 (135)	Apr-26 (116)	May-05 (125)	Apr-30 (120)	Apr-15 (105)	Mar-31 (90)
2007	May-24 (144)	Apr-29 (119)	May-05 (125)	May-09 (129)	Apr-24 (114)	Apr-09 (99)
2008	May-24 (145)	May-04 (125)	May-18 (139)	May-09 (130)	Apr-24 (115)	Apr-09 (100)
2009	Jun-04 (155)	May-06 (126)	May-25 (145)	May-20 (140)	May-05 (125)	Apr-20 (110)
2010	May-21 (141)	Apr-20 (110)	Apr-28 (118)	May-06 (126)	Apr-21 (111)	Apr-06 (96)
2011	May-27 (147)	May-09 (129)	May-19 (139)	May-12 (132)	Apr-27 (117)	Apr-12 (102)

**\*BU = Break-up**

Modifications were also made to the snow on ground data. Brown and Duguay (2011b) noted the importance of accurate snow depths estimates on the lake ice surface because of snow's important role as an insulator and its contribution to the growth of snow ice. Previous studies on high-latitude lakes have found that the fraction of snow-on-land to snow-on-ice usually indicates that less snow is present on the ice than recorded on land (Brown and Duguay, 2011b; Sturm and Liston, 2003). In their study, Brown and Duguay (2011b) found that the fraction of snow-on-ice depth to snow-on-land depth for Back Bay was 0.68. For this study, CLIMo simulations were therefore run using three different scenarios: Scenario 1 (S1), 0% snow cover to represent possible situations

where bare patches of ice may be encountered; scenario 2 (S2), 68% snow cover as suggested by Brown and Duguay (2011b); and scenario 3(S3), 100% snow cover which assumes that the amount of snow measured on land at the Yellowknife airport weather station is equivalent to that measured on lake ice. In total, CLIMo simulations were performed using five methods with each 0%, 68% and 100% snow scenarios (Table 4.3).

**Table 4.3. Summary of the five methods for MODIS integration into CLIMo plus the three snow cover scenarios**

		Snow cover scenarios		
		S1	S2	S3
MODIS integration methods	M1	11-day 0°C isotherm + 0% snow cover	11-day 0°C isotherm + 68% snow cover	11-day 0°C isotherm + 100% snow cover
	M2	31-day 0°C isotherm + 0% snow cover	31-day 0°C isotherm + 68% snow cover	31-day 0°C isotherm + 100% snow cover
	M3	15 days prior to BU + 0% snow cover	15 days prior to BU + 68% snow cover	15 days prior to BU + 100% snow cover
	M4	30 days prior to BU + 0% snow cover	30 days prior to BU + 68% snow cover	30 days prior to BU + 100% snow cover
	M5	45 days prior to BU + 0% snow cover	45 days prior to BU + 68% snow cover	45 days prior to BU + 100% snow cover

## 4.7 Results

### 4.7.1 Ice-off dates: Scenario 1, CLIMo with 0% snow

S1 corresponds to CLIMo run with 0% snow cover added to the model. It is meant to represent the possibility of bare ice on Back Bay during the study period. CLIMo performs well under the S1 scenario, but almost all simulations (with the exception of 2006-2008) appear to overestimate break-up dates when compared to the observations made by the MODIS products for Back Bay (Figure 4.5). This is reinforced in Table 4.4 which shows the statistics used to evaluate the simulated break-up dates. The mean lake ice break-up dates for every simulation method are larger than the mean break-up dates for both observation methods (MxD10A1 and MxD09GA) and the mean bias error (MBE) for both the MxD10A1 and MxD09GA observations are positive for every simulation method. A positive MBE means that each simulated method for CLIMo, on average, overestimates lake ice

**Table 4.4. Error measure statistics to evaluate the performance of the simulated break-up dates to the observed break-up dates for S1 over Back Bay (2000-11).**

Simulated	Mean BU(SD) [DOY]	MxD10A1 BU observation			MxD09GA BU observation		
		RMSE (days)	MAE (days)	MBE (days)	RMSE (days)	MAE (days)	MBE (days)
CLIMo	151 (10)	6	5	4	4	4	3
M1	151 (9)	6	5	5	4	4	3
M2	151 (9)	6	5	5	4	4	3
M3	151 (9)	6	5	5	4	4	3
M4	152 (9)	6	6	5	5	4	4
M5	152 (10)	7	6	6	5	4	4
<hr/>							
Observed							
MxD10A1	146 (7)						
MxD09GA	148 (7)						

break-up under S1. As mentioned earlier, the MxD09GA break-up observations tend to be later than the MxD10A1 break-up observation dates, but they are usually within a few days of each other with the exception of 2010 which was due to cloud interference. The MBE values for MxD10A1 are larger than the MBE values for MxD09GA, because the MxD09GA observations are later and, therefore, closer to the overestimated break-up dates simulated by the S1 scenario. According to the RMSE and MAE values seen in Table 4.4, CLIMo, without the MODIS products integrated into the model, performs just as well or better than some of the simulated break-up dates with the MODIS albedo products integrated into CLIMo for S1. See Appendix A.1 for a detailed description of the performance statistics MBE, MAE, and RMSE. Ménard et al. (2002) reported that CLIMo had an RMSE of 4 days and an MBE of 4 days when comparing the simulated break-up dates to the CID observed break-up dates (1960-91). Using S1, the simulated results for the MxD09GA break-up observations are almost on par with the RMSE results found by Ménard et al. (2002) and have a more accurate (values closer to 0 days) MBE for every method with the exception of M5. The RMSE and MBE values when comparing the simulated break-up dates to the MxD10A1 observations do not perform as well, however. This is expected since observed break-up dates for MxD09GA were an average of two days later than MxD10A1. In hindsight, integrating MODIS albedo data that most likely represents higher snow albedo than bare ice albedo into CLIMo, which has simulated ice growth based on 0% snow conditions thus far, would have an impact on break-up dates that could lead to inaccurate simulations. CLIMo grows thicker ice when snow cover is not present (Brown and Duguay, 2011a) and an increase in albedo would delay ice melt on a system that has assumed 0% snow cover for the entire season. This is reinforced when looking at the mean break-up dates and

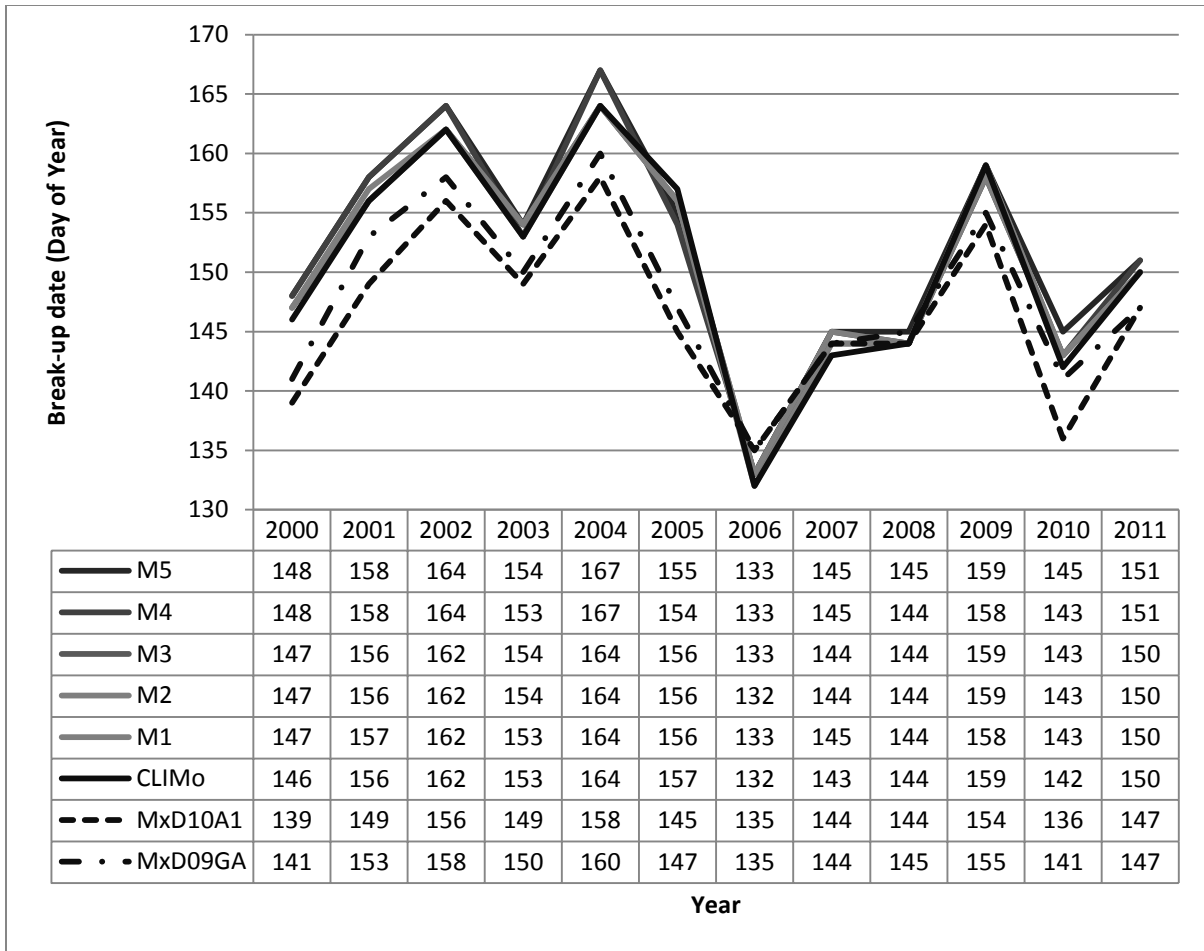


**Figure 4.5. Observed and simulated break-up dates from 2000 to 2011 for S1 (CLIMo with 0% snow) over Back Bay.**

MBE values for M4 and M5, which integrate MODIS albedo data 30 days and 45 days prior to MxD09GA observed break-up, respectively. The increase in albedo observed by MODIS would decrease energy allowed into the system and delay simulated break-up dates.

The incorporation of snow into the model is an important aspect of the simulation of lake ice phenology. Snow's insulating properties and contribution to the top layer of ice are important factors in determining the lake ice thickness and duration throughout the season (Brown and Duguay, 2011a). The next two sections cover the scenarios S2 and S3, which are the 68% and 100% snow cover, respectively.

#### **4.7.2 Ice off dates: Scenario 2, CLIMo with 68% snow**

S2 involves Brown and Duguay's (2011b) 0.68 (or 68%) snow-on-land to snow-on-ice depth fraction for Back Bay when inputting snowfall amount into CLIMo. Compared to the break-up dates found

using S1, S2 appears to match quite well with the observed break-up dates by MxD10A1 and MxD09GA (with the exception of 2006-2008) (Figure 4.6). Unlike S1, the break-up dates for S2 tend to underestimate the observed break-up dates, which can be seen in mean break-up dates for each method in Table 4.5. Each mean break-up date for CLIMo is earlier than the mean break-up dates observed by MxD10A1 and MxD09GA for S2. The MBE values seen in Table 4.5 are all negative compared to the MBE values seen under S1 (see Table 4.4), which also implies that break-up dates simulated under S2 are underestimated (earlier) compared to the observed break-up dates. The RMSE and MAE for S2 are contrary to the values seen in S1. The RMSE and MAE values indicate that the S2 simulations perform better with the MxD10A1 observations. Also, CLIMo without the MODIS products does not perform as well with snow added to the model. M1, M4, and M5 perform better than the other methods where MODIS surface albedo is integrated closer to observed ice break-up for Back Bay and have a lesser influence on the timing of break-up. The RMSE for M1, M4, and M5 with the simulations compared to MxD10A1 break-up date observations are equal to 4 days, which is the same as the RMSE observed by Ménard et al. (2002). The accurate RMSE and MAE values for M1, M4, and M5 indicates that MODIS products integrated for a period that more extensively represent Back Bay's break-up period enhances CLIMo's outputs when snow is added to the model. Assuming that snow is present at the site, MODIS products may well improve break-up date simulations for CLIMo when replacing the current albedo parameterization. CLIMo without MODIS albedo products integrated into the model performed the worst for both the MxD10A1 and MxD09GA break-up date observations with RMSE values of 5 days and 6 days, respectively, and MAE values of 4 days and 5 days, respectively. The dates when albedo is integrated into CLIMo for each method can be found in Table 4.2 (see section 4.6). As mentioned, M5 and M4 usually integrated the MODIS products into CLIMo earlier than the other methods. It can be seen in Table 4.2 that the order is usually first M5, M4, M1, M3, and then M2, which is the order of accuracy when analyzing the RMSE values in Table 4.5 from highest to lowest. M1, M4, and M5 having the same RMSE values compared with MxD10A1 and MxD09GA break-up observations suggests that integrating the MODIS albedo products earlier (e.g. M5) does not noticeably improve CLIMo's break-up simulations. In fact, M4 having the most accurate MAE value compared with MxD09GA break-up observations suggest that early integration of MODIS products into CLIMo may even lessen the accuracy of break-up simulations. Further analysis is required, but integrating MODIS albedo products closer to the break-up date does not appear to be more beneficial for the simulation of break-up using CLIMo, but neither does integrating the MODIS albedo products too far in advance.

**Table 4.5. Error measure statistics to evaluate the performance of the simulated break-up dates to the observed break-up dates for S2 over Back Bay (2000-2011).**

Simulated	Mean BU(SD) [DOY]	MxD10A1 BU observation			MxD09GA BU observation		
		RMSE (days)	MAE (days)	MBE (days)	RMSE (days)	MAE (days)	MBE (days)
CLIMo	144 (10)	5	4	-3	6	5	-4
M1	145 (10)	4	3	-1	4	4	-3
M2	145 (10)	5	4	-2	5	4	-3
M3	145 (10)	5	3	-2	5	4	-3
M4	145 (9)	4	3	-1	4	3	-3
M5	145 (9)	4	3	-2	4	4	-3

**Observed**

MxD10A1 146 (7)

MxD09GA 148 (7)

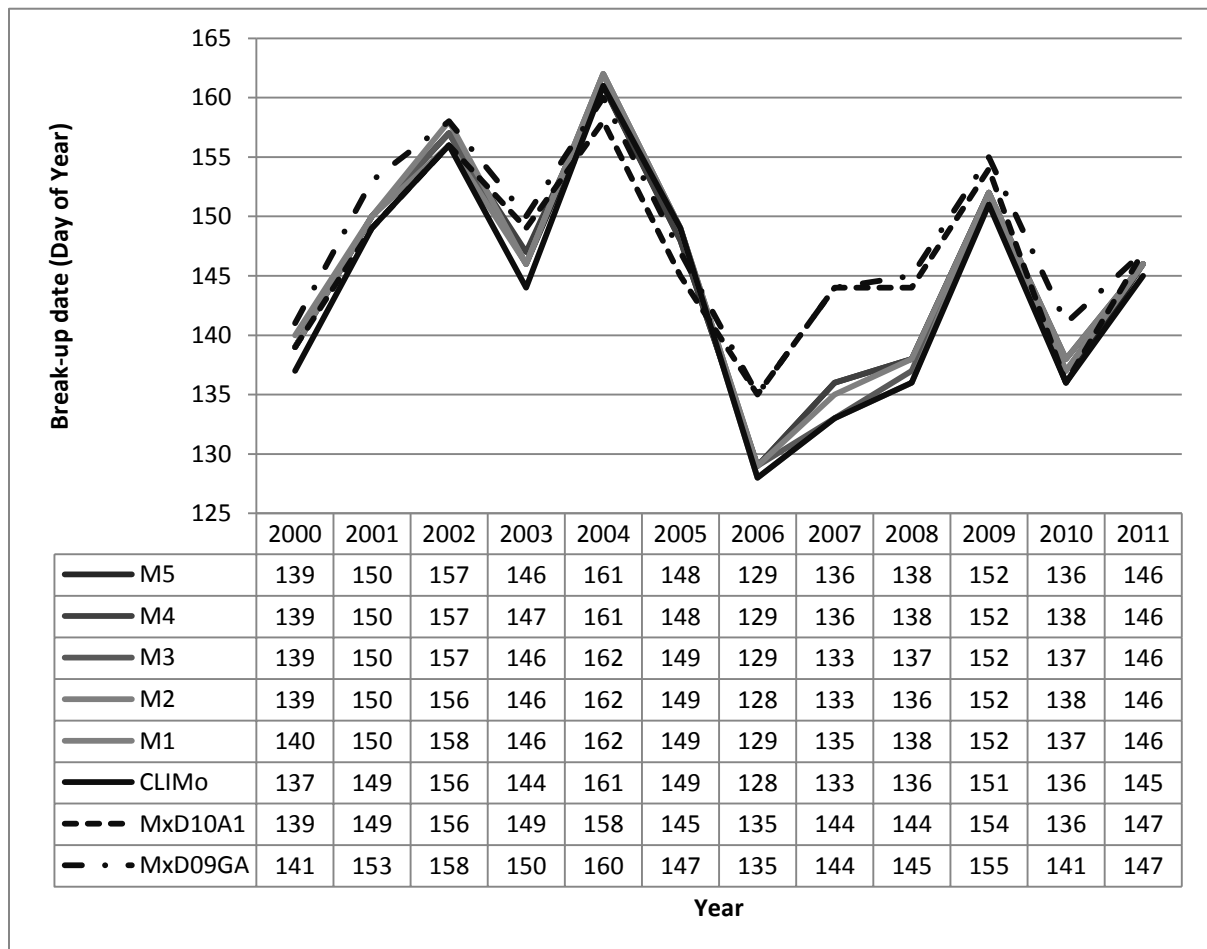


**Figure 4.6. Observed and simulated break-up dates from 2000 to 2011 for S2 (CLIMo with 68% snow) over Back Bay.**

### 4.7.3 Ice off dates: Scenario 3, CLIMo with 100% snow

The S3 simulations correspond to CLIMo run with 100% snow, which was recorded on land near the Yellowknife airport. Like S2, simulated break-up dates using S3 appear to agree with the break-up date observations by MxD10A1 and MxD09GA with the exception of 2006 to 2008 (Figure 4.7). The mean break-up date for each simulation is earlier than the mean observed break-up dates, but the means for the simulations are much closer to observed means than in the previous two scenarios. The mean break-up dates for the simulations are especially close to the mean observed break-up dates using MxD10A1. The MBE values shown in Table 4.6 are negative for all methods when compared to both observation methods. The MBE values for the simulations compared against the MxD10A1 observations are closer to 0 days than the simulations compared against the MxD09G observations. The break-up dates simulated for 2006 to 2008 are noticeably earlier than the observed break-up dates (Figure 4.7). This has an effect on the error statistics results and the averages that indicate underestimation of the break-up dates for S3.

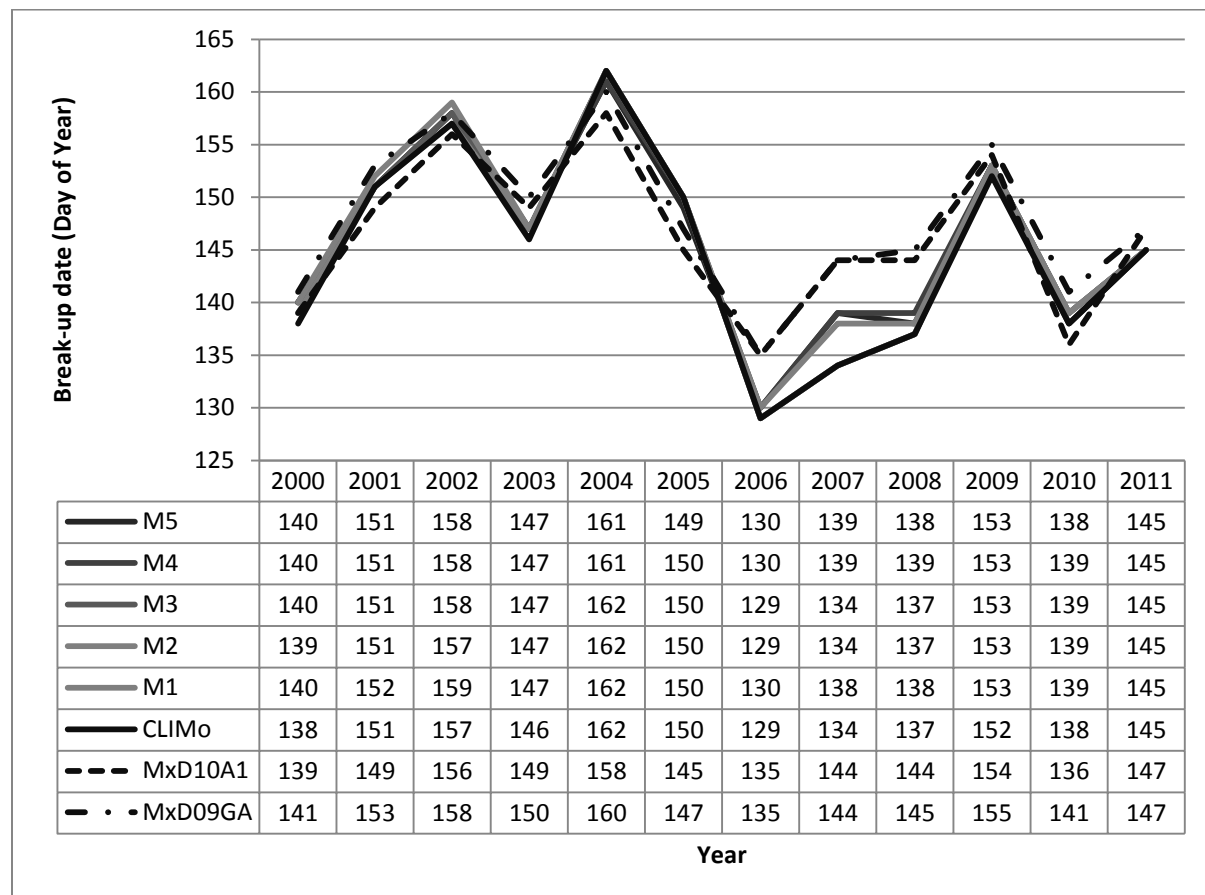


Figure 4.7. Observed and simulated break-up dates from 2000 to 2011 for S3 (CLIMo with 100% snow) over Back Bay.

As noted, S3 is run with 100% snow cover and like S2, which had 68% snow cover, the methods M1, M4, and M5 show RMSE and MAE values that indicate that these methods were more accurate. The M1, M4, and M5 methods were the 11-day 0°C isotherm, and MODIS integration 30 days and 45 days prior to lake ice break-up, respectively. It was also mentioned in section 4.7.2 that the M1, M4, and M5 were usually the methods where MODIS albedo products were integrated into CLIMo at earlier dates. The S3 scenario produced the most accurate results according to the error statistics in Table 4.6 with RMSE and MAE values closer to 0 days than the RMSE and MAE values found in the S1 and S2 scenarios. M4 compared with the MxD09GA break-up date observations agreed the most with an RMSE and MAE of 3 days. The RMSE value of 3 days for M4 is one day better than the RMSE of 4 days obtained by Ménard et al. (2002). CLIMo with the original albedo parameterization performed the worst, but it was still accurate with an RMSE of 5 days compared with the MxD10A1 and MxD09GA break-up observations.

**Table 4.6. Error measure statistics to evaluate the performance of the simulated break-up dates to the observed break-up dates for S3 over Back Bay (2000-2011).**

Simulated	Mean BU (St. Dev.) [DOY]	MxD10A1 BU observation			MxD09GA BU observation		
		RMSE (days)	MAE (days)	MBE (days)	RMSE (days)	MAE (days)	MBE (days)
CLIMo	145 (10)	5	4	-1	5	4	-3
M1	146 (10)	4	3	0	4	3	-2
M2	145 (10)	5	4	-1	5	4	-3
M3	145 (10)	5	4	-1	4	3	-3
M4	146 (9)	3	3	0	3	3	-2
M5	146 (9)	3	3	-1	3	3	-2
<b>Observed</b>							
MxD10A1	146 (7)						
MxD09GA	148 (7)						

## 4.8 Discussion

### 4.8.1 MODIS albedo products and CLIMo's performance

The results show that CLIMo can accurately simulate lake ice break-up on Back Bay within 6 days of observed break-up for all three scenarios. However, with the exception of S1 where CLIMo was run with 0% snow cover, the integration of MODIS products into CLIMo did improve the accuracy of simulated break-up dates for Back Bay. The MODIS products improved the accuracy of CLIMo for

S2 and S3 where snow is present in the model. Figure 4.8 illustrates that snow was present on the ice during the winter from 2003 to 2011 according to Canadian Ice Service (CIS) records (*Ice Thickness Program Collection [2002-2011]*, 2012). No data was available from CIS for winters 2000-2001 and 2001-2002. The fraction of average snow-on-land to average snow-on-ice from 2003 to 2011 was 0.69 which agrees with the S2 scenario (68% or 0.68 snow cover). However, it should be noted that there is more snow accumulated on the ground when the ice first forms and that the ice tends to retain the snow for a longer period of time. Assuming S3, 100% snow cover, is reasonable when considering the different accumulation periods for snow between land and ice (i.e. once the ice forms, the snow will begin to accumulate from snowfall events, but will obviously be less than snow-on-land initially if snow has already previously accumulated on land).

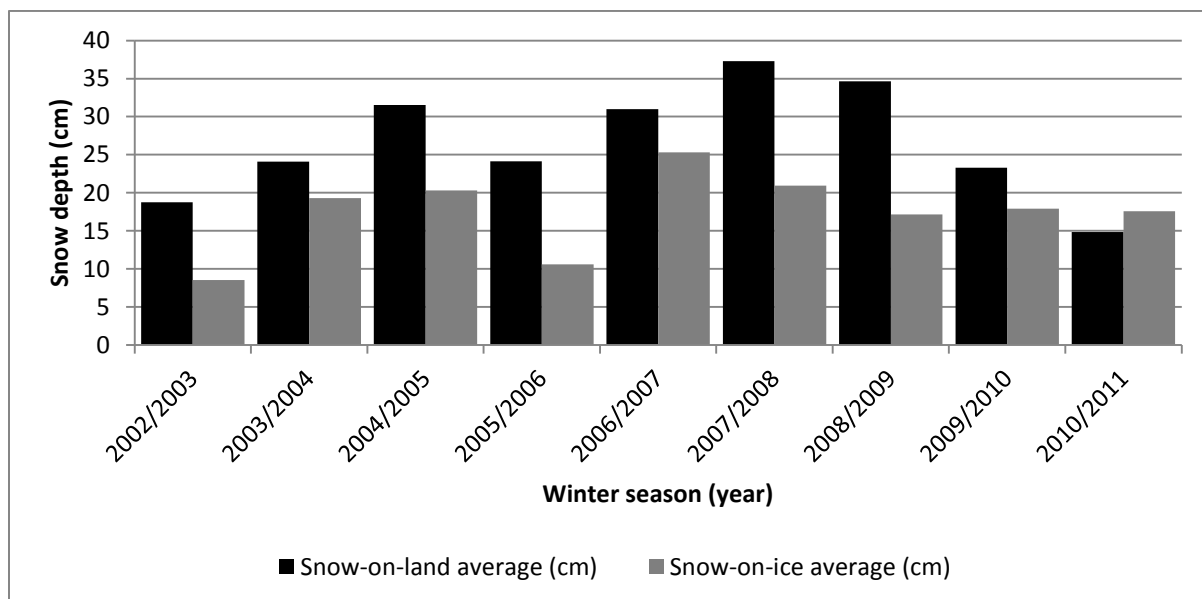


**Figure 4.8. Average snow-on-land and average snow-on-ice for Yellowknife and Back Bay from the 2002/2003 to 2010/2011 winter seasons (*Ice Thickness Program Collection [2002-2012]*, 2012)**

Each method of integration (M1 to M5) improved simulated break-up dates for S2 and S3 although some improvements were negligible. As mentioned in previous sections, the methods of integrations that inserted MODIS albedo products earlier in the break-up season often had the most impact on the simulation results and Figure 4.9 illustrates why this might be. In Figure 4.9, the albedo that would have been integrated as the MODIS snow albedo for 2008 and 2010 are compared against the CLIMo albedo parameterization simulations for each snow cover scenario. Both graphs indicate the specific dates when albedo is integrated into CLIMo for each method. M5, MODIS integration 45 days prior to observed break-up, captures much of the albedo degradation observed by

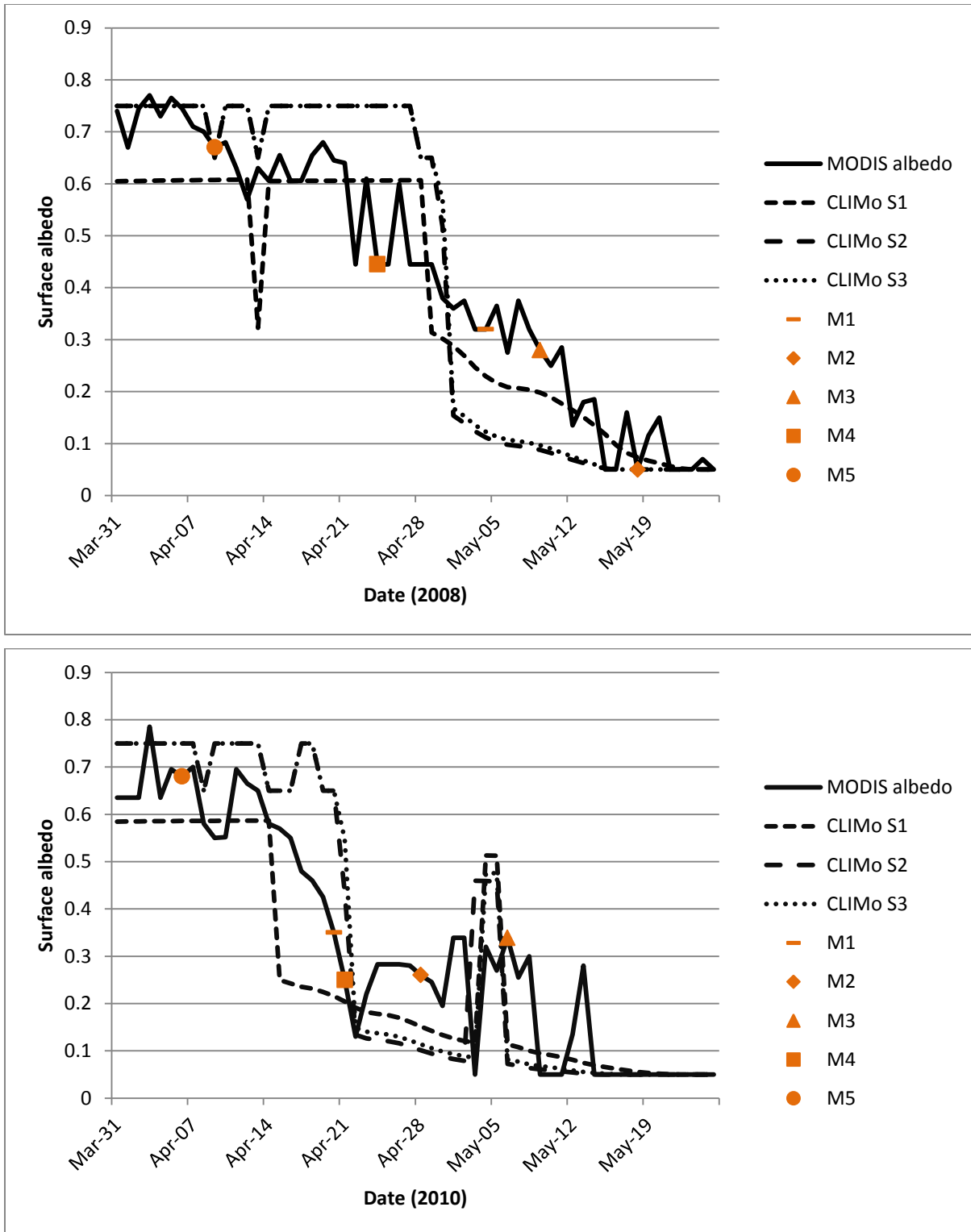


Figure 4.9. A comparison between MODIS surface albedo and CLIMo's surface albedo for the three snow cover scenarios for the years 2008 (Top) and 2010 (Bottom). Also indicated are the dates when the MODIS surface albedo data are integrated into CLIMo for the five different methods.

the MODIS albedo products. M1 and M4, which also performed well in regards to the error statistics in previous sections, are also integrated earlier in the break-up season, but both methods do not capture the beginning of albedo degradation as M5 does (Figure 4.9). Still, M1 and M4 appear to be capable of covering break-up when CLIMo simulates the snow depth to be zero and transfers albedo simulations over to the cold ice and melting ice parameterizations. M2 and M3 integration methods occurred later in the break-up season and often had little impact on the simulation date.

During break-up, S1 appears to agree more with the MODIS acquired albedo in 2008 (Figure 4.9). As mentioned earlier, S1 will simulate thicker ice depths than the other two scenarios due to the lack of snow and the ice albedo parameterization uses ice depth as an important determining factor. Figure 4.9 also shows that the CLIMo S3 bare ice albedo appears to be very slightly higher than CLIMo S2 albedo which contradicts the previous statement that the lack of snow produces larger ice depths. CLIMo S3 produces a slightly higher albedo than CLIMo S2, because the addition of snow ice (100% snow cover for S3 compared to 68% snow cover for S2) is greater than the reduction in ice growth at the ice underside (Brown and Duguay, 2010). The difference between the cold ice and melting ice parameterizations can be seen in 2010 (Figure 4.9), where there is a spike in albedo during the break-up season. This is because the cold ice parameterization, in equation (4.5), puts a much greater emphasis on ice depth than the melting ice parameterization does. When snow is present, the snow albedo parameterization will designate the albedo as 0.75 if the temperature is below melting and 0.65 if the temperature is greater than or equal to melting. As one can see in Figure 4.9, the evolving albedo of snow is a complex process affected by day-to-day elements. The MODIS albedo products appear to do a good job at capturing these variations in the recordings.

M1 and M2 were the 0°C isotherm methods for MODIS integrations. In previous studies, the 0°C isotherm was found to have a strong relationship with freshwater lake ice break-up (Bonsal and Prowse, 2003; Duguay et al., 2006). M1, the 11-day 0°C isotherm, integrated the MODIS albedo products into CLIMo before M2. However, as noted by Bonsal and Prowse (2003), the 11-day 0°C isotherm would sometimes cross the 0°C threshold multiple times and MODIS albedo products would be integrated earlier than other years based on whether or not warming periods followed by a cooling period would occur or not. For each scenario, M1 has RMSE and MAE values closer to 0 days than M2, which indicates that adding MODIS albedo products earlier simulates more accurate break-up dates. With the exception of S1 compared with MxD10A1 observations, M1 performed better than or equal to CLIMo in regards to RMSE and MAE values for each scenario. M2, the 31-day 0°C isotherm, consistently performed worse than the other MODIS integration methods, but was as accurate as or more accurate than CLIMo when snow cover was involved. Unfortunately, the 31-day

0°C isotherm occurs too close to the break-up date for Back Bay and has a smaller influence on the break-up than the other integration methods.

M3 to M5 were the set intervals prior to MxD09GA observed break-up methods for MODIS integrations. The MODIS integration methods M4 and M5 were consistently more accurate than M3 when snow cover was added to CLIMo. In terms of RMSE and MAE, M5 was usually more accurate (lower values) than M4 when compared with the MxD10A1 break-up observations and M4 was more accurate than M5 when compared with the MxD09GA observations. As mentioned earlier, the MxD10A1 observations usually occurred earlier than the MxD09GA observations with mean break-up dates occurring on day 150 and 148 of the year, respectively. The method M5, MODIS integrated into CLIMo 45 days prior to MxD09GA observation, is integrated 15 days earlier than M4. M5 would capture snow albedo before the onset of break-up, as seen in Figure 4.9, and often produced lower albedo values than simulated by CLIMo. With CLIMo, ice growth will usually continue until snow is longer present on the lake ice (available energy is first used to melt the snow) and a lower albedo from the MODIS products would allow more shortwave radiation into the model and slightly delay ice growth and allow for an earlier snow free date. Smaller ice depths and earlier snow free dates with M5 could sometimes lead to earlier break-up dates, as seen in Figures 4.6 and 47, which would then favour the MxD10A1 observations over the MxD09GA observations. The same reasoning can be applied to M4. The insulating properties of snow as well as higher simulated albedo values of snow by CLIMo, which usually hinder ice growth during the cold season, can delay ice degradation during the melt season and can lead to later break-up simulations which would explain M4 agreeing more with the MxD09GA break-up observations for Back Bay. The differences in RMSE and MAE between M4 and M5 for both satellite observations are minor and both are dependent on whether CLIMo is under- or overestimating the observed break-up dates. For the scenarios S2 and S3, the CLIMo and CLIMo with the MODIS albedo products integrated in for break-up appear to agree much better than S1 with the exception of the years 2006 to 2008.

The S2 (68%) and S3 (100%) snow cover scenarios performed well in most years, but not 2006 to 2008, while the scenario with 0% snow cover (S1) only appeared to perform well simulating break-up dates from 2006 to 2008, and overestimating the rest of the study years. A twelve year period (2000-2011) is a relatively small sample size and annual variability such as seen in the years 2006 to 2008 would affect the performance statistics' results. It could be assumed then that Back Bay from 2006 to 2008 experienced bare ice conditions, which would explain why S1 agrees better than the snow cover scenarios for these years, but this is probably not the case. The CIS records recorded low snow-on-ice values for the 2005/2006 winter compared to other winter seasons, but the same

conditions were seen for the 2002/2003 winter (Figure 4.8). CLIMo performed well with the S2 and S3 snow cover scenarios during the 2002/2003 winter season. Furthermore, the 2006/2007 and 2007/2008 winter seasons were recorded to have above average snow cover over Back Bay (Figure 4.8). The 2005/2006 winter season was warmer than average for the study period, but the 2006/2007 and 2007/2008 winter seasons did not show abnormal temperature trends (Figure 4.10). It is hard to determine why CLIMo had difficulty simulating break-up dates for these years, but seeing how CLIMo with 0% snow cover consistently overestimated these break-up dates and the snow cover scenarios underestimated the years 2006 to 2008, it was probably a coincidence that the S1 break-up simulations fell in line with the MODIS observed break-up dates. As mentioned, Brown and Duguay (2010) state that decreasing the snow amount for CLIMo more than 75% would lead to thicker ice depth simulations, because snow's insulating properties would have a lesser influence on the outcome. Therefore, albedo is low during the winter months in CLIMo, but the lack of insulating properties of snow cause the lake ice depth to increase at a faster rate than CLIMo with snow cover. When break-up starts to occur, the cold ice and melting ice albedo parameterization (that increase with larger ice depths) do not allow as much energy into the system as CLIMo with snow present in the model. Larger ice depths plus higher albedo values during break-up lead to later simulated break-up dates as seen in the results for S1. The effect that albedo has on later break-up date simulations can be seen in scenarios S2 and S3 (Tables 4.5 and 4.6) where the mean break-up dates for CLIMo without MODIS integrated into the model are earlier than the mean break-up dates with MODIS and the MBE values are further from 0 days when CLIMo is run without MODIS albedo. The simulated break-up date for 2007 by CLIMo without MODIS albedos was particularly lower than CLIMo with MODIS albedos. CLIMo without MODIS albedos simulated break-up dates for May 13<sup>th</sup> and May 14<sup>th</sup> for the 68% and 100% snow covers scenarios, respectively, while CLIMo with MODIS albedos (M5) simulated break-up dates for May 16<sup>th</sup> and May 19<sup>th</sup> for the 68% and 100% snow cover scenarios, respectively. The higher albedo values from MODIS have been shown to delay the timing of lake ice break-up; however, these large differences in lake ice break-up dates (May 14<sup>th</sup> compared to May 19<sup>th</sup> in particular) are the results of “bad timing” for CLIMo. Air temperatures cooled briefly for two days (May 17<sup>th</sup> to 18<sup>th</sup>, 2007), which delayed Back Bay's ice break-up for the M5 simulation (Figure 4.11). The large differences between CLIMo's lake ice break-up simulations for Back Bay from 2006 to 2008 could be due to other processes in addition to thermodynamic processes, but it cannot be certain without *in situ* observations. Since the years 2006 to 2008 do not line up with the simulated results under the scenarios S2 and S3, it would be interesting to see how these years affect the error statistics.

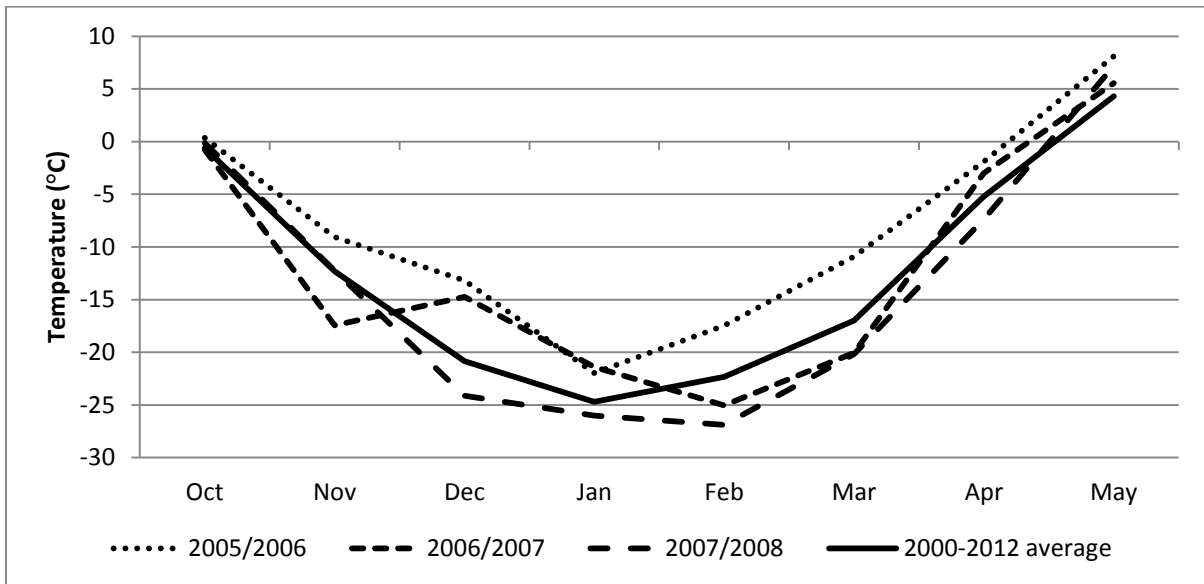


Figure 4.10. Average monthly temperatures for the winter seasons leading up to the 2006-2008 lake ice break-up date simulations.

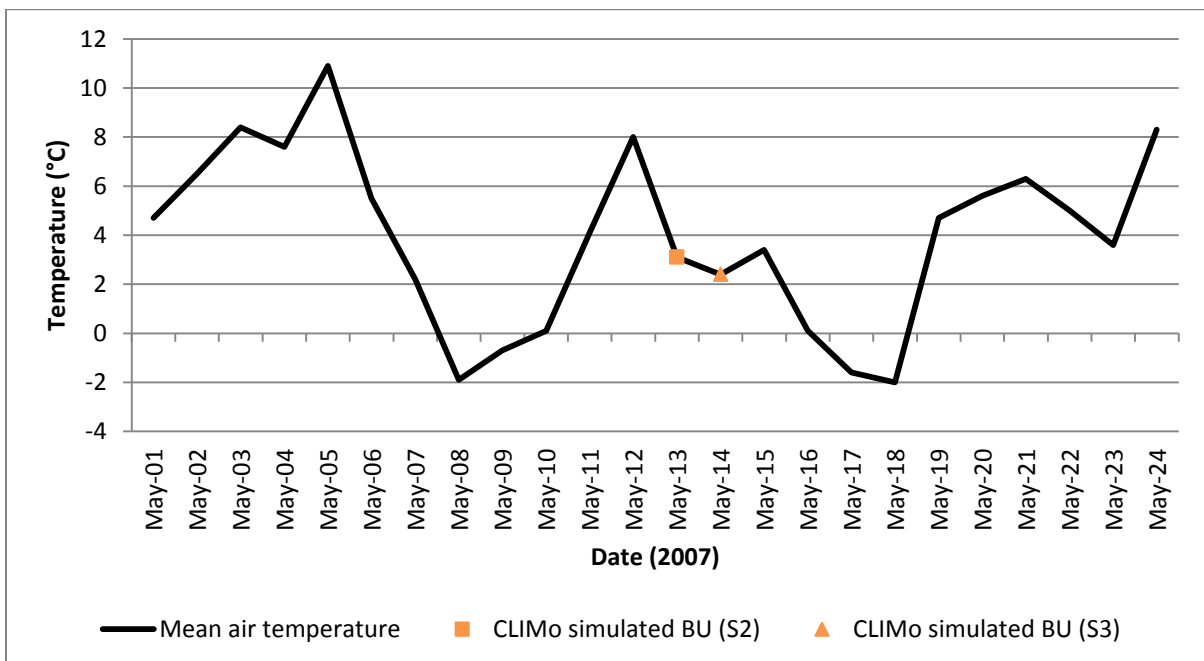


Figure 4.11. Mean air temperatures for Back Bay, GSL leading up to lake ice break-up in 2007.

In Table 4.7, the years 2006 to 2008 were removed from the error analysis. Immediately, it can be seen that the mean break-up date for the MODIS observations and CLIMo simulations increased by several days and the standard deviations decreased. The MBE values for S1 increased in value indicating that CLIMo with 0% snow cover simulated even later break-up dates with 2006 to 2008 removed from the study. The MBE values for the scenarios S2 and S3 indicated that CLIMo simulated earlier break-up dates compared to the MODIS break-up observations. With the years 2006 to 2008 removed, the CLIMo simulations using the MODIS albedo products simulate later break-up dates (by up to two days) when compared with MxD10A1 observations and simulate earlier break-up dates (by up to three days) when compared with MxD09GA observations (Table 4.7). The RMSE and MAE values increased for S1 with the years 2006 to 2008 removed as well. The RMSE and

**Table 4.7. Error measure statistics to evaluate the performance of the simulated break-up dates to the observed break-up dates for S1, S2, and S3 over Back Bay, but with 2006-2008 removed (2000-2005, 2009-2011).**

Scenario	Simulated	Mean BU(SD) [DOY]	MxD10A1 BU observation			MxD09GA BU observation		
			RMSE (days)	MAE (days)	MBE (days)	RMSE (days)	MAE (days)	MBE (days)
S1	CLIMo	154(7)	7	6	6	5	4	4
	M1	154(7)	7	6	6	5	4	4
	M2	155(7)	7	6	6	5	4	4
	M3	155(7)	7	6	6	5	4	4
	M4	155(8)	7	7	7	5	5	5
	M5	156(7)	8	8	8	6	5	5
S2	CLIMo	148(8)	3	2	-1	4	3	-3
	M1	149(8)	2	2	1	3	2	-1
	M2	149(8)	2	2	1	3	2	-2
	M3	149(8)	2	2	1	3	2	-2
	M4	149(8)	2	2	1	2	2	-2
	M5	148(8)	2	2	0	3	2	-2
S3	CLIMo	149(8)	3	2	1	3	3	-1
	M1	150(8)	3	3	2	2	2	-1
	M2	149(8)	3	2	1	2	2	-1
	M3	149(8)	3	2	1	2	2	-1
	M4	149(7)	3	2	1	2	2	-1
	M5	149(8)	2	2	1	2	2	-1
Observed								
	MxD10A1	148(7)						
	MxD09GA	150(7)						

MAE values for the scenarios S2 and S3 all improved in accuracy with the erroneous years removed to having an average error down to 2 to 3 days of the MODIS observations compared to RMSE and MAE values ranging from 3 to 5 days before. With the exception of the RMSE for M4 and the MAE for M1 in S3 compared with the MxD10A1 break-up observations, the removal of the years 2006 to 2008 improved the RMSE and MAE values for the snow cover scenarios by 1 to 3 days. The integration of MODIS products into CLIMo only improved the simulation of break-up dates for Back Bay by 1 to 2 days compared to the MODIS observed break-up dates for the snow cover scenarios. CLIMo with and without the MODIS products integrated for the break-up date simulations were all within an average error of 3 days when compared to the MODIS break-up observations for Back Bay. CLIMo performed very well with just the albedo parameterization. The MODIS albedo products integrated into CLIMo were able to improve the simulation of lake ice break-up dates by 1 to 2 days. The MODIS products had a larger influence on the simulations if the entire melt period was captured.

## **4.9 Summary and conclusion**

The one-dimensional lake ice model, CLIMo, was modified to run with MODIS albedo products integrated into the model during the break-up season. The main purpose was to see if the integration of MODIS albedo products in place of the original albedo parameterization would improve the simulated break-up dates for each year. The results show that both CLIMo with and without MODIS products integrated into the model performed very well. With the MODIS products integrated into CLIMo, there were slight improvements in break-up date simulation for Back Bay by 1 to 2 days. The daily and 16-day MODIS albedo products, MxD10A1 and MCD43A3, respectively, were integrated into CLIMo using five different methods and tested under three different snow cover scenarios. The five methods were integration at the 11 day 0°C isotherm date (M1); the 31 day 0°C isotherm date (M2); 15 days prior to observed lake-ice break-up (M3); 30 days prior to observed lake-ice break-up (M4); and 45 days prior to observed lake-ice break-up (M5). The three different snow cover scenarios were the 0% snow cover scenario (S1); 68% snow cover scenario according to Brown and Duguay's (2011b) snow-on-ice to snow-on-land depth ratio (S2); and the 100% snow cover scenario (S3).

Each scenario with snow cover added into the model (S2 and S3) displayed improvements in simulated break-up dates for Back Bay (Yellowknife). Under the snow cover scenarios, the methods M4 and M5 were the methods that improved simulated break-up dates the most. Under the S2 scenario, CLIMo had an RMSE (MAE) of 5 (4) days and 6 (5) days when compared to the MxD010A1 and MxD09GA break-up date observations, respectively. Under the S3 scenario, CLIMo

had an RMSE (MAE) of 5 (4) days and 5 (4) days when compared to the MxD010A1 and MxD09GA break-up date observations, respectively. CLIMo, as is, performs well in simulating break-up dates having an average accuracy within approximately 5 days of actual lake-ice break-up on Back Bay. However, with MODIS albedo data integrated into CLIMo, the M4 method under S2 had an RMSE (MAE) of 4 (3) days and 4 (3) days when compared to the MxD10A1 and MxD09GA break-up date observations, respectively; the M4 method under S3 had an RMSE (MAE) of 3 (3) days and 3 (3) days when compared to the MxD10A1 and MxD09GA break-up date observations, respectively; the M5 method under S2 had an RMSE (MAE) of 4 (3) days and 4 (4) days when compared to the MxD10A1 and MxD09GA break-up date observations, respectively; and the M5 method under S3 had an RMSE (MAE) of 3 (3) days and 3 (3) days when compared to the MxD10A1 and MxD09GA break-up date observations, respectively. With MODIS albedo products integrated into CLIMo, the accuracy of simulated ice break-up over Back Bay was sometimes improved by 1 to 2 days. The opposite occurred when snow was removed from the model simulations (S1) where CLIMo with the original albedo parameterization performed better than the methods with MODIS albedo product integrations and the products that integrated albedo at earlier dates performed the worst.

The Back Bay lake ice simulations performed the worst under S1. CLIMo without the MODIS albedo products provided the most accurate break-up date simulations, but all simulations (including those with MODIS albedo integrated into CLIMo) simulated later break-up dates than those observed by the MODIS albedo products. Without snow's insulating properties CLIMo simulated thicker ice during the cold season. The cold ice and melting ice albedo parameterizations are very dependent on ice thickness (i.e. thicker ice equals higher modelled albedo), but the MODIS albedo products still retrieved higher albedo values over Back Bay leading up to and during the melt period. Therefore, the results have shown that even slightly higher albedo (Figure 4.9) do affect the timing of modelled lake ice break-up where CLIMo with MODIS albedo simulated break-up dates a day later than CLIMo without MODIS albedo in the case of M4 and M5. However, high Arctic and sub-Arctic lakes can often have variable snow cover across a lake (as seen in Chapter 3) and MODIS' 500 m spatial resolution may capture unwanted snow albedo if simulating lake ice phenology using the 1-D lake ice model CLIMo.

It is unclear why CLIMo had difficulty simulating lake ice break-up for Back Bay from 2006 to 2008, but CLIMo performed exceptionally well with and without MODIS albedo when those years were removed from the results. The atmospheric forcing input variables for CLIMo being collected from a nearby meteorological station on land may have been a factor, but further investigation is required or it may be due to forces other than thermodynamic processes that required *in situ*

observations. The 0% snow cover scenario (S1) performed well from 2006 to 2008, but only during these years so it is believed that it was just a coincidence. The cause of S1 lake ice break-up date simulations agreeing with those years is probably due to CLIMo simulating thicker ice without snow cover present and the bare ice albedo parameterizations dependence on lake ice thickness. MODIS albedo integrated into CLIMo slightly slows the growth of lake ice showing that higher albedos do have an effect on the simulated break-up dates for lake ice. However, it also shows that MODIS albedo products may not represent bare ice scenarios. The S1 scenario was implemented to help cover all snow condition scenarios and bare ice can be experienced at higher latitude environments.

MODIS albedo integrated into CLIMo slightly delays lake ice break-up for Back Bay by 1 to 2 days. The later break-up date simulations usually lead to slightly more accurate simulations. However, it difficult to determine if the improved break-up simulations is significant with such a small sample size (2000-2011). What MODIS albedo has shown is that it provides values similar to CLIMo's albedo parameterization. This is useful because there are many areas in the Northern Hemisphere dominated by lakes that do not have the required atmospheric forcing inputs required for CLIMo to run. Remote sensing products such as the MODIS albedo products are capable of providing alternatives to *in situ* measurements. While it has been noted that MODIS' 500 m spatial resolution may capture unwanted albedo values in certain situations, the product is still able to capture day-to-day variations in albedo in ways that CLIMo's albedo parameterization cannot (e.g. impurities, snow removal by wind processes). In the future, data assimilation techniques may provide CLIMo's albedo parameterization the means to detect such variations.

# Chapter 5

## General Conclusions

### 5.1 Summary

The focus of this research was to examine the importance of accurate snow and lake ice albedo for the simulation of lake ice break-up as well as to explore the potential use of satellite derived albedo from the Moderate Resolution Imaging Spectroradiometer (MODIS) albedo products (MOD10A1, MYD10A1, and MCD43A3) directly integrated into the Canadian Lake Ice Model (CLIMo). Surface albedo of lake ice plays an important role in simulating lake ice break-up as it governs the amount of shortwave solar radiation reflected and absorbed at the surface. It was unclear if CLIMo's albedo parameterization was capable of representing snow and lake ice albedo in the winter months since surface albedo can vary greatly on a daily basis due to many factors (discussed in Chapter 2). Satellite remote sensing via the MODIS albedo products provided the opportunity to obtain albedo retrievals that are capable of capturing such variations albeit over a large area (500 m<sup>2</sup>). However, the MODIS daily albedo products (MOD10A1/MYD10A1) and the 16-day albedo product (MCD43A3) had not yet been evaluated over lake ice. This study evaluated the MODIS albedo products and CLIMo's albedo parameterization by collecting *in situ* albedo measurements at Malcolm Ramsay Lake near Churchill, Manitoba. Also, MODIS albedo products, as mentioned, were directly integrated into CLIMo to examine the effect that satellite retrievals had on simulated lake ice break-up for CLIMo compared to CLIMo using the original albedo parameterization over Back Bay (Great Slave Lake [GSL]) near Yellowknife, Northwest Territories.

Chapter 3 presented the results of CLIMo's albedo parameterization and MODIS albedo products evaluation with *in situ* measurements over Malcolm Ramsay Lake. During the cold winter season in 2012 (February 15<sup>th</sup> to April 25<sup>th</sup>), three albedo measurement stations were set up on Malcolm Ramsay Lake. During the melt period, the stations on Malcolm Ramsay Lake had to be removed due to volatile conditions and a risk that the instruments would fall into the lake. Instead, the MODIS albedo products were compared to the melting ice portion of CLIMo's albedo parameterization to see if similar albedos were obtained between CLIMo and MODIS. Simulated surface albedos from CLIMo (with and without snowfall included in the model) were evaluated with the *in situ* observations for three different surface types (clear ice, snow ice, and snow). The MODIS

albedo products were evaluated against an average of the three stations since the MODIS products have a 500 m spatial resolution. When snow cover was present in the model, CLIMo performed very well, simulating albedo within 10% of *in situ* observations. The MODIS albedo products similarly performed well, retrieving albedo within 10% of average *in situ* observations. The bare ice portion of CLIMo's albedo parameterization overestimated bare ice albedo (both clear and snow ice) and underestimated snow albedo. The comparison between MODIS albedo products and CLIMo albedo simulations (with and without snow in the model) showed differences of at least 0.14 between the two. The differences should be taken lightly since they are not *in situ* measurements and the MODIS albedo products encountered a lot of cloud interference during the melt period. However, the comparisons suggest that MODIS albedo products retrieve higher albedo values than CLIMo's albedo parameterization during the melt season. The results have demonstrated that satellite remote sensing products, specifically the MODIS albedo products (MOD10A1, MYD10A1, and MCD43A3) are capable of retrieving fairly accurate snow and lake ice albedo. This is useful because there are many remote lakes in the Northern Hemisphere that are not easily accessible as well as large lakes that cover vary large areas and MODIS albedo products are capable of retrieving albedo in these areas. The results have also shown that MODIS albedo products may be beneficial to the simulation of lake ice break-up if directly integrated into CLIMo.

Chapter 4 involved the direct integration the MODIS albedo products (MOD10A1, MYD10A1, and MCD43A3) into CLIMo for the break-up period over Back Bay to see if there was a significant improvement in break-up date simulation. MODIS albedo retrievals over Back Bay (near Yellowknife) were collected from 2000 to 2011. Using the MODIS daily products and the MODIS surface reflectance products (MOD09GA/MYD09GA), lake ice break-up for Back Bay was observed for the study period. CLIMo was run using three separate snow cover scenarios (0%, 68%, and 100% snow cover) and MODIS albedo products were integrated at varying increments prior to the MODIS observed ice off dates. The results show that MODIS albedo products, when integrated at least a month in advance of ice off dates for Back Bay, improved CLIMo's simulation by 1-2 days compared to CLIMo using the original albedo parameterization. CLIMo using MODIS albedos and CLIMo using the original albedo parameterization both performed well having average errors of 3-4 days and 4-5 days, respectively. It is difficult to tell whether MODIS albedo retrievals provided a significant improvement in lake ice break-up simulation for CLIMo due to the short study period and evaluation at a single site (Back Bay). However, the results have shown that CLIMo using the original albedo parameterization performs very well in simulating lake ice break-up. The results have also shown that MODIS albedos provide very similar break-up simulation results for CLIMo and could

potentially be used in situations where atmospheric forcing variables are not readily available at other lake locations in remote Arctic and sub-Arctic regions.

Overall, this study has shown that CLIMo's albedo parameterization performs well in simulating lake ice albedo although the albedo parameterization could use some improvement in simulating bare ice albedo. Further investigation of the melting ice albedo is also required. The MODIS albedo products perform well over lake ice and can still be useful in assisting CLIMo's lake ice break-up simulations over large areas.

## 5.2 Limitations

There are a number of limitations present in this study. There was an accumulation of snow in front of the two bare ice stations following snowfall events, which limited the bare ice evaluation of CLIMo's albedo parameterization. A concern for the *in situ* measurements was that they were not checked as often as the World Meteorological Organisation (WMO) suggests (i.e. daily) (WMO, 2008).

There were also some limitations that should be noted for the MODIS albedo products. The MODIS albedo products have a 500 m spatial resolution. Therefore, the albedo retrievals may contain surface albedos from multiple surfaces and not just the surface desired for the one-dimensional lake ice model CLIMo. Cloud cover is also an issue for the MODIS albedo products. Albedo is a measure of shortwave radiation and cloud cover prevents the satellite sensors from observing the surface. High solar zenith angles (SZA) tend to create erroneous albedo values in the MODIS retrievals. To counter this, the albedo retrievals are provided as close to local solar noon as possible when SZAs are lowest. However, in Arctic and sub-Arctic regions, high SZAs are difficult to avoid during the winter, so MODIS albedo products are most reliable later in the winter season when SZA are consistently below 70°. It is also worth noting that the MODIS albedo products only represent approximations of albedo after atmospheric corrections and angular modelling (Schaeppman-Strub *et al.*, 2006).

For CLIMo, atmospheric forcing inputs required for the lake ice model to run cannot always be located as close to the lake as preferred (e.g. Chapter 4 used atmospheric forcing data recorded at Yellowknife's airport near Back Bay). Methods are used to reduce any error caused by the location differences (e.g. Brown and Duguay's [2010] snow-on-land to snow-on-ice ratio for Back Bay), but atmospheric conditions differ at local scales and some slight differences may exist. Also, CLIMo does not account for snow deposition and removal by wind related processes. Snow's insulating

properties have a significant effect on lake ice growth and any aeolian changes in snow cover may lead to altered simulations.

Finally, the Back Bay break-up observations had to be made using MODIS products. Cloud interference during the melt period may have resulted in break-up observations that were slightly off which would affect the error statistics in Chapter 4.

### 5.3 Future work

Future work involving this research can go in many directions. The *in situ* measurements gathered over Malcolm Ramsay Lake can help assess more than just CLIMo's albedo parameterization. Air temperature, wind speed, relative humidity, and net radiation were collected over a frozen lake. Using the net radiation information, CLIMo's surface energy budget can be evaluated in future studies.

Pertaining to the albedo parameterization, it has been shown that the MODIS albedo products perform well over lake ice and should be further investigated. This study used the daily MODIS albedo products, MxD10A1, and the 16-day albedo product, MCD43A3. Wang et al. (2012) used a product developed by Shuai (2010) that utilizes the MCD43 algorithm and produces a daily albedo and 16-day daily products (instead of every eight days). The MCD43 algorithm produces a very robust BRDF and Wang et al. (2012) found the products to be accurate within 0.05 units of albedo when compared to ground based observations on the North Slope of Alaska. These products should be investigated for integration into CLIMo in the future and could potentially replace both the MxD10A1 and MCD43A3 products.

Data assimilation techniques could also be explored using MODIS albedo products with CLIMo in the simulation of lake ice phenology. Malik *et al.* (2012) has explored such techniques and found promising results assimilating satellite retrieved albedo into a land surface model.

Finally, CLIMo simulates the growth of snow ice; therefore, the albedo parameterization could be altered to account for the presence of clear or snow ice to improve bare ice albedo simulations.

# Appendix A

## A.1 Performance statistics

Common statistical difference measures used to measure average model performance error are the mean bias error (MBE), root mean square error (RMSE), and the mean absolute error (MAE) seen in equations (A.1), (A.2), and (A.3):

$$\text{MBE} = n^{-1} \sum_{i=1}^n (P_i - O_i) \quad (\text{A.1})$$

$$\text{RMSE} = \left[ n^{-1} \sum_{i=1}^n (P_i - O_i)^2 \right]^{0.5} \quad (\text{A.2})$$

$$\text{MAE} = n^{-1} \sum_{i=1}^n |P_i - O_i| \quad (\text{A.3})$$

where  $n$  is the sample size;  $P$  is the modelled value; and  $O$  is the observed value. These statistical measures are described as good measures for evaluating a models performance (Willmott, 1982; Willmott and Matsuura, 2005, 2006). MBE illustrates the systematic errors that occur and provides context on whether the modelled values are being over- or under-estimated (Ménard *et al.*, 2002; Willmott and Matsuura, 2005, 2006). The RMSE is squared before being averaged and therefore does not provide information on whether the modelled values are being over- or underestimated, but it does provide information on the deviation of the modelled values from the observed (Ménard *et al.*, 2002). However, Willmott and Matsuura (2005, 2006) note that the RMSE is a “function of the average error (MAE), the distribution of error magnitudes (or squared errors), and  $n^{1/2}$ ” and do not only describe the average error. Without the MAE, which is an absolute measure of the average magnitude of errors between the modelled and observed values, one cannot tell how much the RMSE is affected by the average error or how much it is affected by the variability within the distribution of squared errors or the sample size (Willmott and Matsuura, 2005, 2006). “MAE is the most natural measure of average error magnitude, and that (unlike RMSE) it is an unambiguous measure of average error magnitude” (Willmott and Matsuura, 2005). Still, the RMSE is commonly reported in studies and is included in error evaluation for accurate comparisons with previous validation studies.

# References

- Ackerman, S. A., Strabala, K. I., Menzel, W. P., Frey, R. A., Moeller, C. C., & Gumley, L. E. (1998). Discriminating clear sky from clouds with MODIS. *Journal of Geophysical Research*, 103(D24), 32141-32157.
- Adams, W. P., & Roulet, N. T. (1980). Illustration of the roles of snow in the evolution of the winter cover of a lake. *Arctic*, 33(1), 100-116.
- Aoki, T., Aoki, T., Fukabori, M., Hachikubo, A., Tachibana, Y., & Nishio, F. (2000). Effects of snow physical parameters on spectral albedo and bidirectional reflectance of snow surface. *Journal of Geophysical Research*, 105(D8), 10219-10236.
- Barry, R. G., & Maslanik, J. A. (1993). Monitoring lake freeze-up/break-up as a climatic index. In Barry, R. G., Goodison, B. E., & LeDrew, E. F. (Eds.), *Snow Watch '92* (pp. 66-79). Boulder, CO: Earth-Observations Laboratory, Institute for Space and Terrestrial Science and the World Data Center A for Glaciology Snow and Ice.
- Bengtsson, L. (1986). Spatial variability of lake ice covers. *Geografiska Annaler*, 68A(1-2), 113-121.
- Bolsenga, S. J. (1977). Preliminary observations on the daily variation of ice albedo. *Journal of Glaciology*, 18(80), 517-521.
- Bonsal, B. R., & Prowse, T. D. (2003). Trends and variability in spring and autumn 0°C-isotherm dates over Canada. *Climate Change*, 57, 341-358.
- Brown, L. C., & Duguay, C. R. (2010). The response and role of ice cover in lake-climate interactions. *Progress in Physical Geography*, 34(5), 671-704.
- Brown, L. C., & Duguay, C. R. (2011a). A comparison of simulated and measured lake ice thickness using a Shallow Water Ice Profiler. *Hydrological Processes*, 25, 2932-2941.
- Brown, L. C., & Duguay, C. R. (2011b). The fate of lake ice in the North American Arctic. *The Cryosphere*, 5, 869-892.
- Conway, H., Gades, A., & Raymond, C. F. (1996). Albedo of dirty snow during conditions of melt. *Water Resources Research*, 32(6), 1718,1718.
- Duguay, C. R., Flato, G. M., Jeffries, M. O., Ménard, P., Morris, K., & Rouse, W. R. (2003). Ice-cover variability on shallow lakes at high latitudes: model simulations and observations. *Hydrological Processes*, 17, 3465- 3483.
- Duguay, C. R., Prowse, T. D., Bonsal, B. R., Brown, R. D., Lacroix, M. P., & Menard, P. (2006). Recent trends in Canadian lake ice cover. *Hydrological Processes*, 20, 781-801.

- Ebert, E. E., & Curry, J. A. (1993). An intermediate one-dimensional thermodynamic sea ice model for investigating ice-atmosphere interactions. *Journal of Geophysical Research*, 98(C6), 10,085-10,109.
- Flato, G. M., & Brown, R. D. (1996). Variability and climate sensitivity of landfast Arctic sea ice. *Journal of Geophysical Research*, 101(C10), 26767-25777.
- Gardner, A. S., & Sharp, M. J. (2010). A review of snow and ice albedo and the development of a new physically based broadband albedo parameterization. *Journal of Geophysical Research*, 115, F01009, doi:10.1029/2009JF001444.
- Gerard, R. (1990). Hydrology of floating ice. In Prowse, T. D., & Ommanney, C. S. L. (Eds.), *Northern hydrology: Canadian perspectives* (pp. 103-134). Saskatoon, Saskatchewan: National Hydrology Research Institute.
- Grenfell, T. C., Perovich, D. K., & Ogren, J. A. (1981). Spectral albedos of an alpine snowpack. *Cold Regions Science and Technology*, 4, 121-127.
- Grenfell, T. C., Warren, S. G., & Mullen, P. C. (1994). Reflection of solar radiation by the Antarctic snow surface at ultraviolet, visible, and near-infrared wavelengths. *Journal of Geophysical Research*, 99(D9), 18699-18684.
- Grenfell, T. C., & Perovich, D. K. (2004). Seasonal and spatial evolution of albedo in a snow-ice-land-ocean environment. *Journal of Geophysical Research*, 109, C01001, doi:10.1029/2003JC001866.
- Hall, D. K., Riggs, G. A., Salomonson, V. V., Barton, J. S., Casey, K., Chien, J. Y. L., ... & Tait, A. B. (2001). Algorithm theoretical basis document (ATBD) for the MODIS snow and sea ice-mapping algorithms. *Hydrological Science Branch NASA*.
- Hall, D. K., & Riggs, G. A. (2007). Accuracy assessment of the MODIS snow products. *Hydrological Processes*, 21, 1534-1547.
- Hall, D. K., Nghiem, S. V., Schaaf, C. B., DiGirolamo, N. E., & Neumann, G. (2009). Evaluation of surface and near-surface melt characteristics on the Greenland ice sheet using MODIS and QuikSCAT data. *Journal of Geophysical Research*, 114, F04006, doi:10.1029/2009JF001287, 1-13.
- Henneman, H. E., & Stefan, H. G. (1999). Albedo models for snow and ice on a freshwater lake. *Cold Regions Science and Technology*, 29, 31-48.
- Heron, R., & Woo, M. K. (1994). Decay of a high Arctic lake-ice cover: observations and modelling. *Journal of Glaciology*, 40(135), 283-292.
- Hostetler, S. W. (1991). Simulation of lake ice and its effects on the late-Pleistocene evaporation rate of Lake Lahontan. *Climate Dynamics*, 7, 43-48.
- Hostetler, S. W., Bates, G. T., & Giorgi, F. (1993). Interactive coupling of a lake thermal model with a Regional Climate Model. *Journal of Geophysical Research*, 98(D3), 5045-5057.

- Howell, S. E. L., Brown, L. C., Kang, K. K., & Duguay, C. R. (2009). Variability in ice phenology on Great Bear Lake and Great Slave Lake, Northwest Territories, Canada, from SeaWinds/QuikSCAT: 2000-2006.
- Jeffries, M. O., Morris, K., & Duguay, C. R. (2005a). Lake ice growth and decay in central Alaska, USA: observations and computer simulations compared. *Annals of Glaciology*, 40, 1-4.
- Jeffries, M. O., Morris, K., & Kozlenko, N. (2005b). Ice characteristics and processes, and remote sensing of frozen rivers and lakes. In Duguay, C. R., & Pietroniro, A. (Eds.), *Remote Sensing in Northern Hydrology: Measuring Environmental Change* (pp. 63-90). Washington, DC: American Geophysical Union.
- Jin, Y., Schaaf, C. B., Woodcock, C. E., Gao, F., Li, X., Strahler, ... & Liang, S. (2003). Consistency of MODIS surface bidirectional reflectance distribution function and albedo retrievals: 2. Validation. *Journal of Geophysical Research*, 108(D5), 4159, doi:10.1029/2002JD002804, 1-15.
- Key, J. R., Wang, X., Stroeve, J. C., & Fowler, C. (2001). Estimating the cloudy-sky albedo of sea ice and snow from space. *Journal of Geophysical Research*, 106[D12], 12489-12497.
- Kheyrollah Pour, H., Duguay, C. R., & Martynov, A. (2012). Simulation of surface temperature and ice cover of large northern lakes with 1-D models: a comparison with MODIS satellite data and *in situ* measurements. *Tellus A*, 64, 1-19.
- Klein, A. G., & Stroeve, J. (2002). Development and validation of a snow albedo algorithm for the MODIS instrument. *Annals of Glaciology*, 34, 45-52.
- Knight, C. A. (1962). Studies of Arctic lake ice. *Journal of Glaciology*, 46(1), 397-403.
- Langleben, M.P. (1971). Albedo of melting sea ice in the southern Beaufort Sea. *Journal of Glaciology*, 10[58], 101-104.
- Launiainen, J., & Cheng, B. (1998). Modelling of ice thermodynamics in natural water bodies. *Cold Regions Science and Technology*, 27, 153-178.
- Legates, D. R., & McCabe Jr., G. J. (1999). Evaluating the use of “goodness-of-fit” measures in hydrologic and hydroclimatic model validation. *Water Resources Research*, 35(1), 233-241.
- Leppäranta, M. (2010). Modelling the formation and decay of lake ice. In George, G. (Eds.), *Impact of Climate Change on European Lakes* (pp. 63-83). Dordrecht, NL: Springer Netherland.
- Liang, S. (2000). Narrowband to broadband conversions of land surface albedo I Algorithms. *Remote Sensing of Environment*, 76, 213-238.
- Liang, S., Fang, F., Chen, M., Shuey, C. J., Walthall, C., Daughtry, C., ... & Strahler, A. (2002). Validating MODIS land surface reflectance and albedo products: methods and preliminary results. *Remote Sensing of Environment*, 83, 149-162.

- Liu, J., Schaaf, C., Strahler, A., Jiao, Z., Shuai, Y., Zhang, ... & Dutton, E. G. (2009). Validation of Moderate Resolution Imaging Spectroradiometer (MODIS) albedo retrieval algorithm: Dependence of albedo on solar zenith angle. *Journal of Geophysical Research*, 114, D01106, doi:10.1029/2008JD009969, 1-11.
- Magnuson, J. J., Robertson, D. M., Benson, B. J., Wynne, R. H., Livingstone, D. M., Arai, T., ... & Vuglinski, V. S. (2000). Historical trends in lake and river ice cover in the Northern Hemisphere. *Science*, 289, 1743-1746.
- Malik, M. J., van der Velde, R., Vekerdy, Z., Su, Z., & Salman, M. F. (2011). Semi-empirical approach for estimating broadband albedo of snow. *Remote Sensing of Environment*, 115(8), 2086-2095.
- Malik, M. J., van der Velde, R., Vekerdy, Z., & Su, Z. (2012). Assimilation of satellite-observed snow albedo in a land surface model. *Journal of Hydrometeorology*, 13(3), 1119-1130.
- Martonchik, J. V., Bruegge, C. J., & Strahler, A. H. (2000). A review of reflectance nomenclature used in remote sensing. *Remote Sensing Reviews*, 19, 9-19.
- Martynov, A., Sushama, L., & Laprise, R. (2010). Simulations of temperate freezing lakes by one-dimensional lake models: performance assessment for interactive coupling with regional climate models. *Boreal Environment Research*, 15, 143-164.
- Massom, R., & Lubin, D. (2006). *Polar remote sensing volume II: ice sheet*. Chichester, UK: Praxis Publishing Ltd.
- Maykut, G. A., & Untersteiner, N. (1971). Some results from a Time-Dependent Thermodynamic Model of Sea Ice. *Journal of Geophysical Research*, 76(6), 1550-1575.
- Maykut, G. A. (1982). Large-scale heat exchange and ice production in the Central Arctic. *Journal of Geophysical Research*, 87[C10], 7971-7984.
- Ménard, P., Duguay, C. R., Flato, G. M., & Rouse, W. R. (2002). Simulation of ice phenology on Great Slave Lake, Northwest Territories, Canada. *Hydrological Processes*, 16, 3691-3706.
- Michel, B., & Ramseier, R. O. (1971). Classification of river and lake ice. *Canadian Geotechnical Journal*, 8(1), 36-45.
- Mironov, D. V. (2008). Parameterization of lakes in numerical weather prediction. Description of a lake model. *COSMO Technical Report, 11*, Deutscher Wetterdienst, Offenbach am Main, Germany, 1-41.
- Morris, K., Jeffries, M. O., & Duguay, C. R. (2005). Model simulation of the effects of climate variability and change on lake ice in central Alaska, USA. *Annals of Glaciology*, 40, 113-118.
- Mugnai, A., & Wiscombe, W. J. (1980). Scattering of radiation by moderately nonspherical particles. *Journal of the Atmospheric Sciences*, 37, 1291-1307.

- Mullen, P. C., & Warren, S. G. (1988). Theory of the optical properties of lake ice. *Journal of Geophysical Research*, 93(D7), 8403-8414.
- Nicodemus, F. E., Hsia, F. C., Richmond, J. J., Ginsberg, I. W., & Limperis, T. (1977). Geometrical considerations and nomenclature for reflectance. *Science And Technology*, 160, 1-52. National Bureau of Standards (US).
- Nolan, A. W., & Liang, S. (2000). Progress in bidirectional reflectance modeling and applications for surface particulate media: snow and soils. *Remote Sensing Review*, 18, 307-342.
- Oke, T. R. (1978). *Boundary layer climates*. London, UK: Methuen & Co Ltd.
- Petrenko, V. F., & Whitworth, R. W. (1999). *Physics of ice*. New York, NY: Oxford University Press Inc.
- Riggs, G. A., Hall, D. K., & Salomonson, V.V. (2006). *MODIS snow products user guide to collection 5*. Retrieved on September 7, 2012, from, [http://modis-snow-ice.gsfc.nasa.gov/uploads/sug\\_c5.pdf](http://modis-snow-ice.gsfc.nasa.gov/uploads/sug_c5.pdf).
- Rouse, W. R., Oswald, C. J., Binyamin, J., Spence, C., Schertzer, W. M., Blanken, ... & Duguay, C. R. (2005). The role of northern lakes in a regional energy balance. *American Meteorological Society*, 6, 291-305.
- Rouse, W. R., Binyamin, J., Blanken, P. D., Bussi eres, N., Duguay, C. R., Oswald, C. J., ... & Spence, C. (2008a). The influence of lakes on the regional energy and water balance of the central Mackenzie River Basin. In *Cold Region Atmospheric and Hydrologic Studies. The Mackenzie GEWEX Experience* (pp. 309-325). Springer Berlin Heidelberg.
- Rouse, W. R., Blanken, P. D., Duguay, C. R., Oswald, C. J., & Schertzer, W. M. (2008b). Climate-lake interactions. In *Cold region atmospheric and hydrologic studies. The Mackenzie GEWEX experience* (pp. 139-160). Springer Berlin Heidelberg.
- Salomon, J. G., Schaaf, C. B., Strahler, A. H., Gao, F., & Jin, Y. (2006). Validation of the MODIS Bidirectional Reflectance Distribution Function and albedo retrievals using combined observations from the Aqua and Terra platforms. *IEEE Transactions on Geoscience and Remote Sensing*, 44(6), 1555-1565.
- Salomonson, V. V., Barnes, W., & Masuoka, E. J. (2006). Introduction to MODIS and an overview of associated activities. In J. J. Qu, W. Gao, M. Kafatos, R. E. Murphy, & V. V. Salomonson (Eds.), *Earth science satellite remote sensing volume 1: science and instruments* (pp. 14-32). Berlin: Springer.
- Schaaf, C. B., Gao, F., Strahler, A. H., Lucht, W., Li, X., Tsang, T., ... & Roy, D. (2002). First operational BRDF, albedo nadir reflectance products from MODIS. *Remote Sensing of Environment*, 83, 135-148.
- Schaaf, C. B. (2004, April). *MODIS BRDF/Albedo Product (MOD43B) User's Guide – MOD43B3 Albedo Product*. Retrieved from, <http://www-modis.bu.edu/brdf/userguide/albedo.html>.

- Schaepman-Strub, G., Schaepman, M. E., Painter, T. H., Dangel, S., & Martonchik, J. V. (2006). Reflectance quantities in optical remote sensing—definitions and case studies. *Remote Sensing of Environment*, 103, 27-42.
- Schertzer, W. M. (1997). Freshwater Lakes. In W.G. Bailey, T.R. Oke, & W.R. Rouse (Eds.), *The surface climates of Canada* (pp. 124-148). Montreal: McGill-Queen's University Press.
- Serreze, M. C., & Barry, R. G. (2005). *The Arctic climate system*. Cambridge, UK: Cambridge University Press.
- Shine, K. P. (1984) Parameterization of the shortwave flux over high albedo surfaces as a function of cloud thickness and surface albedo. *Quarterly Journal of the Royal Meteorological Society*, 110, 747-764.
- Shuai, Y. (2010). Tracking daily land surface albedo and reflectance anisotropy with MODerate-Resolution Imaging Spectroradiometer (MODIS), *Dissertation for Doctor of Philosophy*, Boston University.
- Şorman, A. Ü., Akyürek, Z., Şensoy, A., Şorman, A. A., & Tekeli, A. E. (2007). Commentary on comparison of MODIS snow cover and albedo products with ground observations over the mountainous terrain of Turkey. *Hydrology and Earth System Sciences*, 11, 1353-1360.
- Stamnes, K., Tsay, S. C., Wiscombe, W., & Jayaweera, K. (1988). Numerically stable algorithm for discrete-ordinate-method radiative transfer in multiple scattering and emitting layered media. *Applied optics*, 27(12), 2502-2509.
- Stroeve, J., Box, J. E., Gao, F., Liang, S., Nolin, A., & Schaaf, C. (2005). Accuracy assessment of the MODIS 16-day albedo product for snow: comparisons with Greenland *in situ* measurements. *Remote Sensing of Environment*, 94, 46-60.
- Stroeve, J. C., Box, J. E., & Haran, T. (2006). Evaluation of the MODIS (MOD10A1) daily snow albedo product over the Greenland ice sheet. *Remote Sensing of Environment*, 105, 155-171.
- Strugnell, N. C., & Lucht, W. L. (2001). An algorithm to infer continental-scale albedo from AVHRR data, land cover class, and field observations of typical BRDFs. *Journal of Climate*, 14(7), 1360-1376.
- Sturm, M., & Liston, G. E. (2003). The snow cover on lakes of the Arctic Coastal Plain of Alaska. *Journal of Glaciology*, 49[166], 370-380.
- Surface Radiation Budget Monitoring*. (n.d.). Retrieved from <http://www.esrl.noaa.gov/gmd/grad/surfrad/surfpag0.html>.
- Tekeli, A. E., Şensoy, A., Şorman, A., Akyürek, Z., & Şorman, Ü. (2006). Accuracy assessment of MODIS daily snow albedo retrievals with *in situ* measurements in Karasu basin, Turkey. *Hydrological Processes*, 20, 705-721.

- Vavrus, S. J., Wynne, R. H., & Foley, J. A. (1996). Measuring the sensitivity of southern Wisconsin lake ice to climate variations and lake depth using a numerical model. *Limnology and Oceanography*, 41(5), 822-831.
- Wang, K., Liu, J., Zhou, X., Sparrow, M., Ma, M., Sun, Z. S., & Jiang, W. (2004). Validation of the MODIS global land surface albedo product using ground measurements in a semidesert region on the Tibetan Plateau. *Journal of Geophysical Research*, 109, D05107, doi:10.1029/2003JD004229, 1-9.
- Wang, K., Liang, S., Schaaf, C. L., & Strahler, A. H. (2010). Evaluation of Moderate Resolution Imaging Spectroradiometer land surface visible and shortwave albedo products at FLUXNET sites. *Journal of Geophysical Research*, 115, D17107, doi:10.1029/2009JD013101, 1-8.
- Wang, Z., Schaaf, C. B., Chopping, M. J., Strahler, A. H., Wang, J., Roman, M. O., ... & Shuai, Y. (2012). Evaluation of Moderate-resolution Imaging Spectrometer (MODIS) snow albedo product (MCD43A) over tundra. *Remote Sensing of Environment*, 117, 264-280.
- Wanner, W., Strahler, A. H., Hu, B., Lewis, P., Muller, J. P., Li, X., ... & Barnsley, M. J. (1997). Global retrieval of bidirectional reflectance and albedo over land from EOS MODIS and MISR data: Theory and algorithm. *Journal of Geophysical Research*, 102(D14), 17,143-17,161.
- Warren, S. G. (1982). Optical properties of snow. *Reviews of Geophysics and Space Physics*, 20(1), 67-89.
- Weller, G. (1972). Radiation flux investigation. *AIDJEX Bulletin*, 14, 28-30.
- Willmott, C. J. (1982). Some comments on the evaluation of model performances. *Bulletin of the American Meteorological Society*, 63, 1309-1313.
- Willmott, C. J., & Matsuura, K. (2005). Advantages of the mean absolute error (MAE) over the root mean square error (RMSE) in assessing average model performance. *Climate Research*, 30, 79-82.
- Willmott, C. J., & Matsuura, K. (2006). On the use of dimensioned measures of error to evaluate the performance of spatial interpolators. *International Journal of Geographical Information Science*, 20(1), 89-102.
- Wiscombe, W. J., & Warren, S. G. (1980). A model for the spectral albedo of snow. I: Pure snow. *Journal of the Atmospheric Sciences*, 37, 2712-2733.
- WMO. (2008). *Guide to meteorological instruments and methods of observation: WMO-No. 8* (7th ed.). Geneva, Switzerland: World Meteorological Organization.